

**Field Deployable Electrochemical Sensors for
Simultaneous Determination of Cd, Pb and Zn
Heavy Metals in Drinking Water**

BY

ABDULLAH ALI ALALIWI

A Thesis Presented to the
DEANSHIP OF GRADUATE STUDIES

KING FAHD UNIVERSITY OF PETROLEUM & MINERALS

DHAHRAN, SAUDI ARABIA

In Partial Fulfillment of the
Requirements for the Degree of

MASTER OF SCIENCE

In

CHEMISTRY

June, 2012

KING FAHD UNIVERSITY OF PETROLEUM & MINERALS

DHAHRAN 31261, SAUDI ARABIA

DEANSHIP OF GRADUATE STUDIES

This thesis, written by **Abdullah Ali Al-Aliwi** under the direction of his thesis advisor and approved by his thesis committee, has been presented to and accepted by the Dean of Graduate Studies, in partial fulfillment of the requirements for the degree of **MASTER OF SCIENCE in CHEMISTRY**.

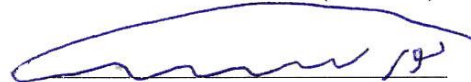
Thesis Committee



Dr. Abdel-Nasser Kawde (Advisor)



Dr. Kalid Alhooshani (Member)



Dr. Nouri M. Hassan (Member)



Dr. Abdullah J. Al-Hamdan

Department Chairman



Dr. Salam A. Zummo

Dean of Graduate Studies

12/9/12

Date



DEDICATED To

My Beloved Parents

Whose constant prayers, support, and inspiration

lead to this accomplishment.

Acknowledgment

I am extremely grateful to almighty Allah who gave me the opportunity, strength and patience to accomplish my goals. Acknowledgement is due to King Fahad University of Petroleum and Minerals for providing all necessary facilities to conduct this research.

I would like to offer my indebtedness and sincere appreciation to my thesis committee chairman Dr. Abdel-Nasser Kawde, for his constant help, patience and guidance during this work. I have learned a lot from him for which I am thankful for.

Dr. Kawde and I would like to express our gratitude to King Abdulaziz City for Science and Technology (KACST) for funding the current research (AT-28-27).

Finally, I am grateful to my family (parents, brothers, sisters and wife) for their extreme support, encouragement and patience during the course of my studies.

Table of Contents

Acknowledgment	iv
Table of Contents	v
List of Figures	x
List of Tables.....	xxv
THESIS ABSTRACT (ENGLISH).....	xxvi
THESIS ABSTRACT (ARABIC).....	xxvii
CHAPTER 1	1
1.0 INTRODUCTION AND LITERATURE REVIEW	1
1.1 FIELD DEPLOYABLE ELECTROCHEMICAL SENSORS	3
1.2 SIMULTANEOUS DETERMINATION OF Zn(II), Cd(II) and Pb(II) IN DRINKING WATER	14
1.3 DETECTION TECHNIQUES AND ELECTRODE SURFACES	16
1.3.1 Electroanalytical Techniques.....	16
1.3.1.1 Cyclic Voltammetry (CV)	17
1.3.1.2 Normal Pulse Voltammetry (NPV).....	20
1.3.1.3 Differential Pulse Voltammetry (DPV)	20
1.3.1.4 Square Wave Voltammetry (SWV)	20

1.3.1.5	Linear Sweep Voltammetry (LSV).....	21
1.3.1.6	Preconcentration and Stripping Techniques	21
1.3.2	Other Techniques.....	28
1.3.2.1	Inductively Coupled Plasma- Mass Spectroscopy (ICP-MS).....	28
1.3.2.2	Scanning Electron Microscopy (SEM)	33
1.3.3	Carbon Electrode Surfaces	35
1.3.3.1	Glassy Carbon Electrode (GCE).....	36
1.3.3.2	Graphite Pencil Electrode (GPE).....	37
1.3.3.3	Carbon Paste Electrode (CPE).....	38
1.3.3.4	Glassy Carbon Paste Electrode (GCPE)	38
1.4	Objectives.....	40
CHAPTER 2		41
2.0	ELECTROCHEMICAL INVESTIGATION AND	
	ANALYTICAL DETERMINATION OF Zn(II), Cd(II) AND	
	Pb(II) USING Bi- & Hg- MODIFIED ELECTRODES.....	41
2.1	INTRODUCTION.....	41
2.2	ELECTROCHEMICAL INVESTIGATION AND ANALYTICAL	
	DETERMINATION USING Bi-MODIFIED ELECTRODES	46
2.2.1	Apparatus.....	46
2.2.2	Electrochemical Transducers Preparation	48
2.2.3	Reagents	48

2.2.4	Procedure.....	49
2.2.5	Results and Discussion.....	49
2.2.5.1	Electrochemical Investigation.....	49
2.2.5.2	Optimization.....	55
2.2.5.3	Reproducibility.....	61
2.2.5.4	Analytical Determination.....	61
2.3	ELECTROCHEMICAL INVESTIGATION AND ANALYTICAL DETERMINATION USING Hg-MODIFIED ELECTRODES.....	65
2.3.1	Apparatus.....	65
2.3.2	Electrochemical Transducers Preparation.....	65
2.3.3	Reagents.....	65
2.3.4	Procedure.....	65
2.3.5	Results and Discussion.....	65
2.3.5.1	Electrochemical Investigation.....	66
2.3.5.2	Optimization.....	72
2.3.5.3	Reproducibility.....	76
2.3.5.4	Analytical Determination.....	80
CHAPTER 3	84
3.0	ELECTROCHEMICAL INVESTIGATION AND ANALYTICAL DETERMINATION OF Zn(II), Cd(II) AND Pb(II) USING Bi/Hg ALLOY-MODIFIED ELECTRODES ..	84
3.1	INTRODUCTION.....	84

3.2	ELECTROCHEMICAL INVESTIGATION AND ANALYTICAL DETERMINATION	85
3.2.1	Apparatus.....	85
3.2.2	Electrochemical Transducers Preparation	85
3.2.3	Reagents	85
3.2.4	Procedure.....	85
3.2.5	Results and Discussion	85
3.2.5.1	Electrochemical Investigation.....	86
3.2.5.2	Optimization	99
3.2.5.3	Reproducibility	103
3.2.5.4	Analytical Determination.....	111
3.2.5.5	Interferences.....	111
CHAPTER 4		121
4.0	FIELD-DEPLOYABLE ELECTROCHEMICAL SENSOR: SETUP AND REAL WATER SAMPLES APPLICATION. 121	
4.1	INTRODUCTION.....	121
4.2	FIELD-DEPLOYABLE ELECTROCHEMICAL SENSORS.....	121
4.2.1	System Setup	121
4.2.2	Procedure.....	123
4.2.3	Results and Discussion	123
4.2.3.1	Real Drinking Water Samples Analysis Using Modified Glassy Carbon Electrodes	125

4.2.3.1.1 Drinking Water Samples Analysis Using Glassy Carbon-Bi Modified Electrodes.....	125
4.2.3.1.2 Drinking Water Samples Analysis Using Glassy Carbon-Hg Modified Electrodes.....	126
4.2.3.1.3 Drinking Water Samples Analysis Using Glassy Carbon- Bi/Hg Alloy Modified Electrodes	126
4.2.3.2 Validation.....	126
CHAPTER 5	131
5.0 CONCLUSION AND REFERENCES.....	131
5.1 CONCLUSION	131
5.2 REFERENCES	132
VITA	147

List of Figures

Figure 1.1: Screen printed electrode sensor (6).	5
Figure 1.2: Electrochemical biosensors (Biorecognition and transduction).	10
Figure 1.3: Potential-time excitation signal in cyclic voltammetric experiment (64).	18
Figure 1.4: Typical cyclic voltammogram, where i_{pc} and i_{pa} show the peak cathodic and anodic current respectively for a reversible reaction (64).	19
Figure 1.5: Normal pulse potential sweep (66).	24
Figure 1.6: Deferential pulse potential sweep (66).	25
Figure 1.7: Square wave potential sweep (66).	26
Figure 1.8: Linear potential sweep (63).	27
Figure 1.9: ICP source (50).	30
Figure 1.10: ICP - MS entrance (69).	31
Figure 1.11: Mass spectroscopy quadrupole filter (69).	32
Figure 1.12: Scanning Electron Microscopy (SEM) (70).	34

Figure 1.13: Schematic diagram of pencil electrode (A) and carbon paste electrode (B).	39
Figure 2.1: (A) The electrochemical work station (B) The cell setup.	47
Figure 2.2: Square-wave stripping voltammograms of 40 ppb of Zn(II), Cd(II) and Pb(II) using GCPE in presence of 600 ppb Bi(III). Accumulation time, 2.0 min at -1.4V; Potential step, 8 mV; Frequency, 100 Hz; Amplitude, 60 mV.	51
Figure 2.3: Square-wave stripping voltammograms of Zn(II), Cd(II) and Pb(II) at GCE in presence of 600 ppb Bi(III) in acetate buffer solution (0.1 M, pH 3.5); amplitude, 60 mV; frequency, 100 Hz; potential increment, 8 mV; accumulation time, 2.0 min at -1.4 V. For Zn(II), Cd(II) and Pb(II) concentrations: (a) 0.0, (b) 20 ppb, (c) 40 ppb, (d) 60 ppb.	52
Figure 2.4: Square-wave stripping voltammograms of Zn(II), Cd(II) and Pb(II) at Carbon Paste Electrode in presence of 600 ppb Bi(III) in acetate buffer solution (0.1 M, pH 3.5); amplitude, 25 mV; frequency, 20 Hz; potential increment, 5 mV; accumulation time, 2.0 min at -1.4 V. For Zn(II), Cd(II) and Pb(II) concentrations: (a) 0.0, (b) 20 ppb, (c) 40 ppb, (d) 60 ppb.	53
Figure 2.5: Square-wave stripping voltammogram of Zn(II), Cd(II) and Pb(II) at pencil in presence of 600 ppb Bi(III) in acetate buffer solution (0.1 M, pH 3.5); amplitude, 25 mV; frequency, 20 Hz; potential increment, 5 mV;	

accumulation time, 2.0 min at -1.4 V. For Zn(II), Cd(II) and Pb(II) concentrations: (a) 0.0, (b) 20 ppb, (c) 40 ppb, (d) 60 ppb.....54

Figure 2.6: Square-wave stripping voltammogram of 40 ppb Zn(II), Cd(II) and Pb(II) at GCE in presence of 600 ppb Bi(III) in acetate buffer solution (0.1 M) at different pH values: (a) pH 3.0, (b) pH 3.5 and (c) pH 4.0; amplitude, 60 mV; frequency, 100 Hz; potential increment, 8 mV; accumulation time, 2.0 min at -1.4 V.56

Figure 2.7: (A) Square-wave stripping voltammograms of 40 ppb Zn(II), Cd(II) and Pb(II) at GCE in presence of 600 ppb Bi(III) in acetate buffer solution (0.1 M, pH 3.5). Accumulation time, 2.0 min at -1.4 V; Potential increment, 5 mV; Amplitude, 25 mV and Frequency: (a) 20 Hz, (b) 40 Hz, (c) 60 Hz, (d) 80 Hz and (e) 100 Hz. (B) The corresponding plot.57

Figure 2.8: (A) Square-wave stripping voltammograms of 40 ppb Zn(II), Cd(II) and Pb(II) at GCE in presence of 600 ppb Bi(III) in acetate buffer solution (0.1 M, pH 3.5). Accumulation time, 2.0 min at -1.4 V; Potential increment, 5 mV; Frequency, 100 Hz; Amplitude: (a) 20 mV, (b) 30 mV, (c) 40 mV, (d) 60 mV. (B) The corresponding plot.58

Figure 2.9: (A) Square-wave stripping voltammograms of 40 ppb Zn(II), Cd(II) and Pb(II) at GCE in presence of 600 ppb Bi(III) in acetate buffer solution (0.1 M, pH 3.5). Accumulation time, 2.0 min at -1.4 V; Amplitude, 60

mV; Frequency, 100 Hz; Potential increment: (a) 2 mV, (b) 4 mV, (c) 6 mV, (d) 8 mV. (B) The corresponding plot.59

Figure 2.10 : (A) Square-wave stripping voltammograms of 40 ppb Zn(II), Cd(II) and Pb(II) at GCE in presence of 600 ppb Bi(III) in acetate buffer solution (0.1 M, pH 3.5). Amplitude, 60 mV; Frequency, 100 Hz; Potential increment, 8 mV; Accumulation time, 2.0 min at: (a) -1.2 V, (b) -1.3 V, (c) -1.4 V and (d) -1.5V. (B) The corresponding plot.60

Figure 2.11: (A) Square-wave stripping voltammograms of 40 ppb Zn(II), Cd(II) and Pb(II) at GCE in presence of 600 ppb Bi(III) in acetate buffer solution (0.1 M, pH 3.5). Amplitude, 60 mV; Frequency, 100 Hz; Potential increment, 8 mV; Accumulation time, 2.0 min at -1.4 V. (B) The corresponding plot.62

Figure 2.12A: Square-wave stripping voltammograms of Zn(II), Cd(II) and Pb(II) at GCE in presence of 600 ppb Bi(III) in acetate buffer solution (0.1 M, pH 3.5); Amplitude, 60 mV; Frequency, 100 Hz; Potential increment, 8 mV; Accumulation time, 2.0 min at -1.4 V. A mixture of Zn(II), Cd(II) and Pb(II) concentrations: (a) 0.0, (b) 5, (c) 10, (d) 15, (e) 20, (f) 30, (g) 40, (h) 50, (i) 100, (j) 150, (k) 200, (l) 250 ppb.....63

Figure 2.12B: The corresponding calibration plots of Zn(II), Cd(II) and Pb(II) concentration ranges (A) 0-50 ppb and (B) 0 – 250 ppb.....64

Figure 2.13: Square-wave stripping voltammograms of 40 ppb Zn(II), Cd(II) and Pb(II) at GCE in presence of 10 ppm Hg(II) in acetate buffer solution (0.1 M, pH 4.5). Accumulation time, 2.0 min at -1.4V; Potential increment, 6 mV; Frequency, 100 Hz; Amplitude, 70 mV..... 67

Figure 2.14: Square-wave stripping voltammograms of Zn(II), Cd(II) and Pb(II) at GCE in presence of 10 ppm Hg(II) in acetate buffer solution (0.1 M, pH 3.5); Amplitude, 70 mV; Frequency, 100 Hz; Potential increment, 6 mV; Accumulation time, 2.0 min at -1.4 V. For Zn(II), Cd(II) and Pb(II) concentrations: (a) 0.0, (b) 20 ppb, (c) 40 ppb, (d) 60 ppb..... 69

Figure 2.15: Square-wave stripping voltammograms of Zn(II), Cd(II) and Pb(II) at Carbon Paste Electrode in presence of 10 ppm Hg(II) in acetate buffer solution (0.1 M, pH 3.5); Amplitude, 25 mV; Frequency, 25 Hz; Potential increment, 5 mV; Accumulation time, 2.0 min at -1.4 V. For Zn(II), Cd(II) and Pb(II) concentrations: (a) 0.0, (b) 20 ppb, (c) 40 ppb, (d) 60 ppb. 70

Figure 2.16: Square-wave stripping voltammograms of Zn(II), Cd(II) and Pb(II) at graphite pencil electrode in presence of 10 ppm Hg(II) in acetate buffer solution (0.1 M, pH 3.5); Amplitude, 25 mV; Frequency, 25 Hz; Potential increment, 5 mV; Accumulation time, 2.0 min at -1.4 V. For Zn(II), Cd(II) and Pb(II) concentrations: (a) 0.0, (b) 20 ppb, (c) 40 ppb, (d) 60 ppb. 71

Figure 2.17: (A) Square-wave stripping voltammograms of 40 ppb Zn(II), Cd(II) and Pb(II) at GCE in presence of 10 ppm Hg(II) in acetate buffer solution (0.1 M) at different pH values: (a) pH 3.0, (b) pH 3.5, and (c) pH 4.0; Amplitude, 70 mV; Frequency, 100 Hz; Potential increment, 6 mV; Accumulation time, 2.0 min at -1.4 V. (B) The corresponding plot. 73

Figure 2.18: (A) Square-wave stripping voltammograms of 40 ppb Zn(II), Cd(II) and Pb(II) at GCE in presence of 10 ppm Hg(II) in acetate buffer solution (0.1 M, pH 3.5); Accumulation time, 2.0 min at -1.4 V ; Potential increment, 5 mV; Amplitude, 25 mV; Frequency: (a) 15 Hz, (b) 35 Hz, (c) 55 Hz, (d) 75 Hz, (e) 95 Hz, (f) 100 Hz, (g) 105 Hz. (B) The corresponding plot..... 74

Figure 2.19: (A) Square-wave stripping voltammograms of 40 ppb Zn(II), Cd(II) and Pb(II) at GCE in presence of 10 ppm Hg(II) in acetate buffer solution (0.1 M, pH 3.5); Accumulation time, 2.0 min at -1.4 V; Potential increment, 5 mV; Frequency, 100 Hz; Amplitude: (a) 50 mV, (b) 60 mV, (c) 70 mV, (d) 80 mV. (B) The corresponding plot. 75

Figure 2.20: (A) Square-wave stripping voltammograms of 40 ppb Zn(II), Cd(II) and Pb(II) at GCE in presence of 10 ppm Hg(II) in acetate buffer solution (0.1 M, pH 3.5); Accumulation time, 2.0 min at -1.4 V; Amplitude, 70 mV; Frequency, 100 Hz; Potential increment: (a) 5 mV, (b) 6 mV, (c) 7 mV. (B) The corresponding plot..... 77

Figure 2.21: (A) Square-wave stripping voltammograms of 40 ppb Zn(II), Cd(II) and Pb(II) at GCE in presence of 10 ppm Hg(II) in acetate buffer solution (0.1 M, pH 3.5); Amplitude, 70 mV; Frequency, 100 Hz; Potential increment, 6 mV; Accumulation time, 2.0 min at: (a) -1.2 V, (b) -1.3 V, (c) -1.4 V, (d) -1.5V. (B) The corresponding plot. 78

Figure 2.22: (A) Square-wave stripping voltammograms of 40 ppb Zn(II), Cd(II) and Pb(II) at GCE in presence of 10 ppm Hg(II) in acetate buffer solution (0.1 M, pH 3.5); Amplitude, 70 mV; Frequency, 100 Hz; Potential increment, 6 mV; Accumulation time, 2.0 min at -1.4 V. (B) The corresponding plot. 79

Figure 2.23A: Square-wave stripping voltammograms of Zn(II), Cd(II) and Pb(II) at GCE in presence of 10 ppm Hg(II) in acetate buffer solution (0.1 M, pH 3.5); Amplitude, 70 mV; Frequency, 100 Hz; Potential increment, 6 mV; Accumulation time, 2.0 min at -1.4 V. A mixture of Zn(II), Cd(II) and Pb(II) concentrations: (a) 0.0, (b) 1, (c) 3, (d) 5, (e) 7, (f) 10, (g) 12, (h) 14, (i) 16, (j) 18, (k) 20 ppb. 81

Figure 2.23B: The corresponding calibration plots of Figure 2.23A. 82

Figure 3.1: Square-wave stripping voltammogram of 20 ppb of Zn(II), Cd(II) and Pb(II) using Glassy Carbon Electrode in the presence of 10 ppm Hg(II) and 600ppb Bi(III) in acetate buffer solution (0.1 M, pH 4.5);

**Accumulation time, 2.0 min at -1.4 V; Potential increment, 6 mV;
 Frequency, 80 Hz; Amplitude, 40 mV.....87**

Figure 3.2: Square-wave stripping voltammograms of 20 ppb Zn(II), Cd(II) and Pb(II) at Glassy Carbon Electrode in presence of: (a) 600 ppb Bi(III), (b) 10 ppm Hg(II) and (c) 10 ppm Hg(II) and 600 ppb Bi(III) alloy, in acetate buffer solution (0.1 M, pH 4.5). Other conditions as in Figure 3.1.89

Figure 3.3: Square-wave stripping voltammograms of 20 ppb Zn(II), Cd(II) and Pb(II) using Glassy Carbon Electrode in acetate buffer solution (0.1 M, pH 4.5) containing 10 ppm Hg(II) and Bi(III) concentrations: (a) 100 ppb, (b) 400 ppb, (c) 600 ppb, (d) 800 ppb. Other working conditions as Figure 3.1.90

Figure 3.4: Square-wave stripping voltammograms of 20 ppb Zn(II), Cd(II) and Pb(II) using Glassy Carbon Electrode in acetate buffer solution (0.1 M, pH 4.5) containing 600 ppb Bi(III) and Hg(II) concentrations: (a) 1 ppm, (b) 5 ppm, (c) 10 ppm, (d) 15 ppm. Other working conditions as Figure 3.1.91

Figure 3.5: Square wave stripping voltammograms of Zn(II), Cd(II) and Pb(II) at Glassy Carbon Electrode (GCE) in presence of 600 ppb Bi(III) and 10 ppm Hg(II) in acetate buffer solution (0.1 M, pH 4.5); Amplitude, 40 mV; Frequency, 80 Hz; Potential increment, 6 mV; Accumulation time, 2.0

min at -1.4 V. For Zn(II), Cd(II) and Pb(II) concentrations: (a) 0.0, (b) 10 ppb, (c) 20 ppb, (d) 30 ppb, (e) 40 ppb, (f) 50 ppb.93

Figure 3.6: Square wave stripping voltammograms of Zn(II), Cd(II) and Pb(II) at Carbon Paste Electrode (CPE) in presence of 600 ppb Bi(III) and 10 ppm Hg(II) in acetate buffer solution (0.1 M, pH 4.5); Amplitude, 40 mV; Frequency, 80 Hz; Potential increment, 6 mV; accumulation time, 2.0 min at -1.4 V. For Zn(II), Cd(II) and Pb(II) concentrations: (a) 0.0, (b) 20 ppb, (c) 40 ppb, (d) 60 ppb.....94

Figure 3.7: Square-wave stripping voltammograms of Zn(II), Cd(II) and Pb(II) at Graphite Pencil Electrode (GPE) in presence of 600 ppb Bi(III) and 10 ppm Hg (II) in acetate buffer solution (0.1 M, pH 4.5); Amplitude, 40 mV; Frequency, 80 Hz; Potential increment, 6 mV; Accumulation time, 2.0 min at -1.4 V. For Zn(II), Cd(II) and Pb(II) concentrations: (a) 0.0, (b) 20 ppb, (c) 40 ppb, (d) 60 ppb.95

Figure 3.8: Square-wave stripping voltammograms of Zn(II), Cd(II) and Pb(II) at Glassy Carbon Paste Electrode (GCPE) in presence of 600 ppb Bi(III) and 10 ppm Hg (II) in acetate buffer solution (0.1 M, pH 4.5); Amplitude, 40 mV; Frequency, 80 Hz; Potential increment, 6 mV; Accumulation time, 2.0 min at -1.4 V. For Zn(II), Cd(II) and Pb(II) concentrations: (a) 0.0, (b) 20 ppb, (c) 40 ppb, (d) 60 ppb.96

Figure 3.9: Square-wave stripping voltammograms of Zn(II), Cd(II) and Pb(II) at Carbon Nanotubes Paste Electrode (CNTPE) in presence of 600 ppb Bi(III) and 10 ppm Hg (II) in acetate buffer solution (0.1 M, pH 4.5); Amplitude, 40 mV; Frequency, 80 Hz; Potential increment, 6 mV; Accumulation time, 2.0 min at -1.4 V. For Zn(II), Cd(II) and Pb(II) concentrations: (a) 0.0, (b) 20 ppb, (c) 40 ppb, (d) 60 ppb.....97

Figure 3.10: Square-wave stripping voltammograms of 20 ppb Zn(II), Cd(II) and Pb(II) at: (a) Bare GCE, (b) CNT/DMF-GCE and (c) CNT/Nafion-GCE. in acetate buffer solution (0.1 M, pH 4.5); Frequency, 80 Hz; Amplitude, 40 mV; Potential increment, 6 mV; Accumulation time 2.0 min at -1.4 V.98

Figure 3.11: (A) Square-wave stripping voltammograms of 20 ppb of Zn(II), Cd(II) and Pb(II) heavy metals at GCE in the presence of 600 ppb Bi(III) and 10 ppm Hg(II), in acetate buffer solution (0.1M) at different pH values: (a) pH 3.5, (b) pH 4.0, (c) pH 4.5, (d) pH 5.0; Amplitude, 40 mV; Frequency, 80 Hz; Potential increment, 6 mV; Accumulation time, 2.0 min at -1.4V. (B) The corresponding plot..... 100

Figure 3.12: (A) Square-wave stripping voltammograms of 40 ppb of Zn(II), Cd(II) and Pb(II) heavy metals at GCE in the presence of 600 ppb Bi(III) and 10 ppm Hg(II), in acetate buffer solution (0.1M) at different pH values: (a) pH 3.5, (b) pH 4.0, (c) pH 4.5, (d) pH 5.0; Amplitude, 40 mV; Frequency,

80 Hz; Potential increment, 6 mV; Accumulation time, 2.0 min at -1.4V.

(B) The corresponding plot..... 101

Figure 3.13: (A) Square-wave stripping voltammograms of 20 ppb Zn(II), Cd(II) and Pb(II) at GCE in presence of 600 ppb Bi(III) and 10 ppm Hg(II), in acetate buffer solution (0.1 M, pH 4.5); Accumulation time, 2.0 min at -1.4V; Amplitude, 40 mV; Potential increment, 6 mV; Frequency: (a) 10 Hz, (b) 20 Hz, (c) 30 Hz, (d) 40 Hz, (e) 50 Hz, (f) 60 Hz, (g) 70 Hz, (h) 80 Hz, (i) 90 Hz. (B) The corresponding plot..... 104

Figure 3.14: (A) Square-wave stripping voltammograms of 20 ppb Zn(II), Cd(II) and Pb(II) at GCE in presence of 600 ppb Bi(III) and 10 ppm Hg(II), in acetate buffer solution (0.1 M, pH 4.5); Accumulation time, 2.0 min at -1.4 V; Accumulation time, 2.0 min at -1.4V; Potential increment, 5 mV; Frequency, 25 Hz; Amplitude: (a) 20 mV, (b) 30 mV, (c) 40 mV, (d) 50 mV, (e) 60 mV. (B) The corresponding plot..... 105

Figure 3.15: (A) Square-wave stripping voltammograms of 20 ppb Zn(II), Cd(II) and Pb(II) at GCE in presence of 600 ppb Bi(III) and 10 ppm Hg(II) in acetate buffer solution (0.1 M, pH 4.5); Accumulation time, 2.0 min at -1.4V; Frequency, 25 Hz; Amplitude, 40 mV; Potential increment: (a) 1 mV, (b) 2 mV, (c) 3 mV, (d) 4 mV, (e) 5 mV, (f) 6 mV, (g) 7 mV, (h) 8 mV. (B) The corresponding plot..... 106

Figure 3.16: (A) Square-wave stripping voltammograms of 20 ppb Zn(II), Cd(II) and Pb(II) at GCE in presence of 600 ppb Bi(III) and 10 ppm Hg(II), in acetate buffer solution (0.1 M, pH 4.5). Amplitude 40 mV; Frequency, 80 Hz; Potential increment, 6 mV; Accumulation time, 2.0 min at: (a) -1.2 V, (b) -1.3 V, (c) -1.4 V, (d) -1.5 V. (B) The corresponding plot. 107

Figure 3.17: (A) Square-wave stripping voltammograms of 20 ppb Zn(II), Cd(II) and Pb(II) at GCE in presence of 600 ppb Bi(III) and 10 ppm Hg (II), in acetate buffer solution (0.1 M, pH 4.5); Amplitude, 40 mV; Frequency, 80 Hz; Potential increment, 6 mV; Accumulation Time at potential - 1.4 V for: (a) 60 Sec, (b) 120 Sec, (c) 180 Sec, (d) 240 Sec, (e) 300 Sec, (f) 360 Sec, (g) 420 Sec, (h) 480 Sec, (i) 540 Sec, (j) 600 Sec and (k) 660 Sec. (B) The corresponding plot. 108

Figure 3.18: (A) Square-wave stripping voltammograms for 20 ppb Zn(II), Cd(II) and Pb(II) at GCE in presence of 600 ppb Bi(III) and 10 ppm Hg(II) in acetate buffer solution (0.1 M, pH 4.5); Amplitude 40 mV; Frequency, 80 Hz; Potential increment, 6 mV; Accumulation time, 2.0 min at -1.4 V. (B) The corresponding histogram showing the degree of reproducibility. . 109

Figure 3.19: (A) Square-wave stripping voltammograms of 40 ppb Zn(II), Cd(II) and Pb(II) at GCE in presence of 600 ppb Bi(III) and 10 ppm Hg(II) in acetate buffer solution (0.1 M, pH 4.5); Amplitude 40 mV; Frequency, 80 Hz; Potential increment, 6 mV; Accumulation time, 2.0 min at -1.4 V. (B) The corresponding histogram showing the degree of reproducibility. . 110

Figure 3.20A: Square-wave stripping voltammograms of Zn(II), Cd(II) and Pb(II) at GCE in presence of 600 ppb Bi(III) and 10 ppm Hg(II) in acetate buffer solution (0.1 M, pH 4.5); Amplitude, 40 mV; Frequency, 80 Hz; Potential increment, 6 mV; Accumulation time, 2.0 min at -1.4 V. A mixture of Zn(II), Cd(II) and Pb(II) concentrations: (a) 0.0, (b) 1, (c) 3, (d) 5, (e) 10, (f) 15, (g) 20, (h) 25, (i) 30, (j) 35, (k) 40, (l) 45, and (m) 50 ppb. 112

Figure 3.20B: The corresponding calibration plots of Figure 3.20A 113

Figure 3.21: Effect of Cu(II) concentrations on the simultaneous determination of the 40 ppb Zn(II), Cd(II) and Pb(II) mixture at GCE in presence of 600 ppb Bi(III) and 10 ppm Hg(II) in acetate buffer solution (0.1 M, pH 4.5); Amplitude, 40 mV; Frequency, 80 Hz; Potential increment, 6 mV; Accumulation time, 2.0 min at -1.4 V. The Cu(II) concentrations: (a) 0.0 ppm, (b) 1.0 ppm, (c) 2.0 ppm, (d) 3.0 ppm. 115

Figure 3.22: Effect of Fe(III) concentrations on the simultaneous determination of the 40 ppb Zn(II), Cd(II) and Pb(II) mixture at GCE in presence of 600 ppb Bi(III) and 10 ppm Hg(II) in acetate buffer solution (0.1 M, pH 4.5). Amplitude 40 mV; Frequency, 80 Hz; Potential increment, 6 mV; Accumulation time, 2.0 min at -1.4 V. The Fe(III) concentrations: (a) 0.0 ppm, (b) 1.0 ppm, (c) 2.0 ppm, (d) 3.0 ppm. 116

Figure 3.23: Effect of Ni(II) concentration on the simultaneous determination of the 40 ppb Zn(II), Cd(II) and Pb(II) mixture at GCE in presence of 600 ppb

**Bi(III) and 10 ppm Hg(II) in acetate buffer solution (0.1 M, pH 4.5);
Amplitude, 40 mV; Frequency, 80 Hz; Potential increment, 6 mV;
Accumulation time, 2.0 min at -1.4 V. The Ni(II) concentrations: (a) 0.0
ppm, (b) 1.0 ppm, (c) 2.0 ppm, (d) 3.0 ppm. 118**

**Figure 4.1: (A) The potentiostat, (B) The electrochemical, (C) The complete setup.
..... 122**

**Figure 4.2: Square wave stripping voltamograms at GCE-Bi modified electrode of
six (1- 6) different drinking water samples in acetate buffer solution (0.1
M, pH 3.5) with standard addition of different Zn(II), Cd(II) and Pb(II)
heavy metals concentration: (a) water sample, (b) 2.0, (c) 4.0, (d) 6.0, (e)
8.0, (f) 10.0 ppb. Other working conditions as in Figure 2.12A. 127**

**Figure 4.3: Square wave stripping voltamograms at GCE-Hg modified electrode of
six (1- 6) different drinking water samples in acetate buffer solution (0.1
M, pH 3.5) with standard addition of different Zn(II), Cd(II) and Pb(II)
heavy metals concentration: (a) water sample, (b) 2.0, (c) 4.0, (d) 6.0, (e)
8.0, (f) 10.0 ppb. Other working conditions as in Figure 2.23A. 128**

**Figure 4.4: Square wave stripping voltamograms at GCE-Bi/Hg alloy modified
electrode of six (1- 6) different drinking water samples in acetate buffer
solution (0.1 M, pH 4.5) with standard addition of different Zn(II), Cd(II)
and Pb(II) heavy metals concentration: (a) water sample, (b) 2.0, (c) 4.0,**

(d) 6.0, (e) 8.0, (f) 10.0 ppb. Other working conditions as in Figure 3.20A.

..... **129**

List of Tables

Table 1.1: Limit values (according to WHO, EPA, and EU) (1).....	2
Table 2.1: Limits of Detection and Quantification Obtained at GC-Hg(II) electrode.	83
Table 3.1: Limits of Detection and Quantification Obtained at GC-Hg(II)/Bi(III) alloy electrode.	114
Table 3.2A: Influence of Several Organic Compounds.	119
Table 3.2B: Influence of Several Organic Compounds.	120
Table 4.1: Locations of the Collected Water Samples.....	124
Table 4.2: Concentration Values of the Analyzed Water Samples.	130

THESIS ABSTRACT (ENGLISH)

Name: Abdullah Ali Al-Aliwi

Title: Field Deployable Electrochemical Sensors for Simultaneous Determination of Cd, Pb and Zn Heavy Metals in Drinking Water

Major Field: Chemistry

Date of Degree: June 2012

This study seeks the development and characterization of new electrochemical sensors for on field monitoring of inorganic contaminants (particularly Cadmium, Lead and Zinc) in drinking water. Among the various trace metal techniques, electrochemical stripping analysis is the most likely candidate to meet the requirements of on field metal analysis. Despite of intensive research efforts and growing concerns on the use of mercury, fortunately a ‘non-mercury’ stripping electrode, truly competitive to mercury ones, has recently emerged. The successful analytical utility of bismuth-coated electrodes depends upon understanding their fundamental behavior. The proposed research aims at gaining such insights into the behavior of the bismuth and mercury-bismuth alloy stripping electrodes, and for using the new knowledge for optimizing the preparation and operation of the bismuth-based heavy metals-sensing devices. We have critically assessed the analytical ‘figure-of-merit’ of the ‘mercury’, ‘mercury-bismuth’ and ‘mercury-free’ stripping sensors. The effort would lead to the emergence of the use of reliable alternative ‘non-mercury’ sensing electrodes that would have a major impact upon the monitoring of heavy metals in drinking water within the Eastern area of Saudi Arabia, and thus on the management of drinking water supplies. It shed some light on the quality of waters in the Eastern area of Saudi Arabia in general and in Dhahran vicinity in particular. Such monitoring offers a rapid return of the chemical information while minimizing errors and costs associated with tedious conventional lab-based analyses.

Master of Science Degree

King Fahd University of Petroleum and Minerals

Dhahran – Saudi Arabia

THESIS ABSTRACT (ARABIC)

الاسم : عبدالله علي العليوي

عنوان الرسالة : حساسات كهروكيميائية قابلة للتطبيق المتزامن للعناصر الثقيلة الكاديوم والرصاص والزنك في مياه الشرب .

التخصص: كيمياء

تاريخ التخرج : يونيو 2012

لقد تمت دراسة السلوك الكشطي الكهروكيميائي للملوثات غير العضوية مثل العناصر الثقيلة الكاديوم والرصاص والزنك في مياه الشرب علي أسطح أقطاب الكربون المختلفة. وقد تم تطوير طريقة كهروكيميائية بسيطة وحساسة لقياس التراكيز المنخفضة من هذه الملوثات غير العضوية علي أسطح أقطاب الكربون باستخدام تقنية الفولتامترية الكشطية رباعية الموجة (Square Wave Stripping Voltammetry) ثم تم مقارنتها مع عدة تقنيات أخرى.

وقد تم دراسة مختلف العوامل المؤثرة علي تقدير تراكيز هذه العناصر بصورة دقيقة علي أسطح أقطاب الكربون التالية : قطب عجينة الكربون الفحمي وقطب الكربون الزجاجي وقطب الكربون الفحمي وتم مقارنة نتائج الطرق التقليديه بنتائج الطريقة الحديثة المطورة.

وقد تم أيضاً دراسة وتحديد أفضل الشروط لكل من هذه الطرق السابقة . ثم تم نقل هذه الطريقة لعمل التحليل في الميدان عوضاً عن المعمل . ثم تم مقارنة النتائج لهذه الطريقة مع طريقة (ICP-MS).

درجة الماجستير في العلوم

جامعة الملك فهد للبترول والمعادن

الظهران – السعوديه

CHAPTER 1

1.0 INTRODUCTION AND LITERATURE REVIEW

Knowledge of the concentration of free metal in drinking water is essential to understand the role of human health. Heavy metals contamination of drinking water is a major global problem. Acute lead poisoning in children can cause anorexia, vomiting, malaise, convulsions and even permanent brain damage. Chronic lead poisoning can cause weight loss, weakness and anemia. Lead can leach into water from either solder used to join copper pipes or from lead pipes in older buildings. Other sources of lead are paints in older buildings, dust/soil contaminated with tetraethyl-lead (formerly a gasoline additive) and also industrial and household waste discharges, whether it was directly or indirectly through leakages in sewage systems into water sources can cause excessive pollution in surface and underground water. Water quality also changes in relation to the properties of physical, chemical and biological components of water.

Investigations of toxic heavy metals such as Pb, Cd, Cu, Zn and Cr place special importance on environmental samples. Thus, there is a pressing need to develop trace element analysis techniques that allow separation of different element species prior to trace element analysis.

The allowed concentrations of several heavy metals are shown in Table 1.1 according to WHO, EPA and EU (1).

Table 1.1: Limit values (according to WHO, EPA, and EU) (1).

Heavy Metal	WHO (mg/L)	EPA (mg/L)	EU (mg/L)
Cd	0.003	0.005	0.005
Pb	0.01	0.015	0.01
Zn	3.0	5.0	Not Mentioned

1.1 FIELD DEPLOYABLE ELECTROCHEMICAL SENSORS

Electrochemistry can play a huge role in protecting the environment. Electrochemical sensors and detectors are very attractive for on-site monitoring of priority pollutants, as well as for addressing other environmental needs, this because of its sensitivity and selectivity toward electro-active species (2).

The pH meter can be a good example that has been used for along time in environmental analysis. In the recent days electrochemical sensors expand the scope of these devices to detect a wide range of organic and inorganic contaminant. These advances include the introduction of modified or ultra modified microelectrodes, the modification of carbon screen-printed electrodes, the design of highly selective chemical or biological recognition layers and developments in the areas of computerized instrumentation and flow detectors (2-4). Many field deployable electrochemical sensors have been introduced and discussed in details.

In 2002 Joachim P. Kloock introduced a micro fabricated potentiometric thin-film sensor array to detect lead, cadmium and zinc simultaneously. The thin film is made in the basis of chalcogenide glass material which consist of several elements and been prepared by pulsed laser deposition technique. This array is compact and can be used at field to the targeted elements (5, 6).

Palmsens introduced an electrochemical sensor interface for heavy metal determination in liquid medium for on field detection. This device can be used with several techniques such as SWV, NPV, LSV and CV (6, 7).

The Centre for Environmental Engineering and Sustainable Energy at School of Engineering department in the Robert Gordon University also have developed 3-electrode-sets (counter, reference and working electrode) screen printed on different substrates (glass, polycarbonate and alumina) for analysis of heavy metals in the marine environment (Figure 1.1), part of their project is the investigating and the development of a multi-capability optical sensors for the real-time onsite monitoring of three key marine environmental and offshore/oil parameters: hydrocarbons, synthetic based fluids and heavy metals (6).



Figure 1.1: Screen printed electrode sensor (6).

X. Poteau and others from Dublin City University, Ireland developed sensor system for real-time and on site sensing of heavy metal ions in water, screening either for a selected metal ion or as a general pollution warning detection of metals (6, 8).

In Italy an on-site reliable concentration measurements of various fractions of trace elements has been developed by using a voltammetric method. The device consists of a voltammetric analyzer module, a mini-flow injection module, an optional multi-parameter probe and reagent/waste containers integrated in a case (9).

In principal we need the electrochemical sensor to give us reliable real-time information that represents the surrounding environment. In the best case the information are taken continuously and without upsetting the rest of the sample. Usually this device consist of the electrochemical sensor covered with suitable layer for detecting the contaminant and a detector that collect the information gathered by the electrical interaction between the targeted analyte and the recognition layer. Mainly there are two types of electrical interaction, the amperometric sensors and the potentiometric sensors.

In the amperometric sensors the signal transduction process is accomplished by controlling the potential of the working electrode at a fixed value (relative to a reference electrode) and monitoring the current as a function of time. Where in voltammetry scanning the potential is the driving force for the oxidation or reduction of the electroactive species, and the resulting current measures directly the rate of the electron transfer reaction which is directly proportional to the concentration of the targeted analyte.

The Potentiometric sensors are where the observed electrical signal is the potential which is proportional (in a logarithmic fashion) to the concentration. This method demands an ion selective electrode which contains a preselective membrane that gives a

signal due to the concentration changes of the targeted analyte (5, 10-13).

Several types of selective electrodes can be used in the field detection, such as electrochemical biosensors, metal based electrodes, modified and ultra modified microelectrodes, and ion and gas selective electrodes.

In order to recognize the biological compounds we need to develop a highly selective biosensing device, because of its high specific formula properties.

Electrochemical biosensors hold a leading position among the bioprobes currently available and hold great promise for the task of environmental monitoring (2). Those types of sensors consist of a biological entity that recognizes the target analyte and the electrode transducer that translates the bio-recognition event into a useful electrical signal (Figure 1.2).

In the biosensing approach the biocompounds are immobilized at the surface of the amperometric or potentiometric electrode. The biocompounds could be enzymes, antibodies, receptors or whole cells (14-16).

The Enzyme electrodes are usually prepared by attaching an enzyme layer to the electrode surface. Amperometric enzyme electrodes monitor changes occurring as a result of the biocatalytic reaction which is either generation or consumption of electroactive species. A large number of hydrogen-peroxide generating oxidases and NAD^+ dependent dehydrogenases have been particularly useful for the measurement of a wide range of substrates which can be detected at moderate potential. Lowering the potential is favorable to avoid the interferences from other electroactive species. Potentiometric enzyme electrodes use ion- or gas-selective electrode transducers, that allow us to determine the contaminant whose biocatalytic reaction results in local pH changes or the formation or consumption of ions or gas. The resulting potential signal depends on the

logarithm of the substrate concentration.

A long term stability of the electrode can be achieved by improving the immobilization of the enzyme layer and use thermophilic enzymes, which are useful in the on-field application. Several enzyme electrodes have already proven useful for the task of environmental monitoring, for example, several groups reported on highly sensitive amperometric biosensors for phenolic compounds and single-use on-site sensing (17-23).

In addition to substrate monitoring, it is possible to employ enzyme electrodes for measuring various toxins (via the perturbation/modulation of the enzyme activity) for example the inhibition of enzymes such as biosensors for cyanide, toxic metals and organophosphates and carbamates pesticides (24-26).

While conventional electrodes are mainly used for carrying electrical current, chemical layers can add higher degree of selectivity. The chemical layer is plated on the surface of the bare electrode by either immobilizing the reagent on it that will led to change the chemical and physical characteristics of the surface or by inclusion of the reagent with the matrix of the electrode.

The new “mercury-free” surfaces address also growing concerns associated with field applications of the classical mercury drop electrode. Adding the chemical layer to the bare electrode can be achieved in two ways either by pre treatment, that is by applying potential to the electrode in the reagent solution and then use it with the analyte or by reducing the reagent along with the analyte by a step called preconcentration, that offers high sensitivity because of the preconcentration procedure. A second major advantage lies in the added dimension of selectivity, which is provided by the chemical requirement of the modifier-analyte interactions. This has been reported for nickel, mercury,

aluminumatdimethylglyoxine, crown-ether or alizarin containing carbon pastes (27-29). Another method has been reported for preparing the electrochemical electrode by covering the sensing surface with a thin film by different mechanism, based on the analyte size, charge and polarity, the electrode selectivity can be enhanced toward specific substrate (30-31).

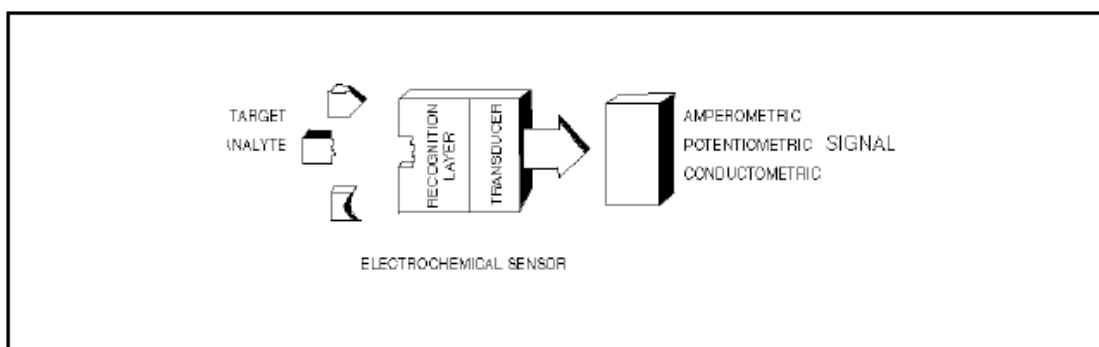


Figure 1.2: Electrochemical biosensors (Biorecognition and transduction).

The stripping based sensors are considered the most sensitive electrochemical technique due to the preconcentration step, in which trace metals are accumulated onto the working electrode. This step is usually followed by the stripping step, in which the metals are stripped away from the electrode during an appropriate potential scan. Stripping analysis gives us a view of the total metal content in the sample, as well as characterization of its chemical form (e.g. oxidation state, labile fraction, etc.) (32).

Several advances in stripping analysis are enhanced the on-site monitoring realization such as automated flow systems for continuous on-line monitoring (33-35), disposable screen-printed stripping electrodes for single-use field applications (36), or remote/submersible devices for down-hole well monitoring or unattended operation (37-38). Portable and compact (hand-held), battery-operated stripping analyzers are currently being commercialized for controlling these field-deployable devices. Adding the remarkable sensitivity of the stripping along with the on site detection, the in-situ devices can minimize the errors due to the low contamination possibility while transporting the sample to the central laboratory.

On the other hand, ion selective electrodes offer direct and selective detection of ionic activities in water samples. They are simple, inexpensive and compatible with the on-line analysis. The sensitivity of such devices is attributed to the selective interaction between the targeted analyte and the membrane material.

There are mainly three types of ion selective electrodes; glass, solid and liquid electrodes. A good example of such electrodes is the pH electrode, which has been used for environmental pH measurements for several decades. New technologies of thin film (dry-reagent) slides or semiconductor chips will certainly facilitate field monitoring of

ionic analyte (39). Gaseous pollutant also can be detected by highly selective gas sensing electrodes. This electrode consists of an ion selective electrode surrounded by an electrolyte solution and enclosed by a gas permeable membrane. By diffusing the gas through the membrane and reacts with the internal electrolyte, detectable electroactive species are consumed or formed.

The electrochemical signal is formed via a process carried away at the surface of the electrode. Therefore the properties of the surface have the main effect on the signal. Because of that a big effort has been focused on the modification on the electrode surface.

The carbon based electrodes gained lots of attention as a substitute of the toxic mercury electrode. The carbon material electrodes are favored because they depend on the carbon material where the electrical conduction between the metal and the semiconductor can vary so a wide range of potential capacitive, adsorption, catalytic and kinetic properties can be achieved (43). Also the carbon can form covalent bonds with some surface modifiers favoring the development of modified electrodes. The carbon electrode is also chemically inert over a wide range of potential. All these features predetermine the use of diverse carbon materials in electroanalysis. Several carbon materials can be used such as glassy carbon, pyrolytic graphite, carbon glass-ceramics, impregnated graphite, carbon fibers, filaments, gauzes, and composite materials. Depending on the type of carbon and the method of using the electrodes, carbon-based electrodes are divided into glassy carbon (GCE), carbon paste (CPE), carbon-containing composite (CCE), impregnated graphite (IGE), thick-film graphite-containing (TFGE) electrodes, carbon microelectrodes (CME), and their arrays (ACME) (43). More types of the modified electrodes are mentioned in details in the later section.

Another type of the modification is by making a carbon screen-printed electrodes (3,

4). One of the main issues on using electrochemical methods on field is the complex setup of the electrode system. A very good way to make it simple and effective is to replace the conventional electrochemical cells by screen printed electrode (SPE) connected with a mini potentiostat and a computer. This will make it easier to convert to a hand-held field analyzers. Since the screen printed electrodes are relatively cheap and easy to handle they are commercially favorable. Several unmodified and modified carbon and metallic working electrode surfaces have been explored (44, 45). But the early work of Wang (46) led to the modification of carbon based electrodes especially glassy carbon along with bismuth which led to the replacement of mercury as an environmental friendly alternative. This breakthrough opened the window to investigate other electrode bases and types such as carbon fibers (47), carbon films (48), edge plane pyrolytic graphite (49) and a variety of modified carbon pastes (50, 51).

Exploring the screen printed carbon electrodes SPCE (18) led to the development of disposable home-use lead detection in water, others fabricated Bi preplated SPCE for simultaneous voltametric detection of Pb(II) and Cd(II) in waste water and soil (53, 54). Microelectronic Bi-film electrode preparations have been also explored (55, 56). Chuanuwatanakul et al. (57) have described a stopped flow system for Zn(II), Cd(II) and Pb(II) in water samples using in situ deposition of Bi film. Recently Rico, and others described the simultaneous determination of the same elements at a novel cell design with improved stirred sample solution accumulation (3, 58).

1.2 SIMULTANEOUS DETERMINATION OF Zn(II), Cd(II) and Pb(II) IN DRINKING WATER

It is essential to know the concentration of heavy metals in water because of its toxicity and direct effect on the human health (40-42). Many different techniques have been introduced to detect heavy metals in different media, yet due to the low concentration of the heavy metals to be detected and the high cost of these analytical devices, the attention has been focused on the electro analytical techniques.

Among the analytical techniques used to determine heavy metals in environmental matrices are: Atomic Absorption Spectrometry (AAS), Inductively Coupled Plasma-Atomic Emission Spectrometry (ICP/AES), Inductively Coupled Plasma-Mass Spectrometry (ICP/MS), Neutron Activation Analysis (NAA), X-ray Fluorescence (XRF), Ion Chromatography (IC) and Electroanalytical technique such as (SWV).

Atomic Absorption Spectrometry (AAS) is an analytical technique that can analyze the concentration of over 62 different metals simultaneously in a solution with high sensitivity. The technique uses the wavelengths of light specifically absorbed by elements. Since each element absorbs characteristic wavelength of light, quantitative analysis could be achieved by measuring the absorbance of solutions with known concentration, draw a calibration curve, and then predict the unknown concentration of that metal (71).

Inductively Coupled Plasma (ICP) is a technique in which both the radio frequency-generated and maintained plasma atomize and ionize the elements in the sample and excite the electrons as well. When the electrons return to the ground state they emit energy in a specific wavelength. The emitted light is focused by lens to the

spectrometer in the case of ICP-AES or throws a high vacuumed mass analyzer in the case of ICP-MS (69, 70).

X-ray Fluorescence is a technique using the X-ray from a tube to remove the electron from the inner shell of the atom. After that the electrons in higher shell will fill the position and expel the excess energy as an X-ray emission with wavelength specific for each element.

Between the above techniques the ICP-MS and the ICP-AES are the best for trace metals detection due to the low detection limit. But considering the high cost and big sized analyzer unit, other techniques should be considered.

1.3 DETECTION TECHNIQUES AND ELECTRODE SURFACES

1.3.1 Electroanalytical Techniques

In electroanalytical techniques we study the interplay between electricity and chemistry, namely the measurements of electrical quantities, such as current, potential, or charge, and their relationship to chemical parameters. Such use of electrical measurements for analytical purposes has found a vast range of applications, including environmental measurements (59), industrial quality control (60), and biomedical analysis (61). They have many advantages such as high sensitivity, good selectivity, rapid response, low cost and simplicity.

There are several electroanalytical techniques such as amperometry, polarography and voltammetry. The voltammetry is considered to be one of the most useful branches of electrochemistry. There are several advantages of the voltammetric techniques such as high sensitivity with a very large useful linear concentration range for both inorganic and organic species, a large number of useful solvents and electrolytes, a wide range of temperatures, rapid analysis times (seconds), simultaneous determination of several analytes, the ability to determine kinetic and mechanistic parameters, a well-developed theory and thus the ability to reasonably estimate the values of unknown parameters, and the ease with which different potential waveforms can be generated and small currents are measured.

1.3.1.1 Cyclic Voltammetry (CV)

Cyclic voltammetry is mainly used for qualitative analysis and usually performed in any electroanalytical studies. It gives clear information about kinetic and thermodynamic of redox processes, electron transfer reactions and adsorption processes. It rapidly provides location potentials of electroactive species (62). Cyclic voltammetry consists of scanning linearly the potential of the working electrode using a triangular wave form, (Figure 1.3), and during the potential sweep the potentiostat measures the resulting current. Single or multiple cycles can be used depending on the information sought. Cyclic voltammogram can be divided into three types; reversible (Figure 1.4), quasi reversible, and irreversible. The characteristic peaks in the cyclic voltammogram are caused by the formation of the diffusion layer near the electrode surface (63).

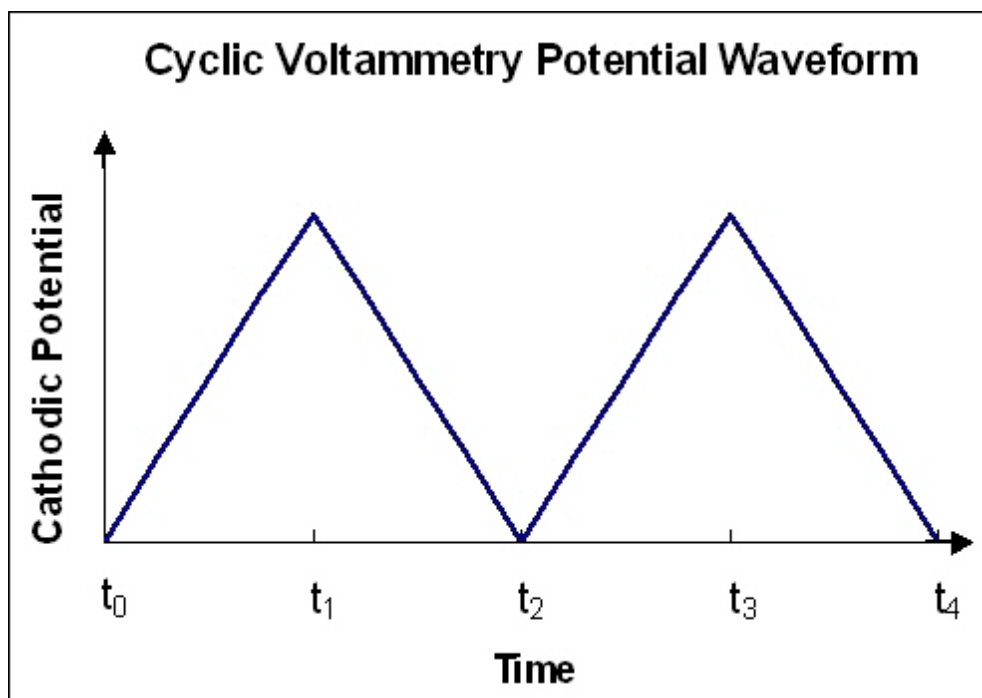


Figure 1.3: Potential-time excitation signal in cyclic voltammetric experiment (64).

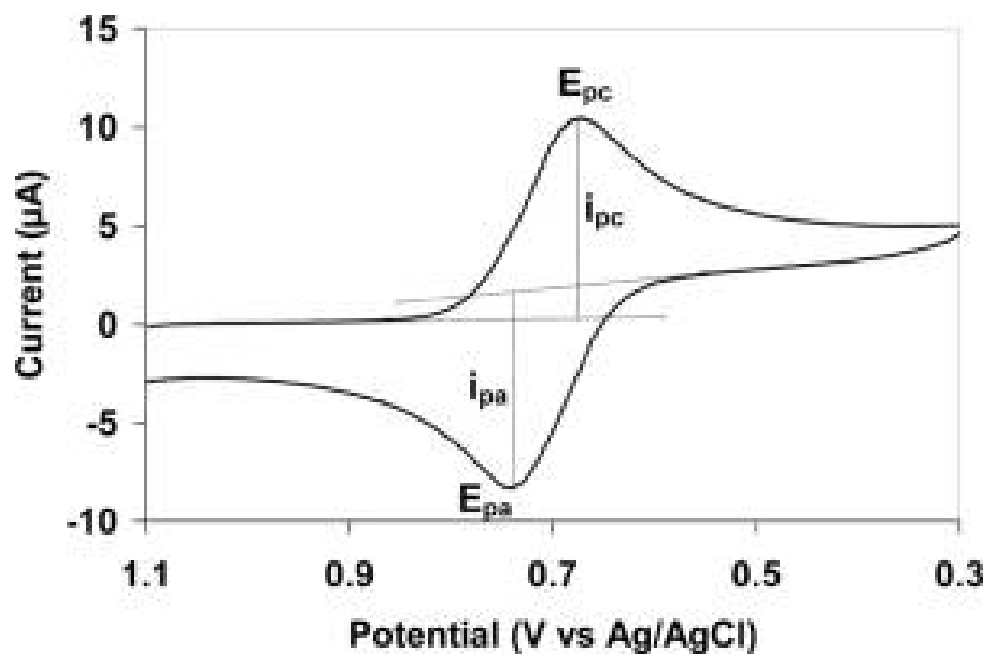


Figure 1.4: Typical cyclic voltammogram, where i_{pc} and i_{pa} show the peak cathodic and anodic current respectively for a reversible reaction (64).

1.3.1.2 Normal Pulse Voltammetry (NPV)

This technique uses a series of potential pulses of increasing amplitude (Figure 1.5). At the end of each pulse the measurement is taken that will give the charging current time to decay (65).

1.3.1.3 Differential Pulse Voltammetry (DPV)

This technique is similar to normal pulse voltammetry because in both of them we use pulses. The potential pulse is fixed in NPV, yet it is not in DPV as shown in Figure 1.6. Current is measured at two points for each pulse, the first point just before the application of the pulse and the second at the end of the pulse. These sampling points are selected to allow for the decay of the non-faradic (charging) current. The difference between current measurements at these points for each pulse is determined and plotted against the base potential (65). The height of the current peaks is proportional to the concentration of the corresponding analytes (64).

1.3.1.4 Square Wave Voltammetry (SWV)

In order to increase speed and sensitivity, many forms of potential modulation (other than just a simple staircase ramp) are developed. Square wave voltammetry is a pulse voltammetric technique in which a waveform composed of a symmetrical square wave is applied on the working electrode (65). The current is measured at the end of the

forward pulse and at the end of the reverse pulse (Figure 1.7). Many advantages for square wave voltammetry such as high speed and very low detection limit near 1×10^{-8} M can be achieved. From the rapid scanning capability and the reversal nature of the square wave voltammetry, kinetic studies can be undertaken. As a comparison between square wave and differential pulse voltammetry for reversible and irreversible cases, results indicate that the square wave currents are higher than the differential pulse response with 4 and 3.3 times respectively (60).

1.3.1.5 Linear Sweep Voltammetry (LSV)

Linear Sweep Voltammetry is a voltammetric method where the current at a working electrode is measured while the potential between the working electrode and a reference electrode is swept linearly in time (63). Oxidation or reduction of species is registered as a peak or trough in the current signal at the potential at which the species begins to be oxidized or reduced (Figure 1.8).

1.3.1.6 Preconcentration and Stripping Techniques

The preconcentration technique is a remarkable way to get the lowest detection limit of detection of any of the commonly used electroanalytical techniques. Any type of preconcentration will mainly consist of two steps. First, the analyte species in the sample solution is concentrated onto a working electrode. It is this crucial preconcentration step that results in the exceptional sensitivity that can be achieved. During the second step, the

preconcentrated analyte is measured or stripped from the electrode by the application of a potential scan. Stripping voltammetry is a very sensitive technique for trace analysis. As with any quantitative technique, care must be taken so that reproducible results are obtainable. Important conditions that should be held constant include the electrode surface, rate of stirring, and deposition time. Every effort should be made to minimize contamination.

Anodic stripping voltammetry (ASV) is the most widely used form of stripping analysis (67). This is attributed to the fast response and low detection limit. This low detection limit is coupled with the ability to determine simultaneously four to six trace metals using relatively inexpensive instrumentation (65). It is usually done by using a mercury electrode either by using a thin layer or a hanging mercury drop. The metal ions are concentrated at the surface of the mercury electrode by applying a negative potential for a sufficient time (accumulation time) which will force the metals to form amalgam with mercury. These amalgamated metals are then stripped (oxidized) out of the mercury by scanning the applied potential in the positive direction. The resulting current is proportional to the concentration i_p and its position depends on the metal E_p .

Having more than one metal possibly could make complicated inter metallic compounds. Thus affects the position of the peaks or distort it. These problems can often be avoided by adjusting the deposition time or by changing the deposition potential.

The cathodic stripping voltammetry (CSV) is the mirror image of the anodic stripping. It is using appositve potential to deposit the analyte at the surface of the mercury and then scan the potential towards the negative direction to reduce the analyte. This method has been used to determine inorganic anions such as halides, selenide, and sulfide, and oxyanions such as MoO_4^{-2} and VO_3^{-1} . In addition, many organic compounds,

such as nucleic acid bases, also form insoluble mercury salts and may be determined by CSV (68).

Adsorptive stripping voltammetry (AdSV) is similar to anodic and cathodic stripping methods. The main difference is that the analyte is preconcentrated on the electrode surface by adsorption or by specific reactions at chemically modified electrodes rather than accumulation by electrolysis. This method is suitable for trace metals along with organic compounds that have surface active properties (68).

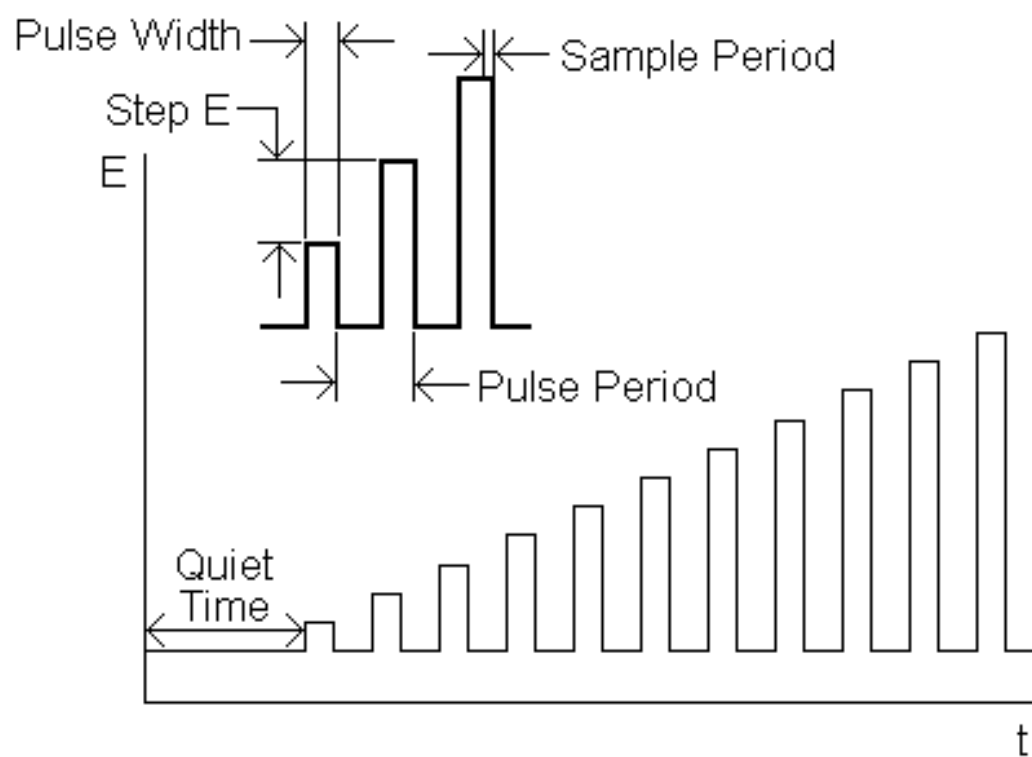


Figure 1.5: Normal pulse potential sweep (66).

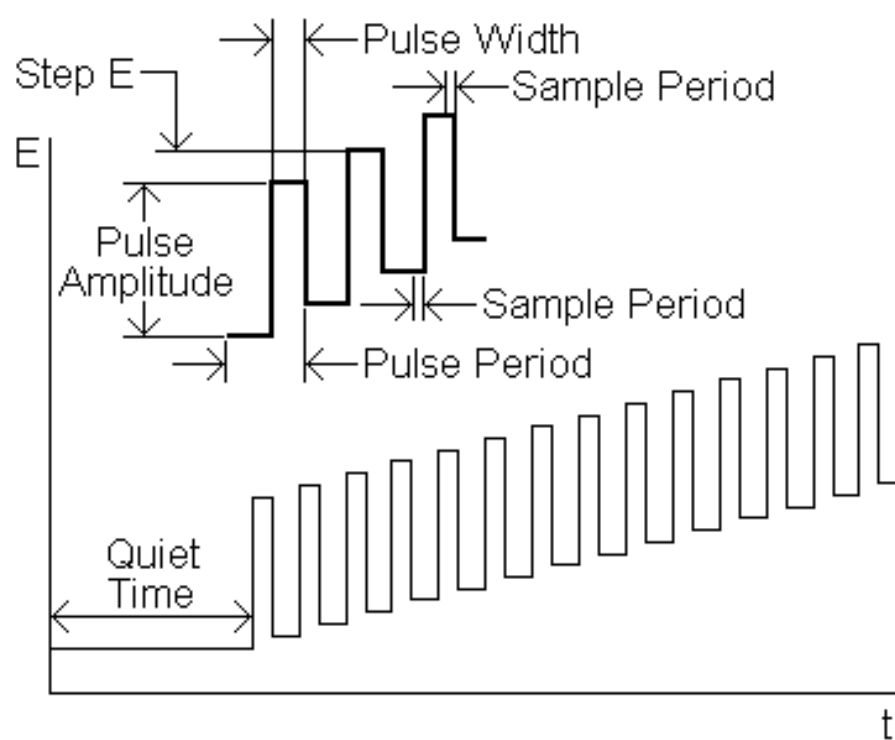


Figure 1.6: Differential pulse potential sweep (66).

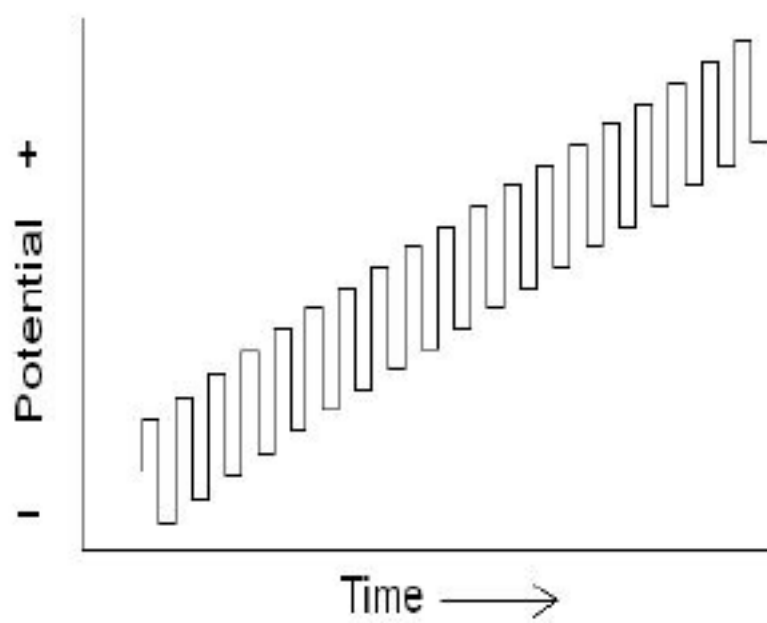


Figure 1.7: Square wave potential sweep (66).

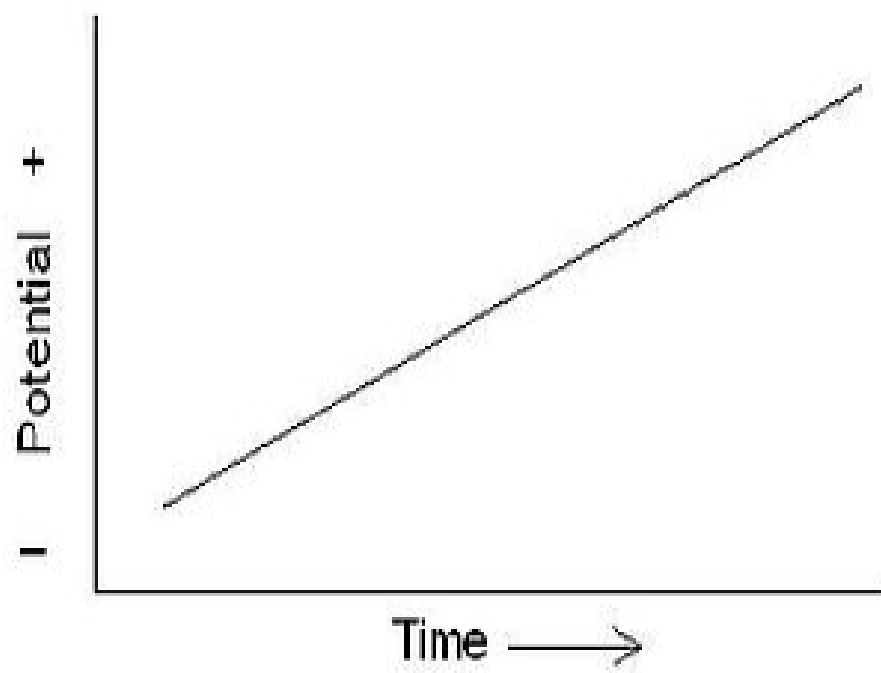


Figure 1.8: Linear potential sweep (63).

1.3.2 Other Techniques

1.3.2.1 Inductively Coupled Plasma- Mass Spectroscopy (ICP-MS)

Elemental determination can be achieved by Inductively Coupled Plasma Mass Spectrometry or ICP-MS. Which has been introduced commercially in 1983 (69), It has a very good detection limits for most elements, the ability to handle both simple and complex matrices and the ability to obtain isotopic information.

This device combines a high-temperature ICP (Inductively Coupled Plasma) source which will convert the atoms into ions (Figure 1.9), and a mass spectrometer which will separate the atoms.

The aerosol flows in the inner channel and the Argon gas flows inside the concentric channels of the ICP torch. The torch is surrounded by an RF load coil connected to a radio-frequency (RF) generator. This coil makes an electric and a magnetic field at the end of the torch. When a spark is applied to the argon flowing through the ICP torch, electrons are stripped off of the argon atoms forming argon ions. These ions will hit other argon atoms, forming an argon discharge or plasma. The sample is added to the aerosol flow which will carry it to the ICP torch and ionizes it then carry it to the end of the torch then to the mass spectra.

After the flow enters the mass spectrometer with a pressure of 1-2 torr it passes by vacuum region which will decrease the pressure into less than 1×10^{-5} torr. To prevent the ICP torch photons from entering the mass spectrometer a similar device is placed at the entrance of the MS called the shadow stop (Figure 1.10). The ions from the ICP source

are then focused by the electrostatic lenses in the system by electrostatic lens charged with a positive charge.

Once the ions enter the mass spectrometer, they are separated by their mass-to-charge ratio usually by a quadrupole filter (Figure 1.11). In a quadrupole mass filter, alternating AC and DC voltages are applied to opposite pairs of the rods. These voltages are then rapidly switched along with an RF-field. An electrostatic filter is established that only allows ions of a single mass-to-charge ratio (m/e) pass through the rods to the detector at a given instant in time. Typical quadrupole mass spectrometers used in ICP-MS have resolutions between 0.7 – 1.0 amu. Those ions after separation will strike the detector which translates the number of ions into an electrical signal that can be measured and related to the number of atoms of that element in the sample via the use of calibration standards (69).

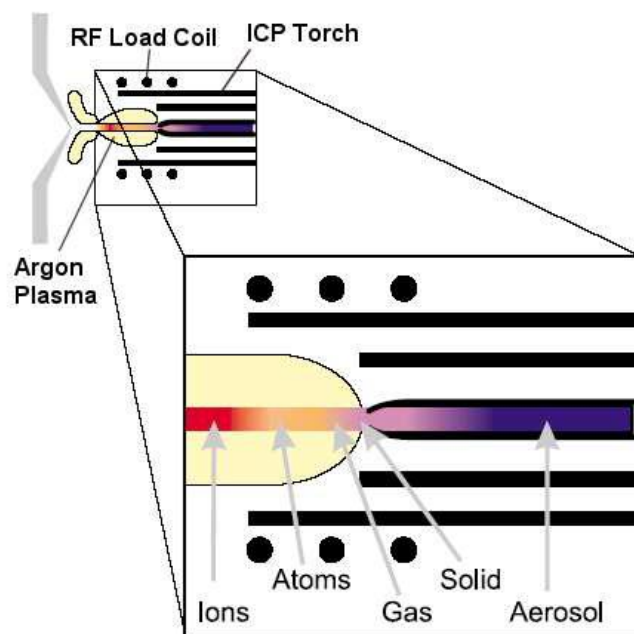


Figure 1.9: ICP source (50).

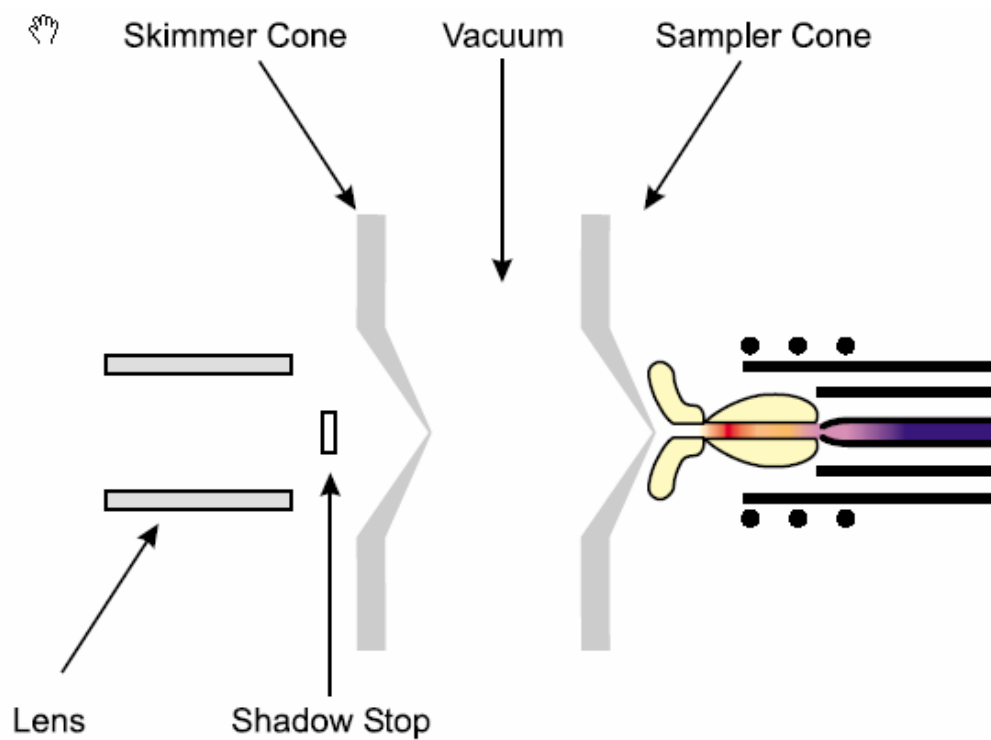


Figure 1.10: ICP - MS entrance (69).

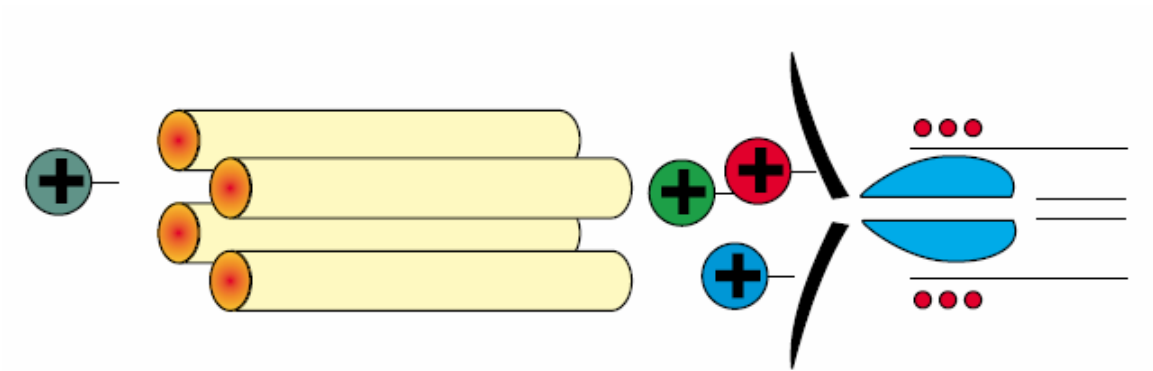
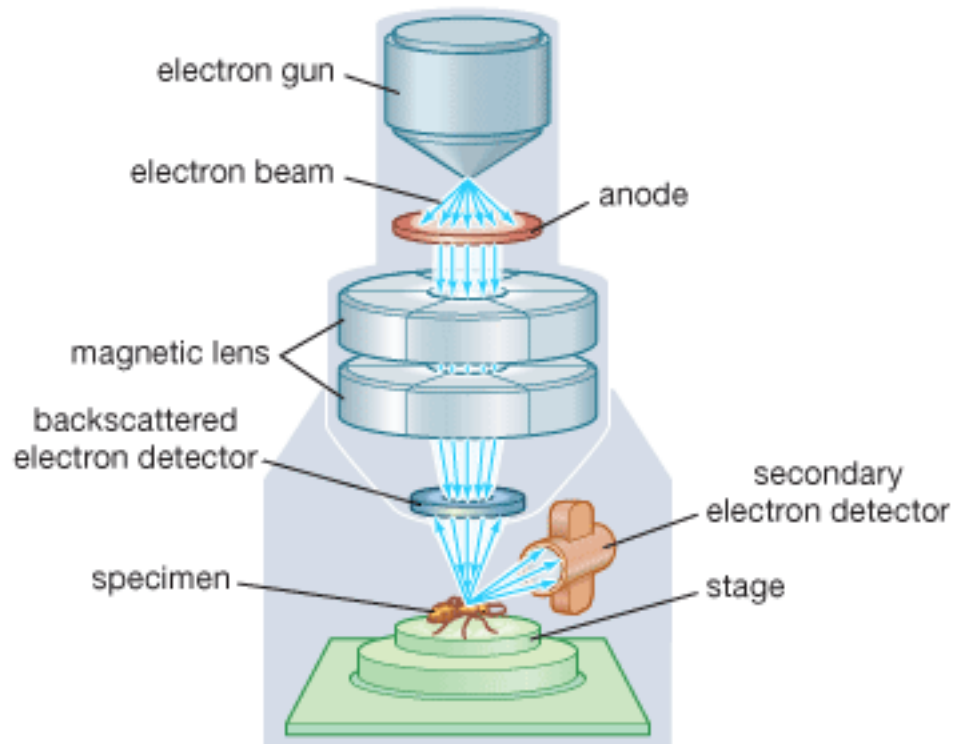


Figure 1.11: Mass spectrometry quadrupole filter (69).

1.3.2.2 Scanning Electron Microscopy (SEM)

In scanning electron microscopy (SEM) an electron beam is focused into a small probe and scanned across the surface of a specimen. Several interactions with the sample that result in the emission of electrons or photons as the electrons penetrate the surface. These emitted particles can be collected with the appropriate detector to yield valuable information about the material. The most immediate result of observation in the scanning electron microscopy is that the shape of the sample. Their resolution is determined by beam diameter (Figure 1.12).



© 2008 Encyclopædia Britannica, Inc.

Figure 1.12: Scanning Electron Microscopy (SEM) (70).

The work of the electron microscopy is similar to the work of optical one. The main difference between them is that we use electrons instead of light and magnetic field instead of lenses. The interaction between the electrons and the sample surface produce signals that are converted into topography, composition and electrical conductivity. There are three types of signals produced by the SEM. Secondary electrons are electrons generated by the ionization process using any source of radiation. This technique can produce very high-resolution images of a sample surface, revealing details less than 1 nm in size. Back-scattered electrons (BSE) are the beam of electron reflected from the sample by scattering. Since the intensity of the scattered electron beam depends on the sample properties such as atomic number, the BSE will give us a good idea about the distribution of different elements at the surface. The applied electron beam can also affect the inner orbitals of the atoms in the surface of the samples. That may cause the inner orbitals to loss its electrons and force the higher levels electrons to fill the position and release energy. This type is called the characteristic X-rays. The characteristics of this energy are used to identify the compositions and measure the abundance of the element in the sample. This technique can be used for almost any kind of samples and will give us a three-dimension image of the surface (71, 72).

1.3.3 Carbon Electrode Surfaces

Carbonaceous materials have many desirable properties that have attracted their use in electrochemistry especially for electrodes and other cell component for batteries, and these properties are good electrical conductivity, acceptable corrosion resistance,

availability in high purity, high thermal conductivity, dimensional and mechanical stability, light in weight and ease of handling, availability in a variety of physical structures, ease of fabrication into composite structures and low cost. Many forms of carbon are suitable for electroanalysis such as glassy carbon and graphite carbon (69).

1.3.3.1 Glassy Carbon Electrode (GCE)

Glassy carbon, also called vitreous carbon, is isotropic with low porosity. It can be fabricated as different shapes, sizes and sections, is a non-graphitizing carbon which combines glassy and ceramic properties with those of graphite. The most important properties are high temperature resistance, hardness, low porosity, low adsorptivity, low density, low electrical resistance, low friction, low thermal resistance, extreme resistance to chemical attack and impermeability to gases and liquids (69). Although the low adsorptivity results in low sensitivity, modifying the surface or increasing the electrochemical accumulation time can enhance the analysis and increase the detection limit or enhance the selectivity (73). Glassy carbon is widely used as an electrode material in electrochemistry, as well as for high temperature crucible and as a component of some prosthetic devices.

Several modifiers can be used with the glassy carbon electrode but the metals are the most common such as mercury (74), gold (75), copper (76), lead (77), platinum (78), bismuth (79-81) and bismuth nanoparticles (82) which facilitate the precipitation of amalgam forming and electropositive elements. Other studies suggested the use of dimetallic alloy to enhance the detection such as tin-bismuth (83), mercury-bismuth (84).

Organic substances can also be used as a modifier such as macrocyclic compounds (85), ethylene diaminetetraacetic (86), nafion (80), polymers (87), bioactive compounds (88, 89) and nanotubes (90).

The voltammetric behavior of a glassy carbon electrode is also known to change because of the degradation of the modified surface which results in displacing the current peak position, distortion of the peak height or even adding a new peak due to the contamination possibility, which affects the reproducibility (91).

Several methods have been used as a treatment to the electrode surface prior to use such as mechanical polishing (92), treatment with reagents (93), and exposure to microwaves (94, 95). Usually most glassy carbon electrodes are treated mechanically by polishing using sub-micron alumina powder (Al_2O_3) and then washed with deionized water.

1.3.3.2 Graphite Pencil Electrode (GPE)

Renewable graphite pencil writing devices have been available for many years. A few years ago, the pencil lead has been used in electroanalytical chemistry as a material for electrodes. For example, it has been used in anodic stripping voltammetric measurements of trace metals (67) and for adsorptive stripping potentiometry of nucleic acids (96), also as a renewable biosensor for label-free electrochemical detection of DNA hybridization (97).

One of the advantages of graphite pencil electrode (GPE) is that it can be extruded to different lengths to yield different surface areas which make this electrode very suitable for many applications. Usually a pentel pencil (Japan) is used as a holder for the pencil

lead. Electrical contact with the lead is achieved by soldering a metallic wire to the metallic part that holds the lead in place inside the pencil (Figure 1.13A).

1.3.3.3 Carbon Paste Electrode (CPE)

A carbon-paste electrode (CPE) is made from a mixture of conductive graphite powder and a pasting liquid (Figure 1.13B). These electrodes are simple to make and offer an easily renewable surface for electron exchange. Carbon paste electrodes belong to a special group of heterogeneous carbon electrodes. These electrodes are widely used mainly for voltammetric measurements. Carbon pastes are easily obtainable at minimal costs and are especially suitable for preparing an electrode material modified with admixture of other compounds (98).

1.3.3.4 Glassy Carbon Paste Electrode (GCPE)

Glassy carbon paste electrode (GCPE) is a new carbon composite electrode material based on mixing glassy carbon (GC) micro particles with mineral oil. The glassy carbon paste electrode has the electrochemical properties of glassy carbon with the advantages of composite electrodes. Glassy carbon paste electrode (GCPE) have many advantages such as high electrochemical reactivity, a wide accessible potential window, a low background current, inexpensive, easy to prepare, to modify, and to renew. Comparing with the conventional carbon paste electrode (CPE), the new material has a lower double-layer capacitance and a higher heterogeneous rate constant.

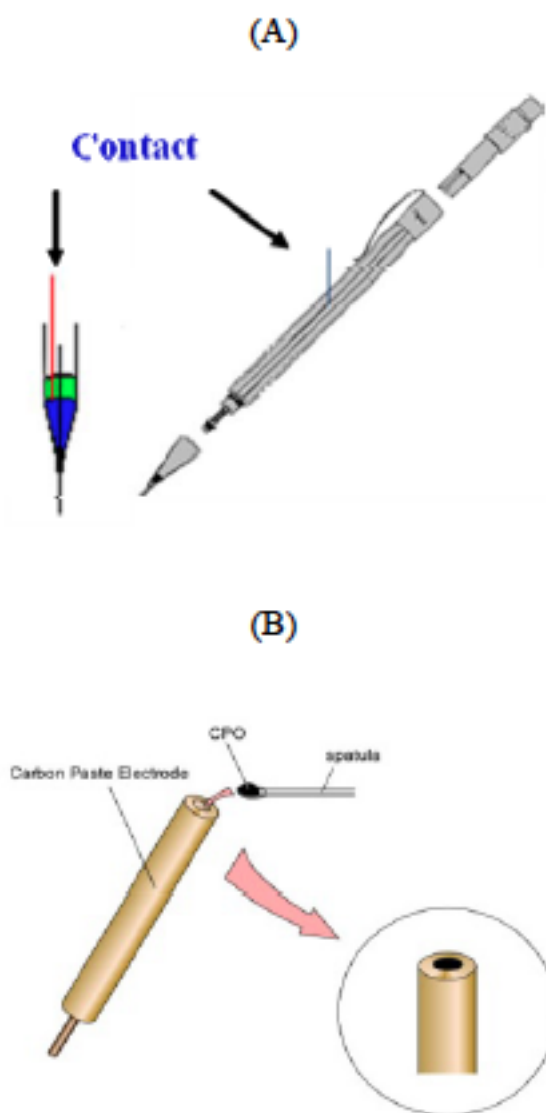


Figure 1.13: Schematic diagram of pencil electrode (A) and carbon paste electrode (B).

1.4 Objectives

The main objectives of the current research are as on the following:

- Screen for toxic heavy metals contaminants in drinking water samples.
- Fabricate suitable transducers for the sensor.
- Develop field-deployable sensors.
- Characterize the developed sensors.
- Test the developed sensors.
- Run on field detection assays.
- Decentralize the water testing of heavy metals in water samples.
- Introduce an effective alternative sensing electrodes and easy-to-use microanalyzers that would have a major impact upon the monitoring of toxic heavy metals particularly Cd(II), Pb(II) and Zn(II) in drinking water.

CHAPTER 2

2.0 ELECTROCHEMICAL INVESTIGATION AND ANALYTICAL DETERMINATION OF Zn(II), Cd(II) AND Pb(II) USING Bi- & Hg- MODIFIED ELECTRODES.

2.1 INTRODUCTION

Several pollutants can be found in the drinking water. Heavy metals pollution is considered to be a major problem in the world due to its toxicity at low concentration levels. Several heavy metals such as lead, cadmium and zinc have been studied and represent a major public health concerns because they are ubiquitous and affects several organs in humans. For these reasons, lead, cadmium and zinc measurements are critically important in industrial, food and environmental safety, clinical diagnosis and toxicology (99).

Many analytical methods have been certified as standard techniques for heavy metals determination such as electro-thermal atomic absorption spectrometry (ET-AAS), flame atomic absorption spectrometry (FAAS), inductively coupled plasma mass spectrometry (ICP-MS), and inductively coupled plasma optical emission spectrometry (ICP-OES) (100). Those techniques are costly, complex instrumentation and cannot be taking on field.

Because of the accuracy, low detection limits and low cost electrochemical stripping analysis is considered to be a very important tool for the trace determination of various

elements and compounds.

The remarkable sensitivity of electrochemical stripping analysis is attributed to the combination of an effective preconcentration step with advanced electrochemical measurements of the accumulated analytes (101-103), especially for adsorptive stripping voltammetry (AdSV) where the analyte is deposited on the working electrode by adsorption. However, the electrode material plays a major role to give a good adsorption of the analyte and stable and reproducible electrode surface (99). The most commonly used working electrode material utilizing this method is the glassy carbon electrode plated with mercury film (104).

However, the toxicity and volatility of the mercury electrode limits its applicability for in situ measurements as a platform of disposable sensor. Several plated Bi film-electrodes have been reported as an alternative electrode to mercury electrodes because Bi is an environmentally-friendly material and has a similar performance compared with mercury in the measurement of heavy metals using anodic stripping voltammetry (ASV) (105).

Even though the Bi film electrode can be a good (green) replacement of the mercury film, the detection limit and the sensitivity of the mercury is better. Several studies were carried out using polymers, such as ethylenediaminetetraacetic acid, crown ether, EDTA, phenol red and aniline has reported as an enhancer to the Bi film (100,103,106). Also using nanoparticles to enhance the trace metals detection has been reported where screen-printed carbon electrodes with bismuth (Bi) nanoparticles has been used for the detection of trace Zn^{2+} , Cd^{2+} and Pb^{2+} (107).

In 2000, Wang, for the first time, reported a Bi-coated carbon electrode as a sensor for the stripping voltammetric analysis of lead, cadmium and zinc (105). The Bi coated electrode is considered to be a good replacement as a green element and gives results comparing to the mercury one

Bismuth film electrodes (BiFEs) have drawn considerable interests due to its remarkable low toxicity and its ability to form alloy with many other metals, as well as its partial insensitivity to dissolved oxygen. On the other hand, it has a wide potential window for determination trace metals combining electrochemical stripping techniques (108), those attractive performances make it preferable comparing to the toxic mercury. The detection at the surface of a Bi electrode is due to the capacity of Bi to form a 'fused alloy' with some heavy metals (e.g., lead) and it has the advantage of not requiring the removal of dissolved oxygen during stripping analysis (102).

In the electrochemical-stripping analysis technique with Bi electrodes there are two different steps; a preconcentration step, where the heavy metals (zinc, cadmium and lead) are reduced to form an alloy with Bi, and a reduction step, where the heavy metals are reoxidized and goes back in solution. The concentrations of the targeted heavy metals are determined by SWV technique.

Earlier study was reported by Wang et al (109), where a screen-printed electrode (SPE) was first coated with a Bi film using square-wave voltammetric stripping analysis, a linear range for lead detection (10-100 $\mu\text{g/L}$) with a good precision was obtained. The main problem in this method was that the Bi film may degrade due to its poor adhesively to the working electrode surface. An interesting investigation was carried out by the

Ogorevics group, adding NaBr salt to the acetate working solution, because this salt seems to promote a denser growth of smaller Bi crystals (99, 110). However, at Bi(III) concentrations greater than 1 mg/L, a reduction in the peak intensity was observed, associated to the formation of a thick layer of Bi on the electrode surface that partially blocks the conductive surface of the electrode, reducing the number of sites (99, 111, 112)

Several methods have been studied in order to enhance the detection. In 2001 Vijakumar and Ashwini reported the using carbon paste mixed with 18-crown-6 ether as a working electrode for the trace analysis of lead. The strong complexation of 18-crown-6 with lead has been advantageously used to enhance the voltammetric signals and to decrease the interference from other transition-metals (106).

Similar study by Md. Aminur-Rahman and others in 2003 report the EDTA-bonded conducting polymer modified electrode. The electrode was used for the selective electrochemical analysis of various trace metal ions such as, Cu(II), Hg(II), Pb(II), Co(II), Ni(II), Fe(II), Cd(II), and Zn(II). The technique offers an excellent way for the selective trace determination of various heavy metal ions in a solution (113).

In 2006 Wei Wei Zhu developed a novel study by voltammetric method (anodic) using a bismuth/poly(aniline) film electrode for simultaneous measurement of Pb(II) and Cd(II) at low concentration levels by stripping voltammetry. The results confirmed that the bismuth/poly(aniline) film electrode offered high-quality stripping performance compared with the bismuth film electrode. Well-defined sharp stripping peaks were observed for Pb(II) and Cd(II), along with an extremely low baseline (114).

In 2007 Gongjun Yang also reported the behavior of lead(II) at poly(phenol red)

modified glassy carbon electrode, and its trace determination by differential pulse anodic stripping voltammetry. The electrode offers attractive properties such as simplicity of electrode preparation, good reproducibility and ability of anti-jamming. The detection limit obtained here is very close to what obtained by the well-known Hg- based DPSV approach (115).

Later on several studies aimed to improve the voltammetric response the nanomaterials such as nanotubes gain lots of interest due to its high surface area. This property made them ideal to be used as a surface for the anodic stripping (116). Janegitz and co-workers made an electrode consisted of carbon nanotube paste modified with cross-linked chitosan, a hydroxyl and amine-rich polysaccharide capable of chelating heavy metals, this electrode have the capability of sensitive detection of copper (117). Similar study had been reported by Morton and co-workers using Cysteine-modified multiwalled carbon nanotubes (MWCNTs) were cast onto glassy carbon electrodes for the detection of lead and copper in water. After 10 minutes accumulation time they achieved a 1.0 and 15.0 ppb limit of detection for lead and copper respectively (118).

Bismuth accompanied by carbon nanotube took advantage of the wide potential window and insensitivity of Bi to O_2 , as well as the high surface area and strong adsorptive capabilities of the MWCNTs, this sensors exhibited limits of detections for lead and cadmium of 25 and 40 ppt, respectively (119).

Several approaches have been used to apply bismuth on the surface of the electrode, one is by casting Bi solution on the electrode, resulting in particle formation after solvent evaporation. This study was carried out by Rico and colleagues, they modified screen-

printed carbon electrodes with bismuth (Bi) nanoparticles for the detection of trace zinc, cadmium and lead. Their method achieved limit of detection from 0.9 to 4.9 ppb after 120 seconds accumulation (120).

2.2 ELECTROCHEMICAL INVESTIGATION AND ANALYTICAL DETERMINATION USING Bi-MODIFIED ELECTRODES

2.2.1 Apparatus

Voltammetry measurements were performed with an electrochemical work station (CHI1140A, CH Instruments Inc, Austin, TX, USA). The Ag/AgCl reference electrode (in 3M KCl, CHI111, CH Instruments Inc), Glassy carbon working electrode (CHI 112, CH Instruments Inc) and platinum wire counter electrode (CHI115, CH Instruments Inc) were inserted into the 5 ml plastic cell through holes in its Teflon cover (Figure 2.1 A and B).

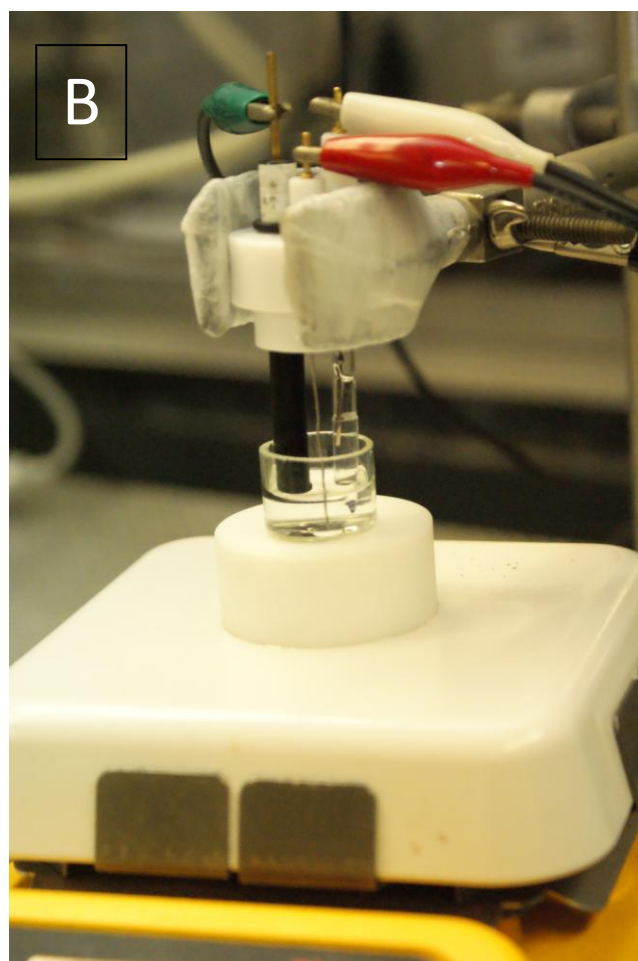
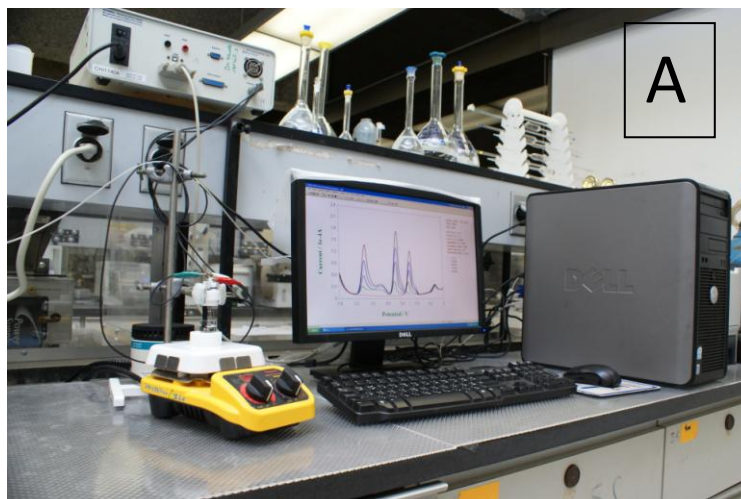


Figure 2.1: (A) The electrochemical work station (B) The cell setup.

2.2.2 Electrochemical Transducers Preparation

Glassy carbon Paste electrode (GCPE) was prepared by hand-mixing 70 mg of 20-50 μm glassy carbon with 30 mg of mineral oil. A small portion of the resulting paste was then packed firmly into a cavity of the PTFE sleeve. Electrical contact was established via copper wire. The paste surface was smoothed with a weighing paper. Also glassy carbon electrode (GCE), 3 mm diameter, was polished with 0.3 μm alpha alumina powder and was washed with double distilled water then tested. Carbon-paste electrodes (CPEs) were prepared by hand mixing of 70 mg of carbon powder with 30 mg of mineral oil, handled the same as the GCPE, and then was tested as well.

Other materials were tested as well. A pencil Model P205 (Pentel, Japan) was used as a holder for the pencil lead. Electrical contact with the lead was achieved by soldering a metallic wire to the metallic part that holds the lead in place inside the pencil. The pencil was fixed vertically with 11 mm of the pencil extrude outside and 10 mm of the lead that immersed in the solution. Such length corresponds to an active electrode area of about 16.36 mm^2 .

2.2.3 Reagents

Standard solutions prepared from Mercury, Bismuth, Zinc, Lead and Cadmium solutions from 1000 ppm AAS standard solution Fuluka analytical. Sodium acetate pH 3.5 (0.1 M) buffer prepared from sigma-Aldrich 3M stock solution.

2.2.4 Procedure

Square wave voltammetry (SWV) measurements were performed by treating the surface at +0.6 V for 60s followed by 120 sec accumulation at -1.4 V in a stirred solution of 0.1 M acetate buffer (pH 3.5). This was followed by a subsequent stripping using a square wave voltammetric waveform, with an 8 mV potential increment, 100 Hz frequency and amplitude of 60 mV for the GC-Bi and with a 6 mV potential increment, 80 Hz frequency and amplitude of 40 mV in the case of GC-Hg. The electrode surface was smoothed and rinsed carefully with deionized water prior to every measurement.

2.2.5 Results and Discussion

After studying several material transducer types we have concluded that the glassy carbon electrode gives the best response for heavy metals determination in drinking water.

2.2.5.1 Electrochemical Investigation

In this work the simultaneous detection of the zinc, cadmium and lead heavy metals using SWV technique is possible. Figure 2.2 shows the square-wave stripping voltammogram for 40 ppb of Zn(II), Cd(II) and Pb(II) at GCE-Bi the peaks were identified for the three metals and the peak area or peak height are proportional directly to the concentration.

Transducer selection:

We have screened different transducers in the presence of Bi(III), the response of GCE-Bi has been taken at four different concentrations, 0.0, 20, 40 and 60 ppb of Zn(II), Cd(II) and Pb(II). The transducers that were used here are the glassy carbon (GCE) (Figure 2.3), the carbon paste (CPE) (Figure 2.4), and the graphite pencil (GPE) (Figure 2.5). As shown clearly, GC is the best transducer among the tested transducers, and thus used for the subsequent experiments.

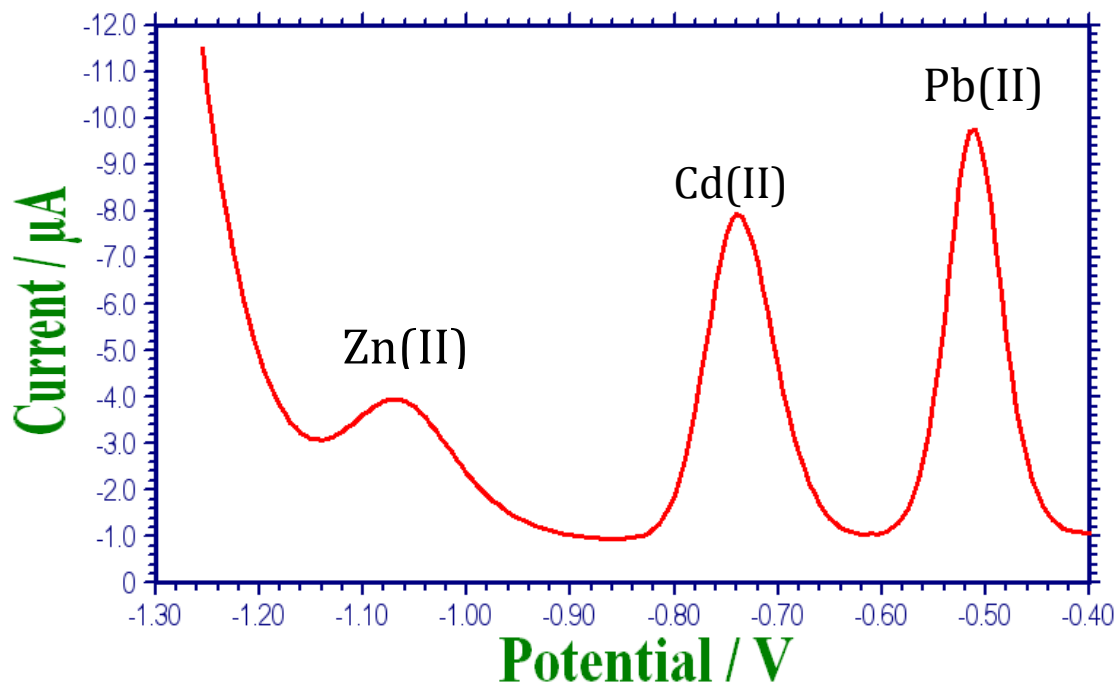


Figure 2.2: Square-wave stripping voltammograms of 40 ppb of Zn(II), Cd(II) and Pb(II) using GCPE in presence of 600 ppb Bi(III). Accumulation time, 2.0 min at -1.4V; Potential step, 8 mV; Frequency, 100 Hz; Amplitude, 60 mV.

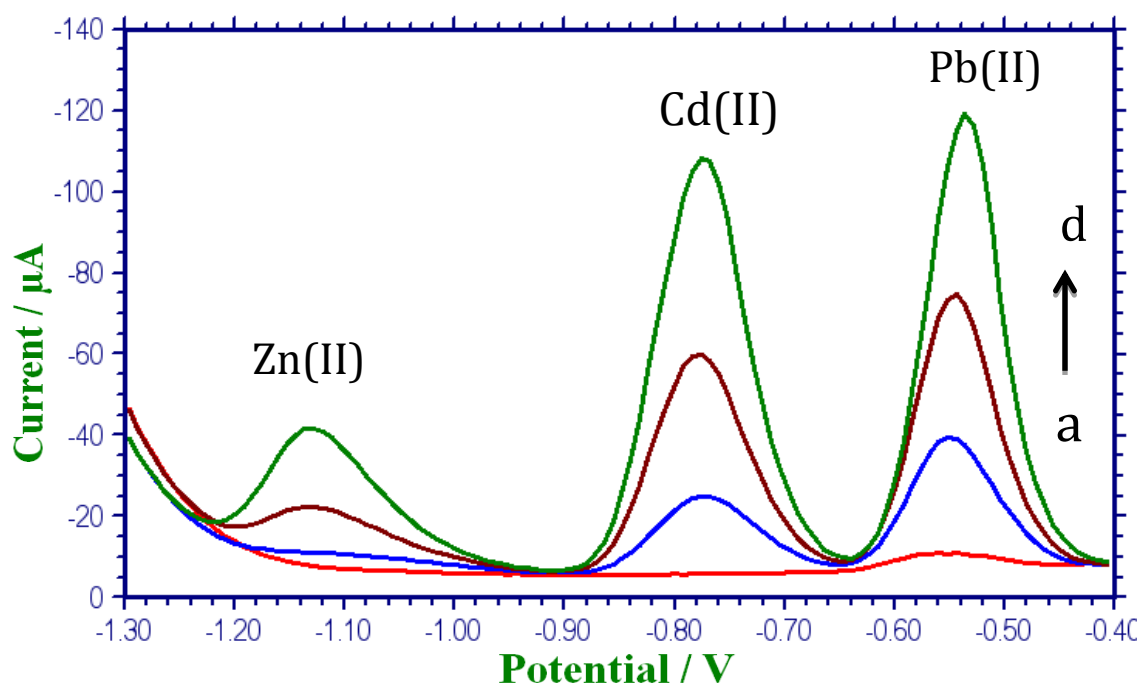


Figure 2.3: Square-wave stripping voltammograms of Zn(II), Cd(II) and Pb(II) at GCE in presence of 600 ppb Bi(III) in acetate buffer solution (0.1 M, pH 3.5); amplitude, 60 mV; frequency, 100 Hz; potential increment, 8 mV; accumulation time, 2.0 min at -1.4 V. For Zn(II), Cd(II) and Pb(II) concentrations: (a) 0.0, (b) 20 ppb, (c) 40 ppb, (d) 60 ppb.

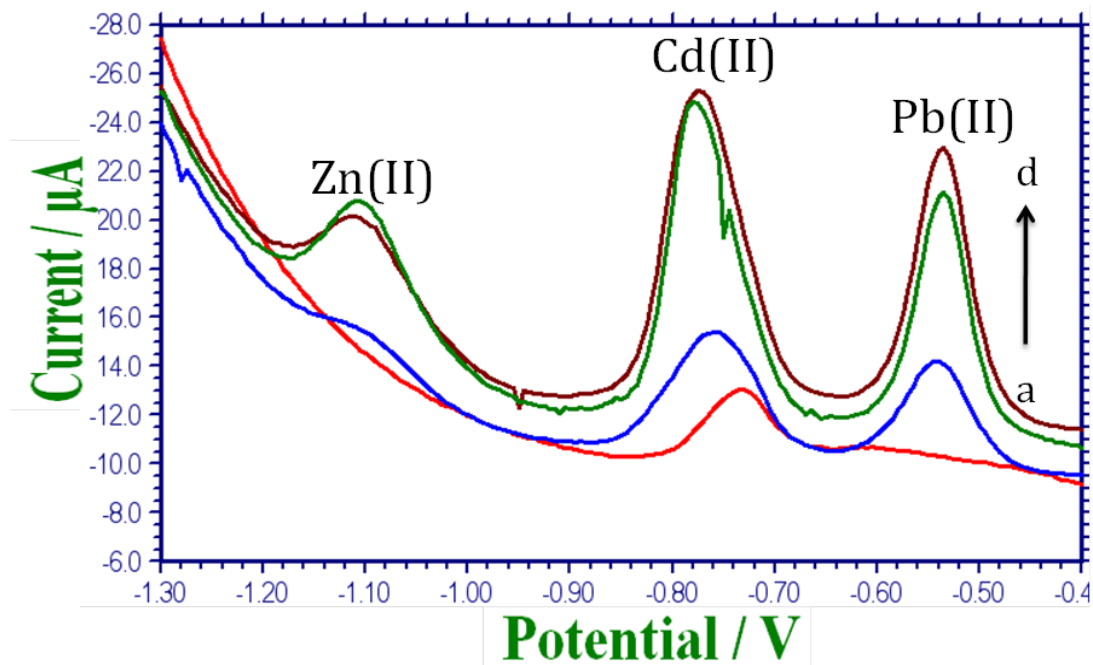


Figure 2.4: Square-wave stripping voltammograms of Zn(II), Cd(II) and Pb(II) at Carbon Paste Electrode in presence of 600 ppb Bi(III) in acetate buffer solution (0.1 M, pH 3.5); amplitude, 25 mV; frequency, 20 Hz; potential increment, 5 mV; accumulation time, 2.0 min at -1.4 V. For Zn(II), Cd(II) and Pb(II) concentrations: (a) 0.0, (b) 20 ppb, (c) 40 ppb, (d) 60 ppb.

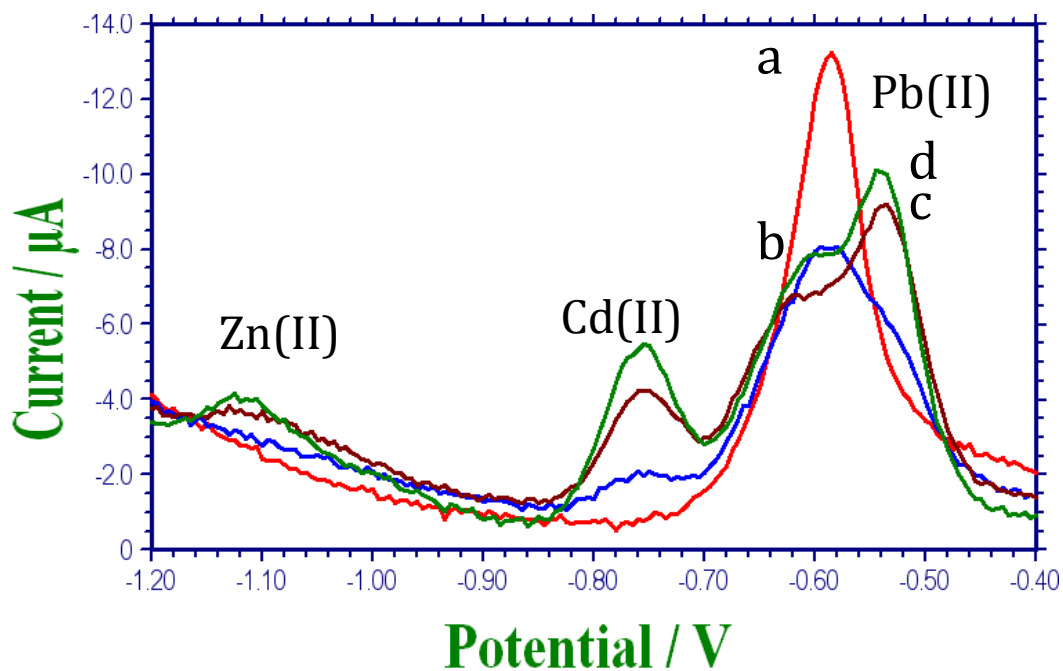


Figure 2.5: Square-wave stripping voltammogram of Zn(II), Cd(II) and Pb(II) at pencil in presence of 600 ppb Bi(III) in acetate buffer solution (0.1 M, pH 3.5); amplitude, 25 mV; frequency, 20 Hz; potential increment, 5 mV; accumulation time, 2.0 min at -1.4 V. For Zn(II), Cd(II) and Pb(II) concentrations: (a) 0.0, (b) 20 ppb, (c) 40 ppb, (d) 60 ppb.

2.2.5.2 Optimization

Figure 2.6 shows the square-wave stripping voltammetric responses of 40 ppb of Zn(II), Cd(II) and Pb(II) at the bismuth modified-glassy carbon electrode (Bi-GCE) in acetate buffer solutions with different pHs. There is a ~50 mV cathodic potential shift for the Zn(II), Cd(II) and Pb(II) oxidation peak position with the increase of the pH from 3.0 to 3.5. In the acetate medium, pH 3.5 was the optimum pH among all examined pHs with respect to the height and shape of the obtained oxidation peaks especially for Cd(II) and Zn(II) peaks.

The SWASV for Zn(II), Cd(II) and Pb(II) was studied at different frequencies as shown in (Figure 2.7A). The plots are linear up to 100 Hz, and level off thereafter (Figure 2.7B) for that 100 Hz was chosen as the optimum value. On the other hand, it was found that the larger the pulse amplitude, the higher the Zn(II), Cd(II) and Pb(II) signals as shown in Figure 2.8A. The plots are linear up to 60 mV and start to decrease thereafter. For that 60 mV was chosen as optimum pulse amplitude (Figure 2.8B). Figure 2.9A shows the influence of varying the potential increment, where all signals increase linearly and start to decrease after 8.0 mV (Figure 2.9B). So 8 mV was chosen as the optimum potential increment.

The effect of the accumulation potential was done by varying the potential from -1.2, -1.3, -1.4 to -1.5 V (vs. Ag/AgCl) (Figure 2.10A). The accumulation potential -1.4 V was selected as the optimum potential for subsequent experiments as in the corresponding plot (Figure 2.10B).

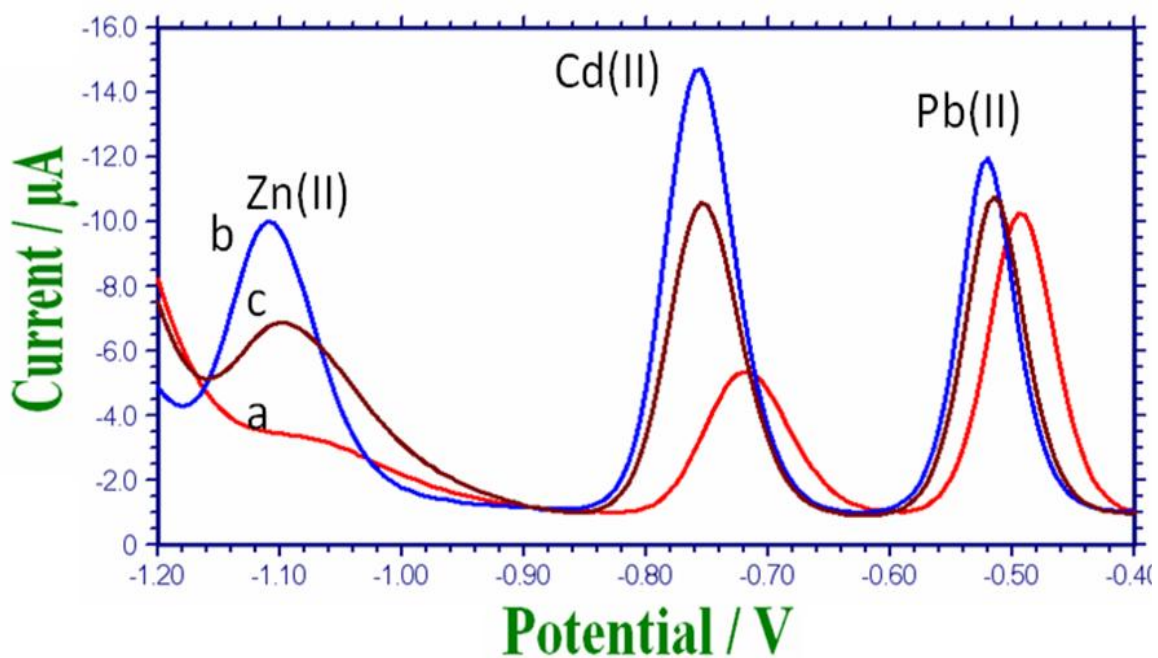


Figure 2.6: Square-wave stripping voltammogram of 40 ppb Zn(II), Cd(II) and Pb(II) at GCE in presence of 600 ppb Bi(III) in acetate buffer solution (0.1 M) at different pH values: (a) pH 3.0, (b) pH 3.5 and (c) pH 4.0; amplitude, 60 mV; frequency, 100 Hz; potential increment, 8 mV; accumulation time, 2.0 min at -1.4 V.

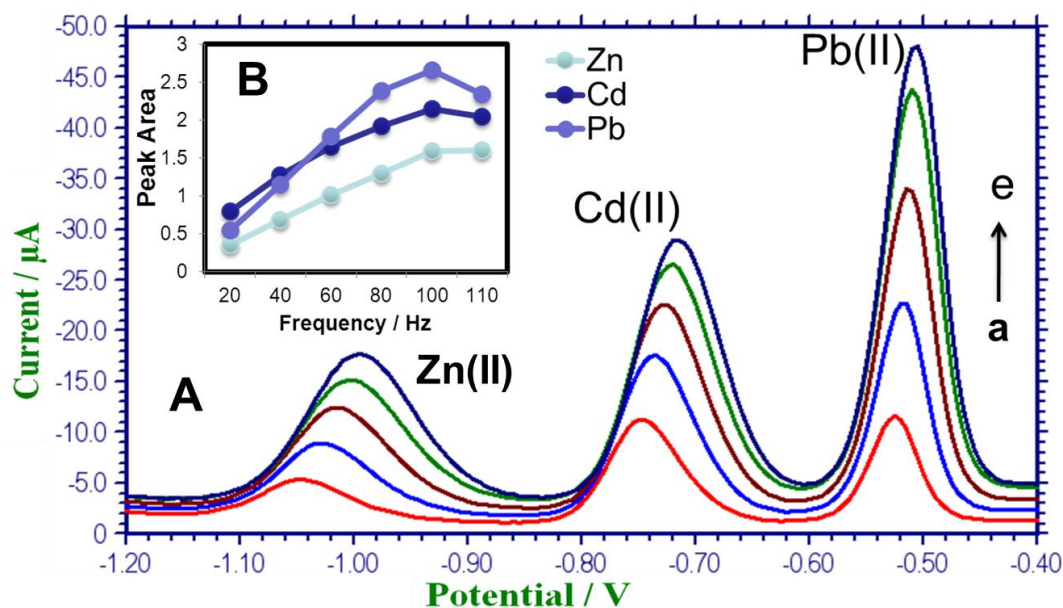


Figure 2.7: (A) Square-wave stripping voltammograms of 40 ppb Zn(II), Cd(II) and Pb(II) at GCE in presence of 600 ppb Bi(III) in acetate buffer solution (0.1 M, pH 3.5). Accumulation time, 2.0 min at -1.4 V; Potential increment, 5 mV; Amplitude, 25 mV and Frequency: (a) 20 Hz, (b) 40 Hz, (c) 60 Hz, (d) 80 Hz and (e) 100 Hz. (B) The corresponding plot.

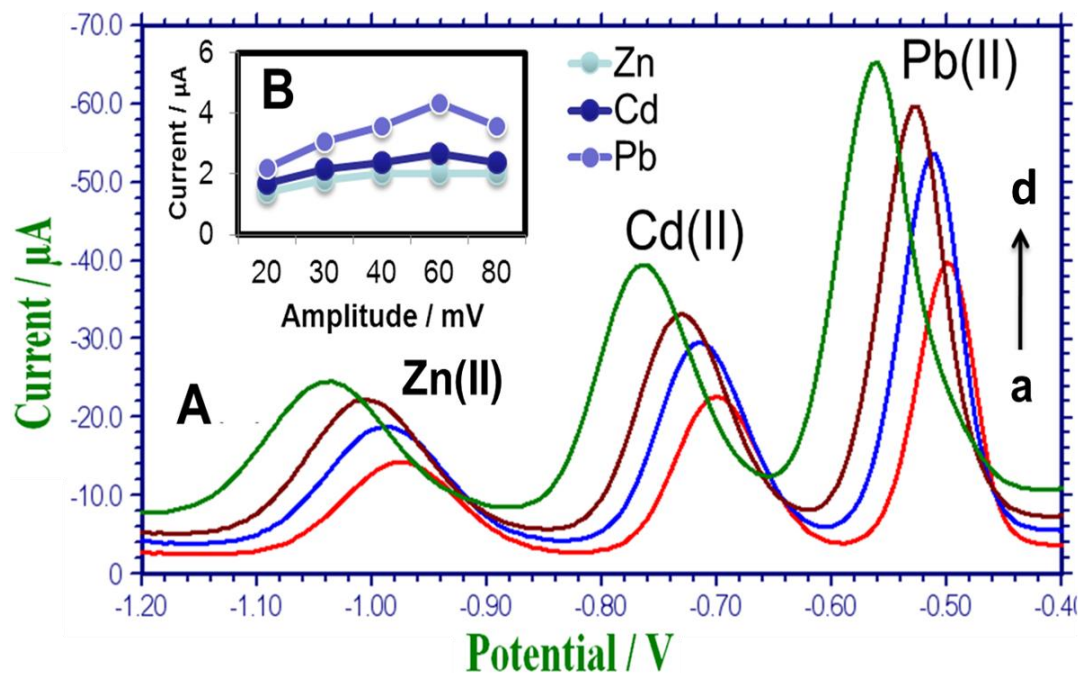


Figure 2.8: (A) Square-wave stripping voltammograms of 40 ppb Zn(II), Cd(II) and Pb(II) at GCE in presence of 600 ppb Bi(III) in acetate buffer solution (0.1 M, pH 3.5). Accumulation time, 2.0 min at -1.4 V; Potential increment, 5 mV; Frequency, 100 Hz; Amplitude: (a) 20 mV, (b) 30 mV, (c) 40 mV, (d) 60 mV. (B) The corresponding plot.

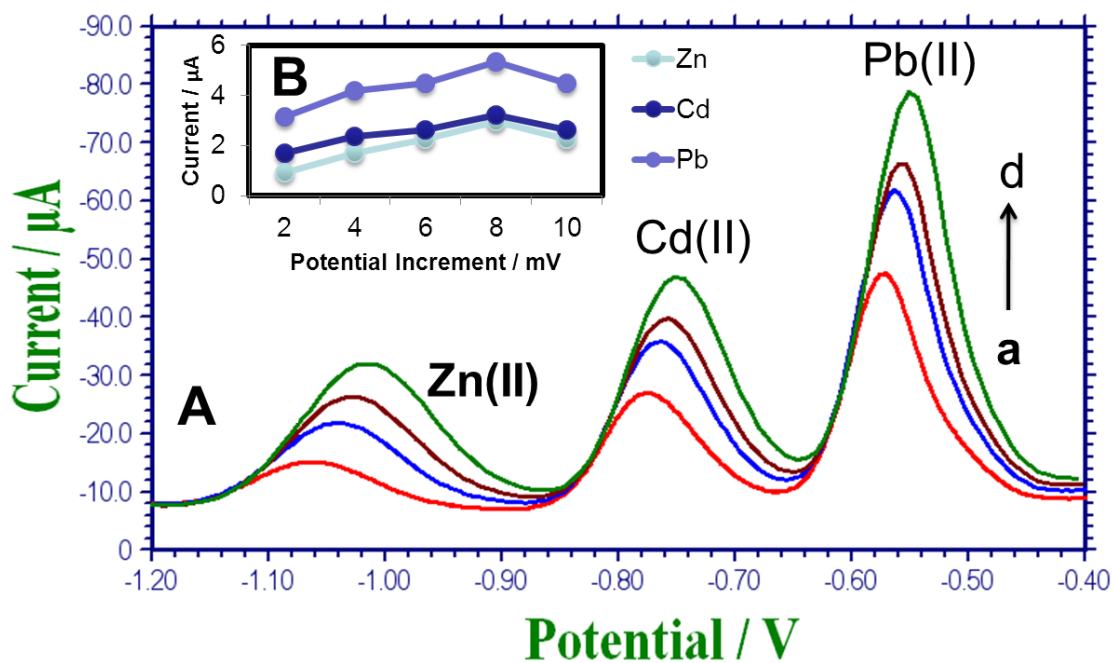


Figure 2.9: (A) Square-wave stripping voltammograms of 40 ppb Zn(II), Cd(II) and Pb(II) at GCE in presence of 600 ppb Bi(III) in acetate buffer solution (0.1 M, pH 3.5). Accumulation time, 2.0 min at -1.4 V; Amplitude, 60 mV; Frequency, 100 Hz; Potential increment: (a) 2 mV, (b) 4 mV, (c) 6 mV, (d) 8 mV. (B) The corresponding plot.

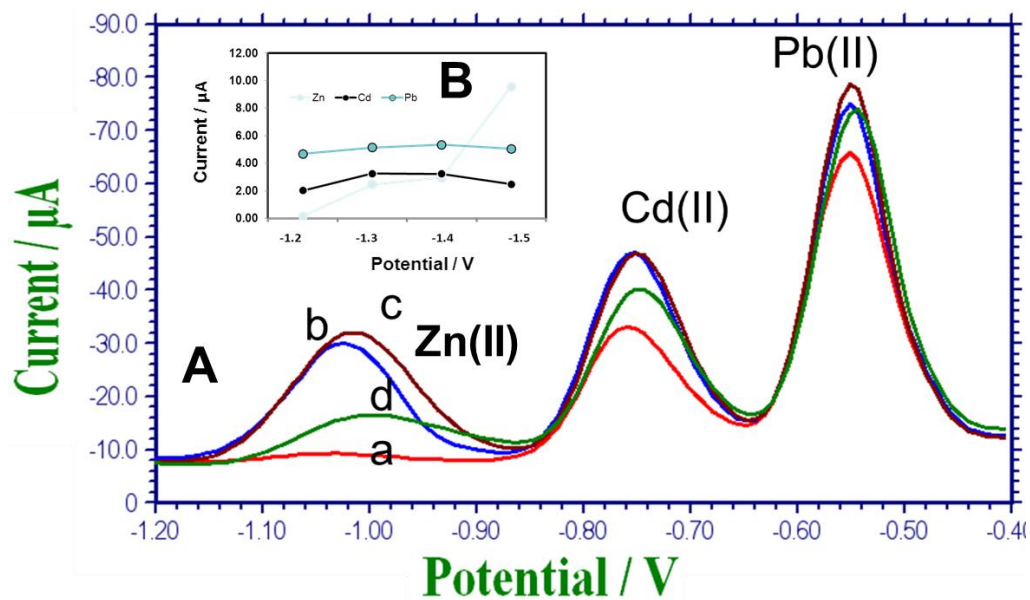


Figure 2.10 : (A) Square-wave stripping voltammograms of 40 ppb Zn(II), Cd(II) and Pb(II) at GCE in presence of 600 ppb Bi(III) in acetate buffer solution (0.1 M, pH 3.5). Amplitude, 60 mV; Frequency, 100 Hz; Potential increment, 8 mV; Accumulation time, 2.0 min at: (a) -1.2 V, (b) -1.3 V, (c) -1.4 V and (d) -1.5V. (B) The corresponding plot.

2.2.5.3 Reproducibility

The reproducibility study has been carried out by using the optimum parameters for a solution containing 40 ppb of Zn(II), Cd(II) and Pb(II) at GCE in presence of 600 ppb Bi(III) in acetate buffer solution (0.1 M, pH 3.5) and repeated for seven times (Figure 2.11A). The recorded signals of Zn(II), Cd(II) and Pb(II) varied in response as in shown in Figure 2.11B.

2.2.5.4 Analytical Determination

To obtain a calibration curve under the optimum parameters, the SWASV responses of Pb(II), Cd(II) and Zn(II) were recorded in a concentration rang from 5.0 ppb to 250.0 ppb as shown in (Figure 2.12A). Figure 2.12B shows the corresponding calibration plots.

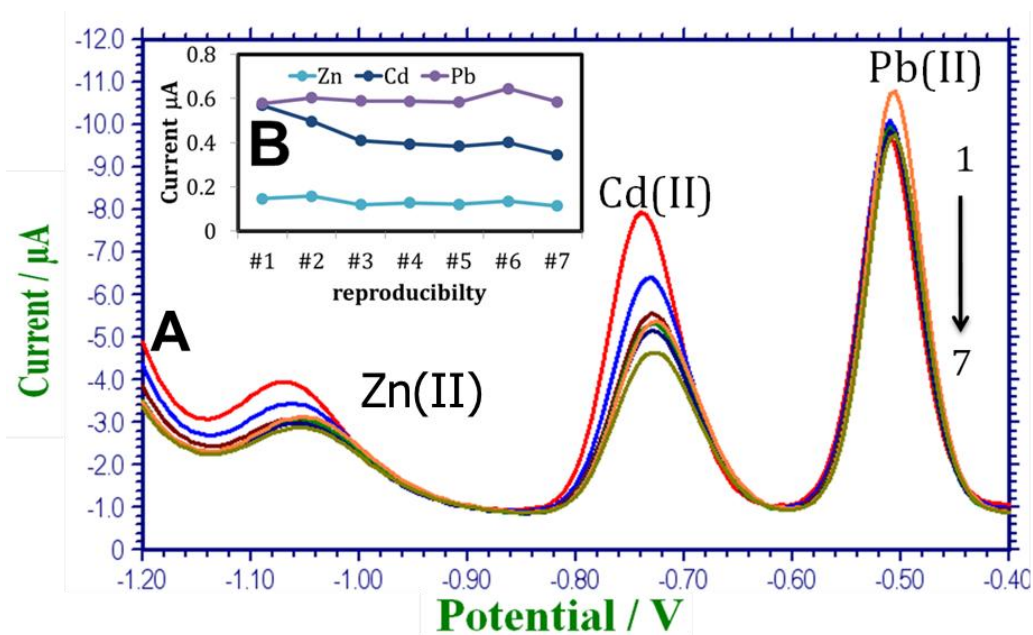


Figure 2.11: (A) Square-wave stripping voltammograms of 40 ppb Zn(II), Cd(II) and Pb(II) at GCE in presence of 600 ppb Bi(III) in acetate buffer solution (0.1 M, pH 3.5). Amplitude, 60 mV; Frequency, 100 Hz; Potential increment, 8 mV; Accumulation time, 2.0 min at -1.4 V. (B) The corresponding plot.

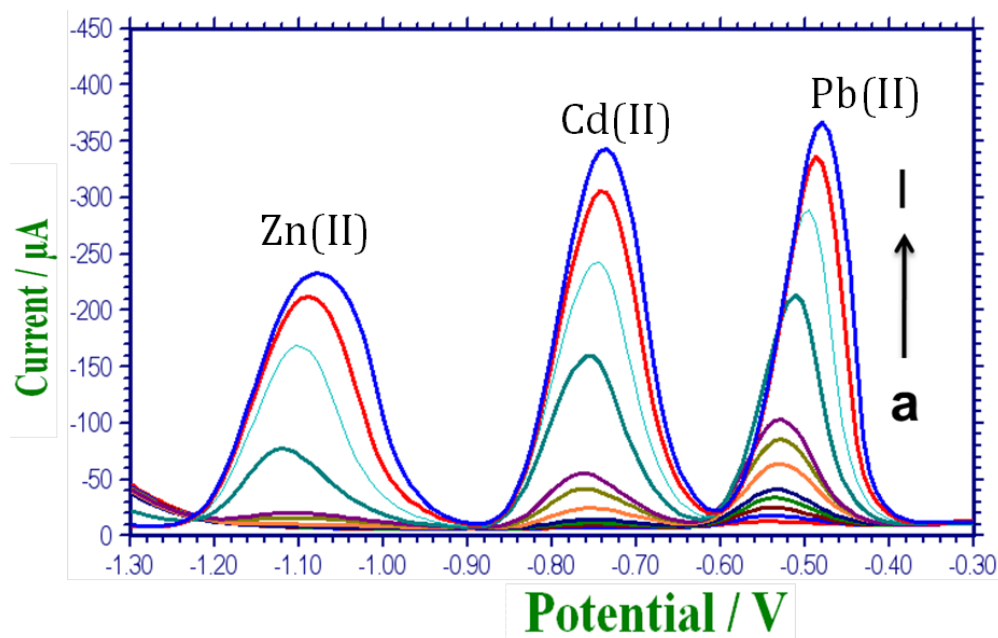


Figure 2.12A: Square-wave stripping voltammograms of Zn(II), Cd(II) and Pb(II) at GCE in presence of 600 ppb Bi(III) in acetate buffer solution (0.1 M, pH 3.5); Amplitude, 60 mV; Frequency, 100 Hz; Potential increment, 8 mV; Accumulation time, 2.0 min at -1.4 V. A mixture of Zn(II), Cd(II) and Pb(II) concentrations: (a) 0.0, (b) 5, (c) 10, (d) 15, (e) 20, (f) 30, (g) 40, (h) 50, (i) 100, (j) 150, (k) 200, (l) 250 ppb.

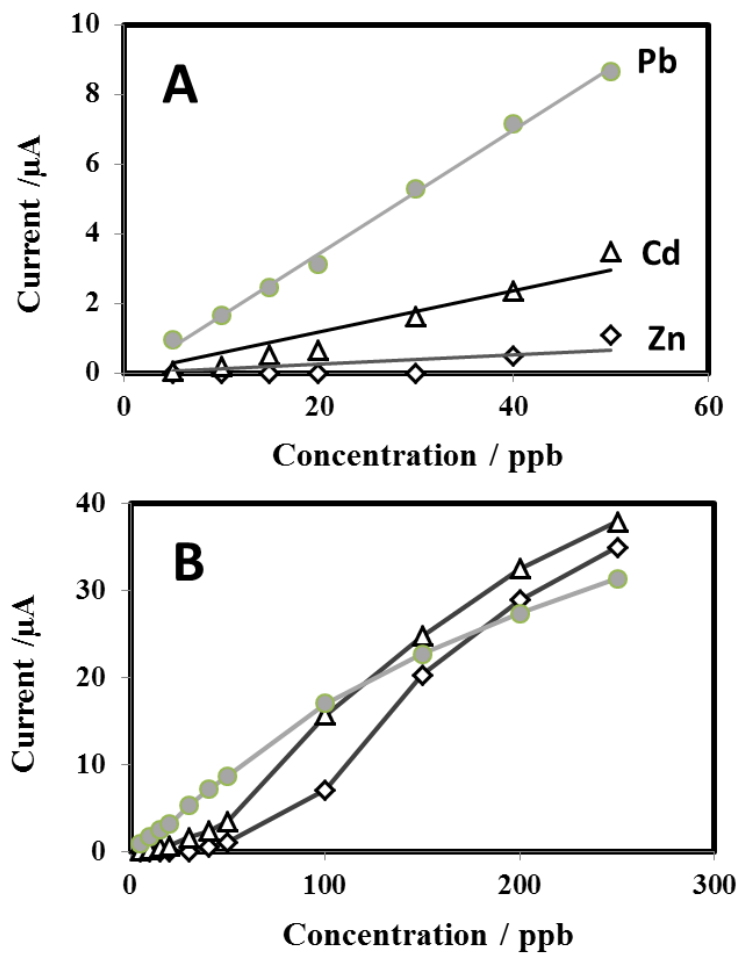


Figure 2.12B: The corresponding calibration plots of Zn(II), Cd(II) and Pb(II) concentration ranges (A) 0-50 ppb and (B) 0 – 250 ppb.

2.3 ELECTROCHEMICAL INVESTIGATION AND ANALYTICAL DETERMINATION USING Hg-MODIFIED ELECTRODES

2.3.1 Apparatus

Details of apparatus were described earlier on the subsection 2.2.1.

2.3.2 Electrochemical Transducers Preparation

Details of the electrochemical transducers preparation were described earlier on the subsection 2.2.2.

2.3.3 Reagents

Details of the reagents were described earlier on the subsection 2.2.3.

2.3.4 Procedure

Details of the procedure were described earlier on the subsection 2.2.4.

2.3.5 Results and Discussion

Glassy carbon electrode as a transducer gives the best response for heavy metals determination in drinking water.

2.3.5.1 Electrochemical Investigation

In this work the simultaneous detection of the zinc, cadmium and lead heavy metals using SWV technique is possible. Figure 2.13 shows the square-wave stripping voltammogram for 40 ppb of Zn(II), Cd(II) and Pb(II) at GCE-Hg. The peaks were identified for the three metals and the peak area or peak heights are proportional directly to the concentration.

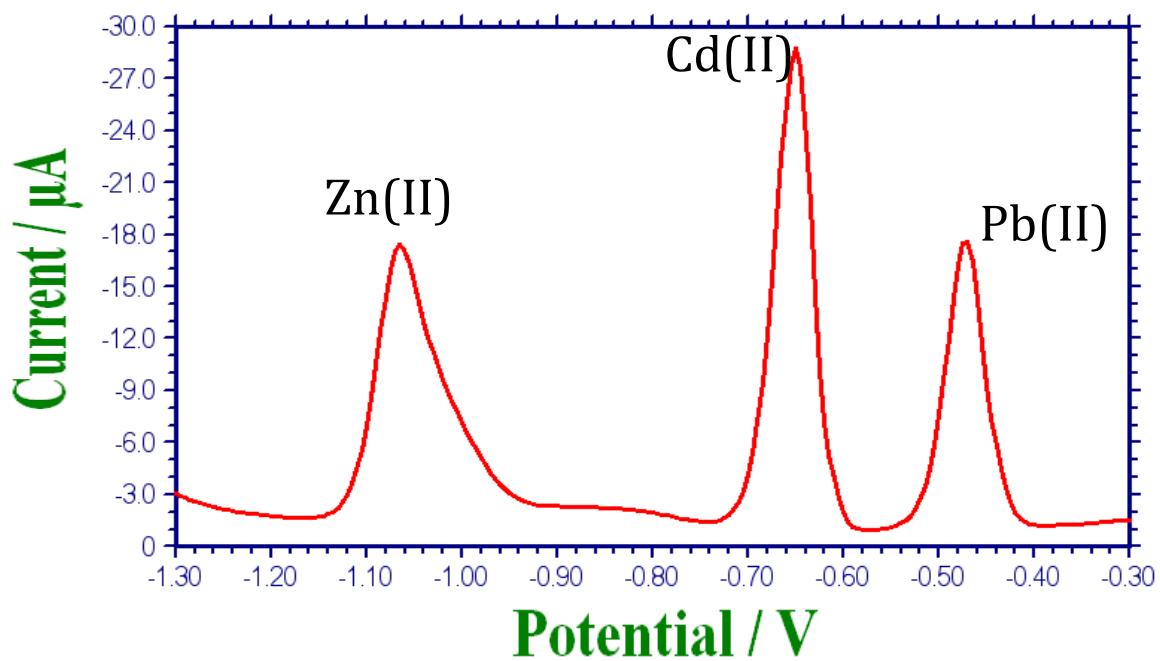


Figure 2.13: Square-wave stripping voltammograms of 40 ppb Zn(II), Cd(II) and Pb(II) at GCE in presence of 10 ppm Hg(II) in acetate buffer solution (0.1 M, pH 4.5). Accumulation time, 2.0 min at -1.4V; Potential increment, 6 mV; Frequency, 100 Hz; Amplitude, 70 mV.

Transducer selection:

Different transducers have been studied in the presence of mercury. The transducers we have used here are the glassy carbon (GC), the carbon paste (CP) and the graphite pencil (GP) electrodes.

- **Glassy Carbon Electrode (GCE) in the presence of Hg(II)**

Figure 2.14 shows the response of GCE-Hg at four different concentration levels (0.0, 20, 40 and 60 ppb) of Zn(II), Cd(II) and Pb(II).

- **Carbon Paste Electrode (CPE) in the presence of Hg(II)**

The response of CPE-Hg at four different concentration levels of Zn(II), Cd(II) and Pb(II) is shown in (Figure 2.15).

- **Graphite Pencil Electrode (GPE) in the presence of Hg(II)**

Figure 2.16 shows the response of GPE-Hg at four different concentration levels of Zn(II), Cd(II) and Pb(II).

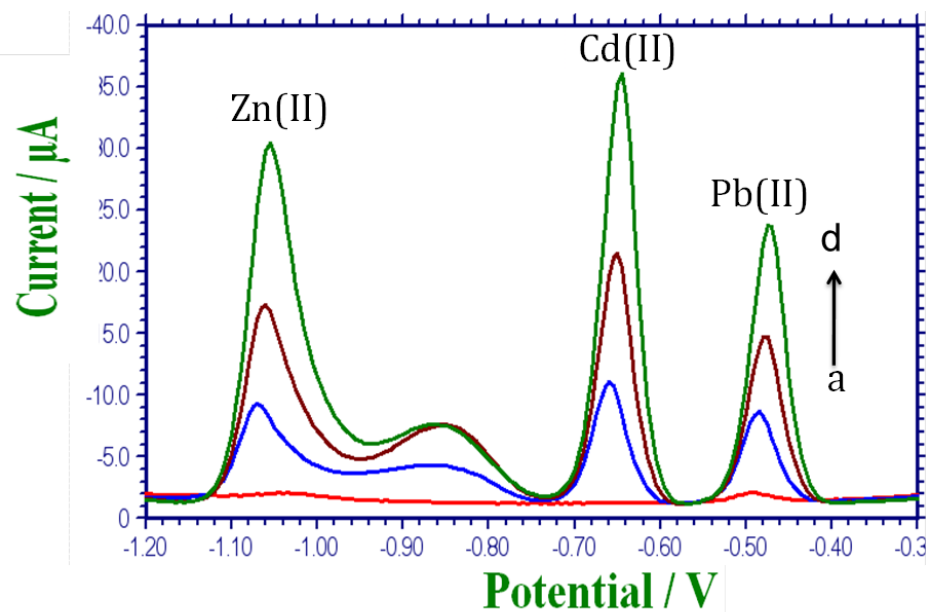


Figure 2.14: Square-wave stripping voltammograms of Zn(II), Cd(II) and Pb(II) at GCE in presence of 10 ppm Hg(II) in acetate buffer solution (0.1 M, pH 3.5); Amplitude, 70 mV; Frequency, 100 Hz; Potential increment, 6 mV; Accumulation time, 2.0 min at -1.4 V. For Zn(II), Cd(II) and Pb(II) concentrations: (a) 0.0, (b) 20 ppb, (c) 40 ppb, (d) 60 ppb.

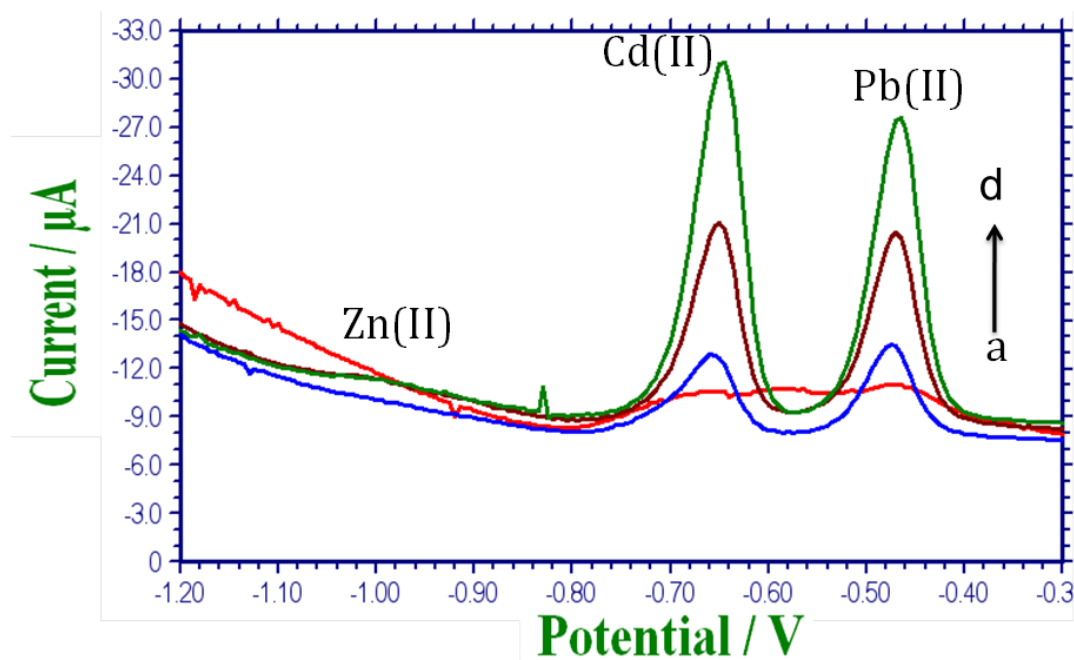


Figure 2.15: Square-wave stripping voltammograms of Zn(II), Cd(II) and Pb(II) at Carbon Paste Electrode in presence of 10 ppm Hg(II) in acetate buffer solution (0.1 M, pH 3.5); Amplitude, 25 mV; Frequency, 25 Hz; Potential increment, 5 mV; Accumulation time, 2.0 min at -1.4 V. For Zn(II), Cd(II) and Pb(II) concentrations: (a) 0.0, (b) 20 ppb, (c) 40 ppb, (d) 60 ppb.

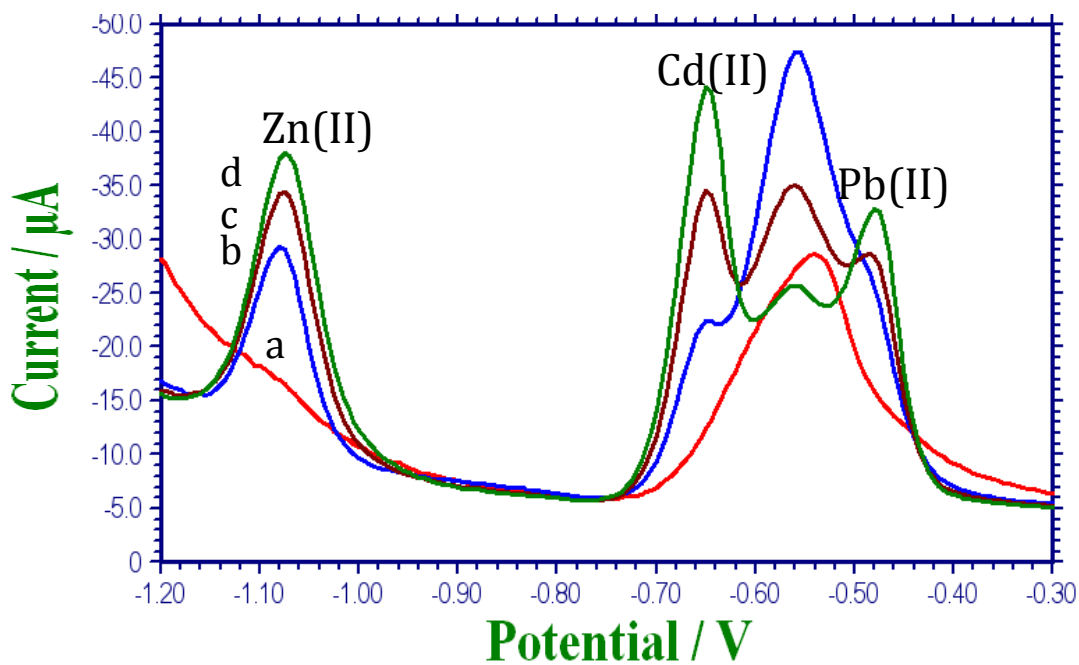


Figure 2.16: Square-wave stripping voltammograms of Zn(II), Cd(II) and Pb(II) at graphite pencil electrode in presence of 10 ppm Hg(II) in acetate buffer solution (0.1 M, pH 3.5); Amplitude, 25 mV; Frequency, 25 Hz; Potential increment, 5 mV; Accumulation time, 2.0 min at -1.4 V. For Zn(II), Cd(II) and Pb(II) concentrations: (a) 0.0, (b) 20 ppb, (c) 40 ppb, (d) 60 ppb.

2.3.5.2 Optimization

Because of the buffer huge role in the detection, several acetate pHs media have been studied to find out the best pH suitable for detection, as shown in Figure 2.17A.

Figure 2.17A shows the square-wave stripping voltammetric responses of 40 ppb Zn(II), Cd(II) and Pb(II) at the glassy carbon electrode (GCE) in presence of 10 ppm Hg(II) in acetate buffer solution (0.1 M) with different pHs: pH 3.0 (a), pH 3.5 (b), and pH 4.0 (c). The lead peaks are not affected by the variation in the pH, the cadmium highest peak is at pH 3.5 while the zinc decreases with increasing the pH in the acetate medium. pH 3.5 was the optimum pH among all examined pHs taking into consideration the three targeted metals (Figure 2.17B).

Effect of frequency has been studied on the response of 40 ppb of Zn(II), Cd(II) and Pb(II) as shown in Figure 2.18A, the electrochemical responses of 40 ppb of Zn(II), Cd(II) and Pb(II) at frequencies 15, 35, 55, 75, 95, 100 and 105 Hz were obtained. Peak current versus frequency were plotted in Figure 2.18B. It has been noticed that the plot is linear up to 100 Hz, and levels off thereafter. For that 100 Hz was chosen for the optimum conditions

It was found also that the larger the pulse amplitude, the higher the Zn(II), Cd(II) and Pb(II) signals as shown in Figure 2.19 with a shift toward the anodic side (Figure 2.19A). The corresponding plot is linear up to 70 mV and levels off thereafter. For that 70 mV was chosen as the optimum pulse amplitude (Figure 2.19B).

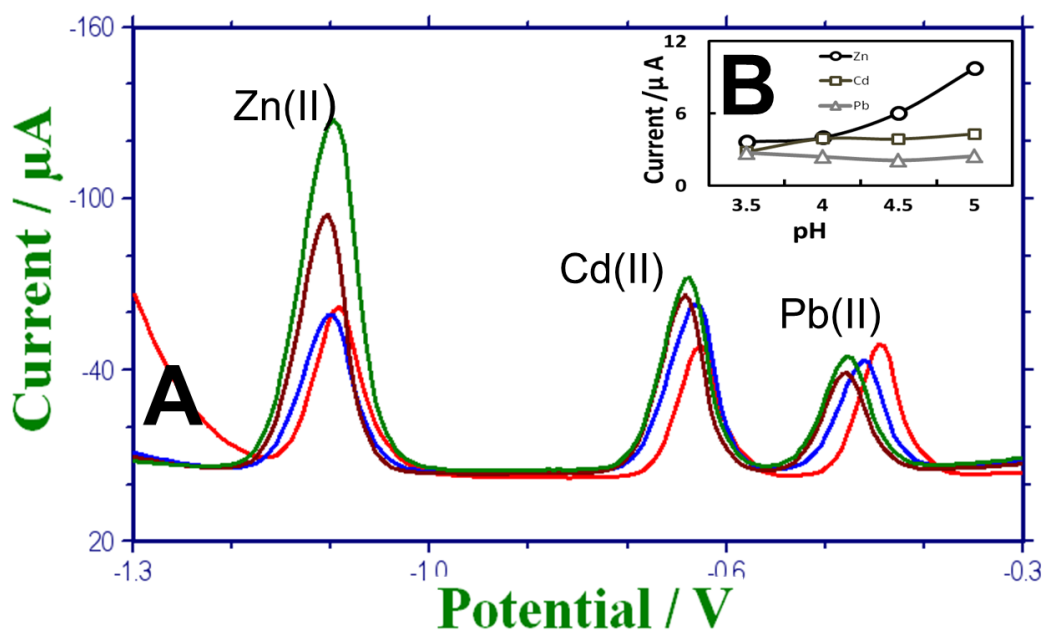


Figure 2.17: (A) Square-wave stripping voltammograms of 40 ppb Zn(II), Cd(II) and Pb(II) at GCE in presence of 10 ppm Hg(II) in acetate buffer solution (0.1 M) at different pH values: (a) pH 3.0, (b) pH 3.5, and (c) pH 4.0; Amplitude, 70 mV; Frequency, 100 Hz; Potential increment, 6 mV; Accumulation time, 2.0 min at -1.4 V. (B) The corresponding plot.

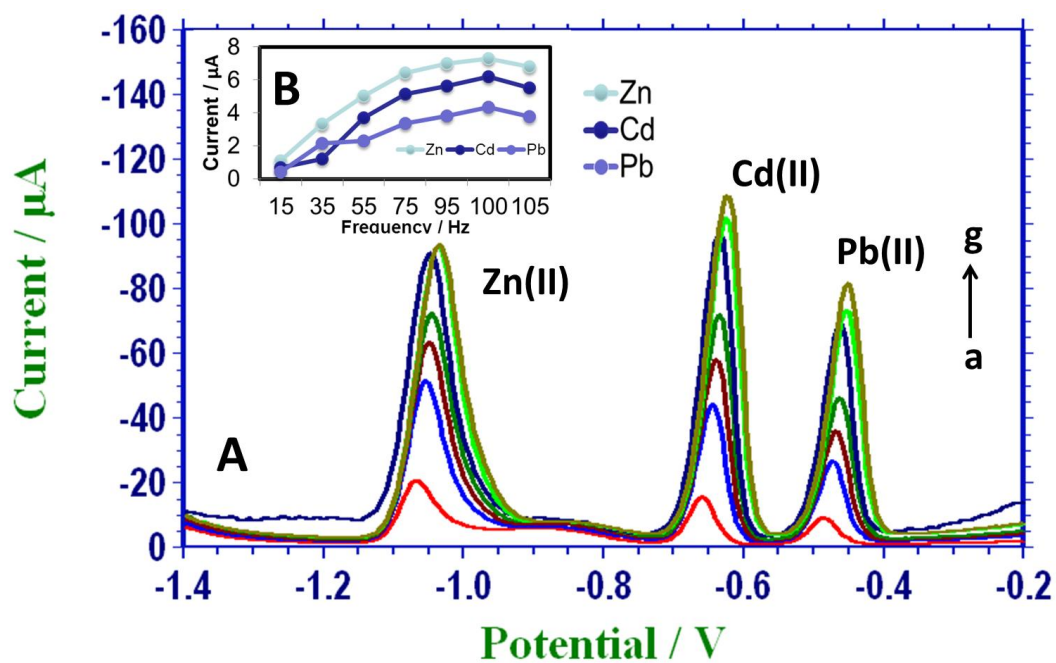


Figure 2.18: (A) Square-wave stripping voltammograms of 40 ppb Zn(II), Cd(II) and Pb(II) at GCE in presence of 10 ppm Hg(II) in acetate buffer solution (0.1 M, pH 3.5); Accumulation time, 2.0 min at -1.4 V ; Potential increment, 5 mV; Amplitude, 25 mV; Frequency: (a) 15 Hz, (b) 35 Hz, (c) 55 Hz, (d) 75 Hz, (e) 95 Hz, (f) 100 Hz, (g) 105 Hz. (B) The corresponding plot.

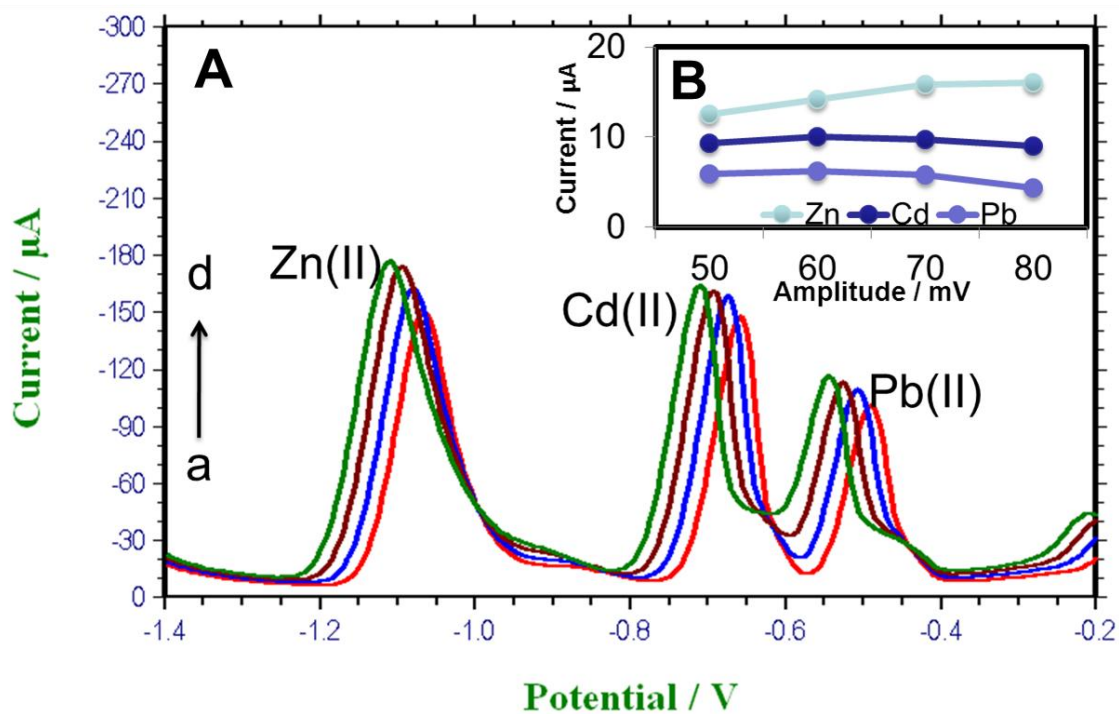


Figure 2.19: (A) Square-wave stripping voltammograms of 40 ppb Zn(II), Cd(II) and Pb(II) at GCE in presence of 10 ppm Hg(II) in acetate buffer solution (0.1 M, pH 3.5); Accumulation time, 2.0 min at -1.4 V; Potential increment, 5 mV; Frequency, 100 Hz; Amplitude: (a) 50 mV, (b) 60 mV, (c) 70 mV, (d) 80 mV. (B) The corresponding plot.

In Figure 2.20 we have studied the influence of varying the potential increment. The signals increase slightly with the increase of the potential increment. We have chosen 7 mV as the optimum potential increment.

We have studied the accumulation potential from -1.2, -1.3, -1.4 to -1.5 V (vs. Ag/AgCl) (Figure 2.21). We have found that there is no big influence on varying the accumulation potential (Figure 2.21B). We choose the optimum potential to be -1.4 V.

2.3.5.3 Reproducibility

The reproducibility study has been carried out by using the optimum parameters for a solution containing 40 ppb of Zn(II), Cd(II) and Pb(II) at GCE in presence of 10 ppm Hg(II) in acetate buffer solution (0.1 M, pH 3.5) and repeated for seven times (Figure 2.22A). The recorded signals of Zn(II), Cd(II) and Pb(II) varied in response as shown in Figure 2.22B.

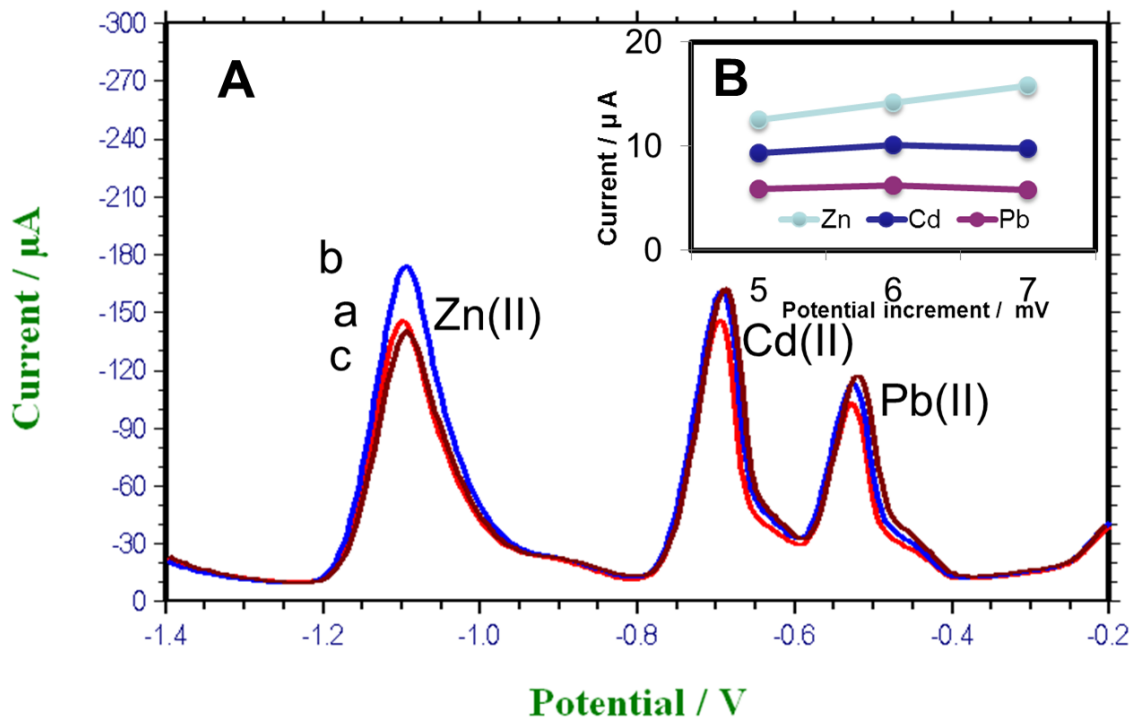


Figure 2.20: (A) Square-wave stripping voltammograms of 40 ppb Zn(II), Cd(II) and Pb(II) at GCE in presence of 10 ppm Hg(II) in acetate buffer solution (0.1 M, pH 3.5); Accumulation time, 2.0 min at -1.4 V; Amplitude, 70 mV; Frequency, 100 Hz; Potential increment: (a) 5 mV, (b) 6 mV, (c) 7 mV. (B) The corresponding plot.

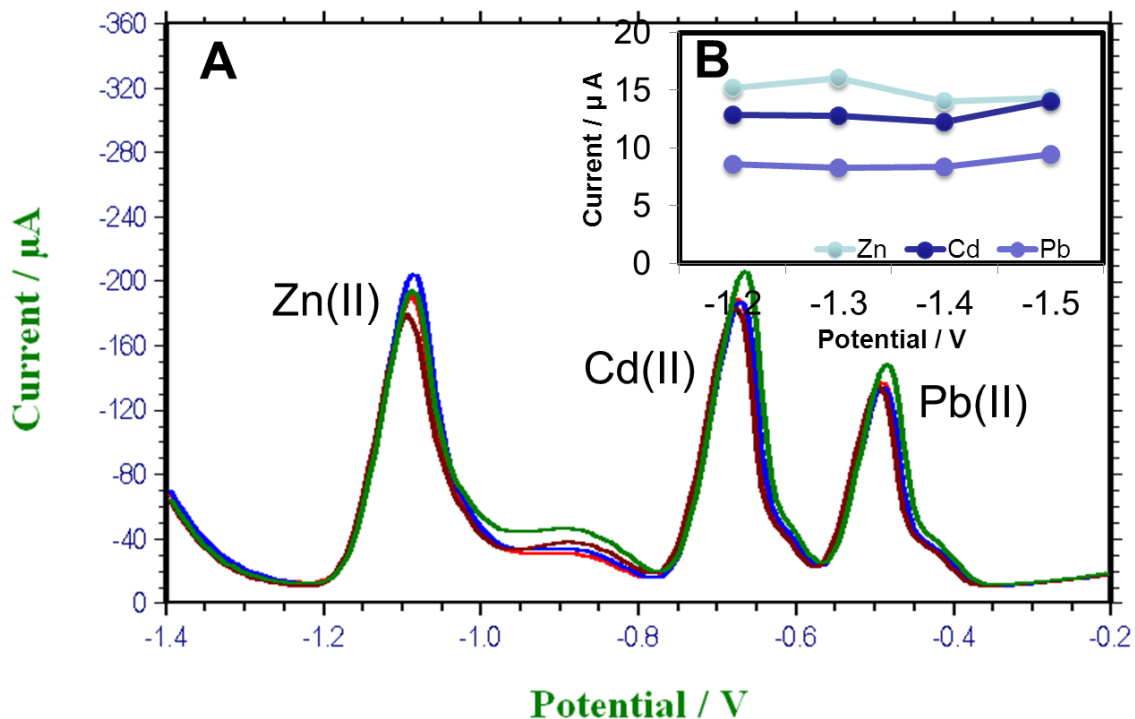


Figure 2.21: (A) Square-wave stripping voltammograms of 40 ppb Zn(II), Cd(II) and Pb(II) at GCE in presence of 10 ppm Hg(II) in acetate buffer solution (0.1 M, pH 3.5); Amplitude, 70 mV; Frequency, 100 Hz; Potential increment, 6 mV; Accumulation time, 2.0 min at: (a) -1.2 V, (b) -1.3 V, (c) -1.4 V, (d) -1.5V. (B) The corresponding plot.

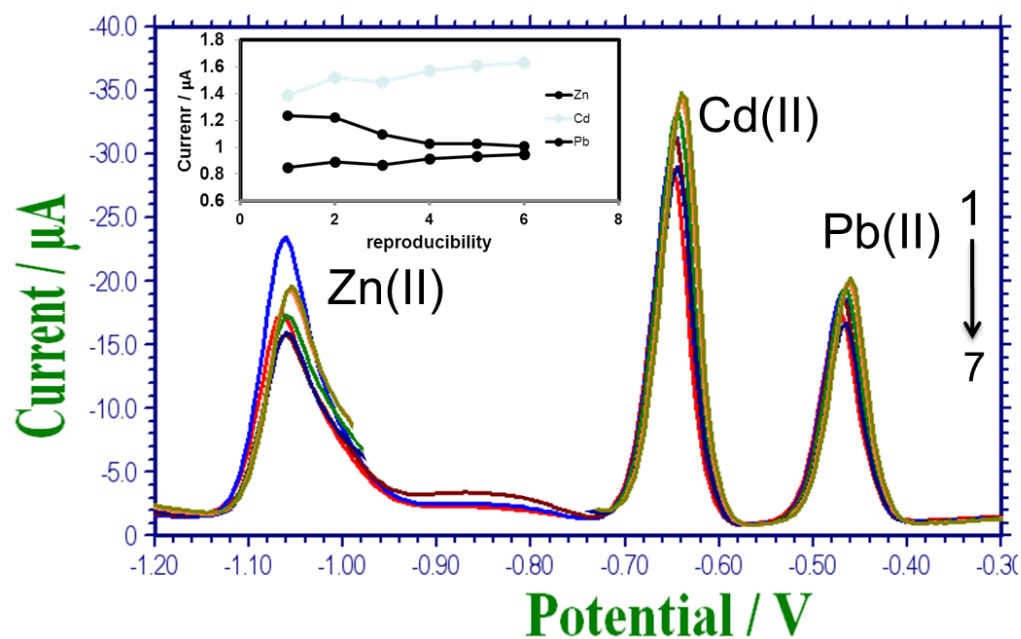


Figure 2.22: (A) Square-wave stripping voltammograms of 40 ppb Zn(II), Cd(II) and Pb(II) at GCE in presence of 10 ppm Hg(II) in acetate buffer solution (0.1 M, pH 3.5); Amplitude, 70 mV; Frequency, 100 Hz; Potential increment, 6 mV; Accumulation time, 2.0 min at -1.4 V. (B) The corresponding plot.

2.3.5.4 Analytical Determination

To study the calibration curve we have used the optimum parameters on the solution containing a mixture of Zn(II), Cd(II) and Pb(II) with the following concentrations: blank, 1, 3, 5, 7, 10, 12, 14, 16, 18 and 20 ppb (Figure 2.23A). Figure 2.23B shows the corresponding calibration plots.

The measured limit of quantitations (LOQs) and the calculated detection limits (DL) obtained using the Hg-GCE modified electrodes as well as the standard deviations are tabulated in Table 2.1.

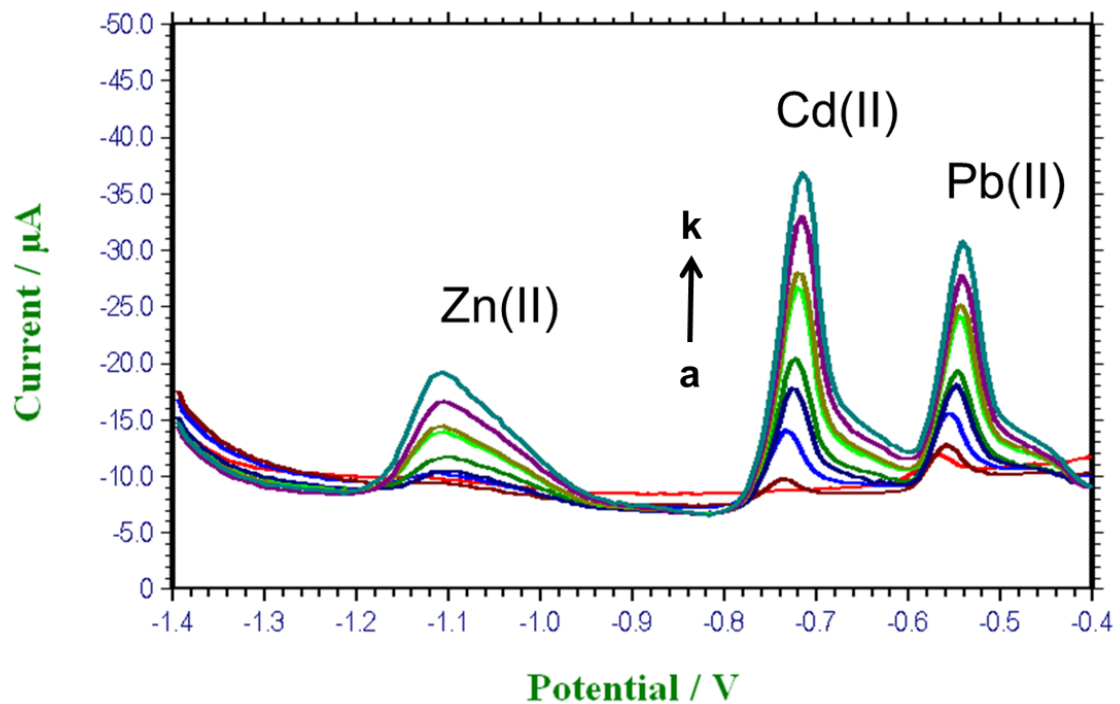


Figure 2.23A: Square-wave stripping voltammograms of Zn(II), Cd(II) and Pb(II) at GCE in presence of 10 ppm Hg(II) in acetate buffer solution (0.1 M, pH 3.5); Amplitude, 70 mV; Frequency, 100 Hz; Potential increment, 6 mV; Accumulation time, 2.0 min at -1.4 V. A mixture of Zn(II), Cd(II) and Pb(II) concentrations: (a) 0.0, (b) 1, (c) 3, (d) 5, (e) 7, (f) 10, (g) 12, (h) 14, (i) 16, (j) 18, (k) 20 ppb.

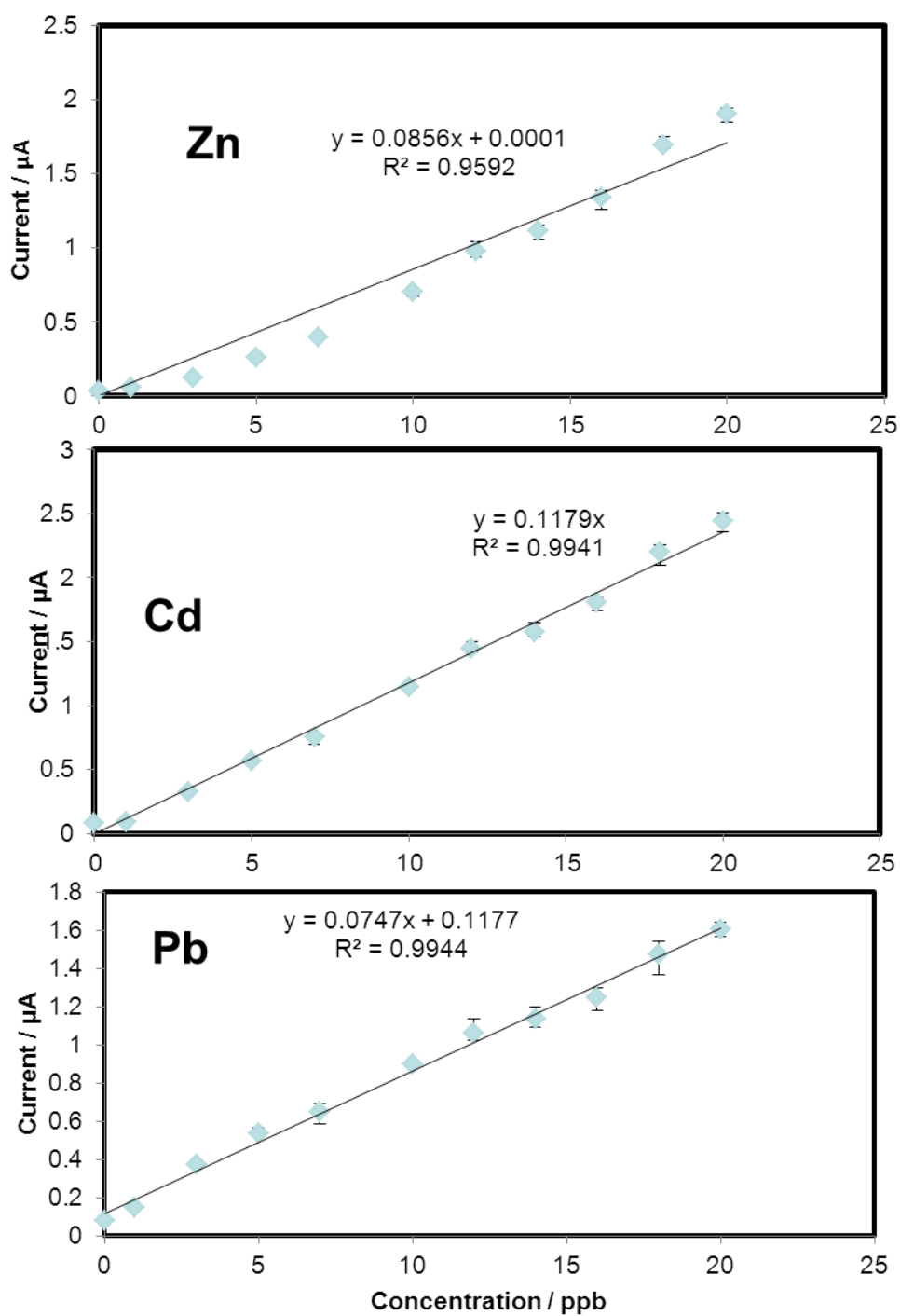


Figure 2.23B: The corresponding calibration plots of Figure 2.23A.

Table 2.1: Limits of Detection and Quantification Obtained at GC-Hg(II) electrode.

Heavy Metal	LOD (ppb)	LOQ (ppb)	RSD (%)
Zn(II)	1.5	3.0	11.9
Cd(II)	1.5	3.0	7.4
Pb(II)	0.3	1.0	6.7

CHAPTER 3

3.0 ELECTROCHEMICAL INVESTIGATION AND ANALYTICAL DETERMINATION OF Zn(II), Cd(II) AND Pb(II) USING Bi/Hg ALLOY-MODIFIED ELECTRODES

3.1 INTRODUCTION

Square wave stripping voltammetry (SWSV) is a powerful technique used for the rapid determination of trace levels of metal ions. Due to the toxicity of the mercury and the environmental concern, stripping voltammetric techniques have been used to develop mercury-free electrodes (65). Several modifiers have been explored such as mercury (74), gold (75), copper (76), lead (77), platinum (78), bismuth (79-81) and bismuth nanoparticles (82) which facilitated the precipitation of amalgam forming and electropositive elements. Other studies suggested the use of dimetallic alloy to enhance the detection such as tin-bismuth (83, 84). In this chapter we are going to explore the Bi/Hg dimetallic alloy to the analytical determination of Zn(II), Cd(II) and Pb(II) heavy metals.

3.2 ELECTROCHEMICAL INVESTIGATION AND ANALYTICAL DETERMINATION

3.2.1 Apparatus

Details of apparatus were described earlier on the subsection 2.2.1.

3.2.2 Electrochemical Transducers Preparation

Details of the electrochemical transducer preparation were described earlier on the subsection 2.2.2.

3.2.3 Reagents

Details of the reagents were described earlier on the subsection 2.2.3. Acetate buffer solution (0.1 M, pH 4.5) was obtained from Sigma (USA).

3.2.4 Procedure

Square wave voltammetry (SWV) measurements were performed by treating the surface at +0.6V for 60s followed by 120s accumulation at -1.4 V in a stirred solution of 0.1 M acetate buffer (pH 4.5). This was followed by a subsequent stripping using a square wave voltammetric waveform, with a 6 mV potential increment, 80 Hz frequency and amplitude of 40 mV. The electrode surface was smoothed and rinsed carefully with deionized water prior to every measurement.

3.2.5 Results and Discussion

After studying several material transducer types we have concluded that the glassy carbon electrode gives the best response for heavy metals determination in drinking water.

3.2.5.1 Electrochemical Investigation

In this work the simultaneous detection of the Zn(II), Cd(II) and Pb(II) heavy metals using SWV technique is possible. (Figure 3.1) shows the square-wave stripping voltammogram for 20 ppb of Zn(II), Cd(II) and Pb(II) at GCE-Hg/Bi alloy. The peaks were identified for the three metals and the peaks area or peaks height are proportional directly to the concentration.

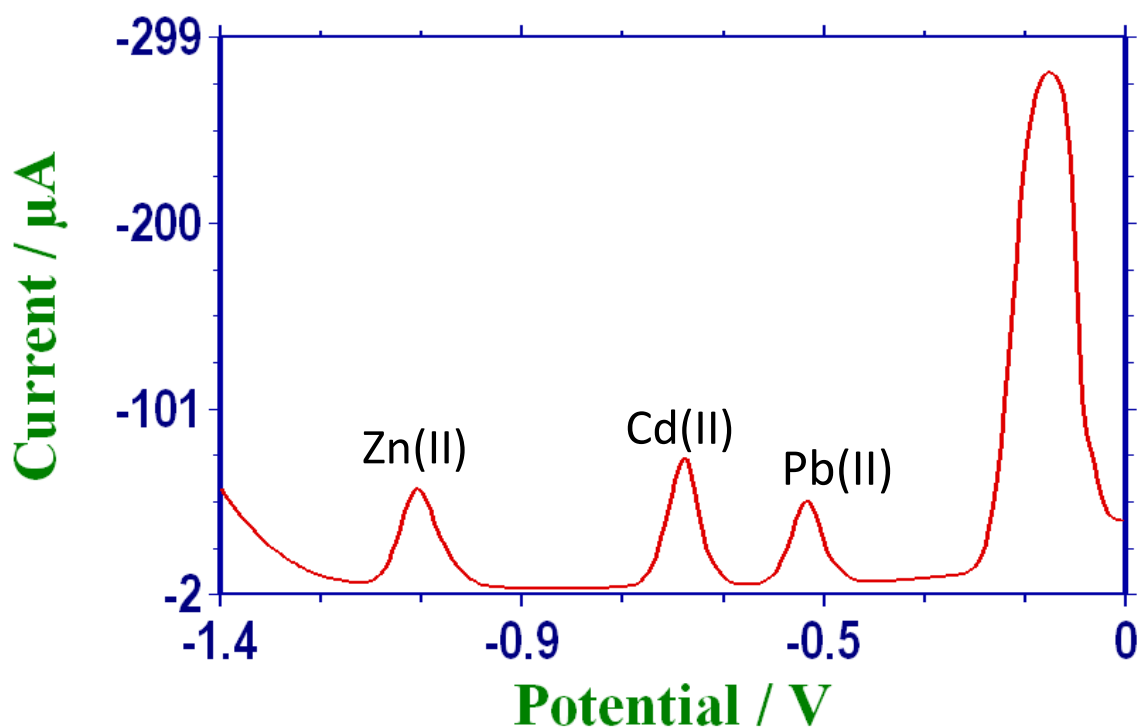


Figure 3.1: Square-wave stripping voltammogram of 20 ppb of Zn(II), Cd(II) and Pb(II) using Glassy Carbon Electrode in the presence of 10 ppm Hg(II) and 600ppb Bi(III) in acetate buffer solution (0.1 M, pH 4.5); Accumulation time, 2.0 min at -1.4 V; Potential increment, 6 mV; Frequency, 80 Hz; Amplitude, 40 mV.

The surface of the working electrode has a huge effect on the detection. A solution containing 20 ppb concentration of Zn(II), Cd(II), and Pb(II) mixture has been detected using three different surfaces, we have found that the voltammogram responses for the GCE-Hg/Bi alloy (c) is better than that obtained at the GCE-Bi (a) or GCE-Hg (b), as shown in Figure 3.2.

Since the influence of adding the two metals together are obvious, more studies have been done to find out the optimum composition of mercury and bismuth concentrations. This is done by keeping the concentration of the mercury constant while varying the concentration of the Bismuth (Figure 3.3) and vice versa (Figure 3.4).

The concentration of the Hg(II) has been fixed at 10 ppm and several voltamograms have been obtained by varying the Bi(III) concentration. The Bi(III) optimum concentration has been found to be 600 ppb as shown in Figure 3.3.

After finding the optimum Bi(III) concentration it is fixed to 600 ppb and we started to vary the Hg(II) as shown in Figure 3.4. After adding 10 ppm of Hg(II) there was no more enhancement in the peak area for the targeted metals. The optimum Hg(II) concentration is 10 ppm (Figure 3.4).

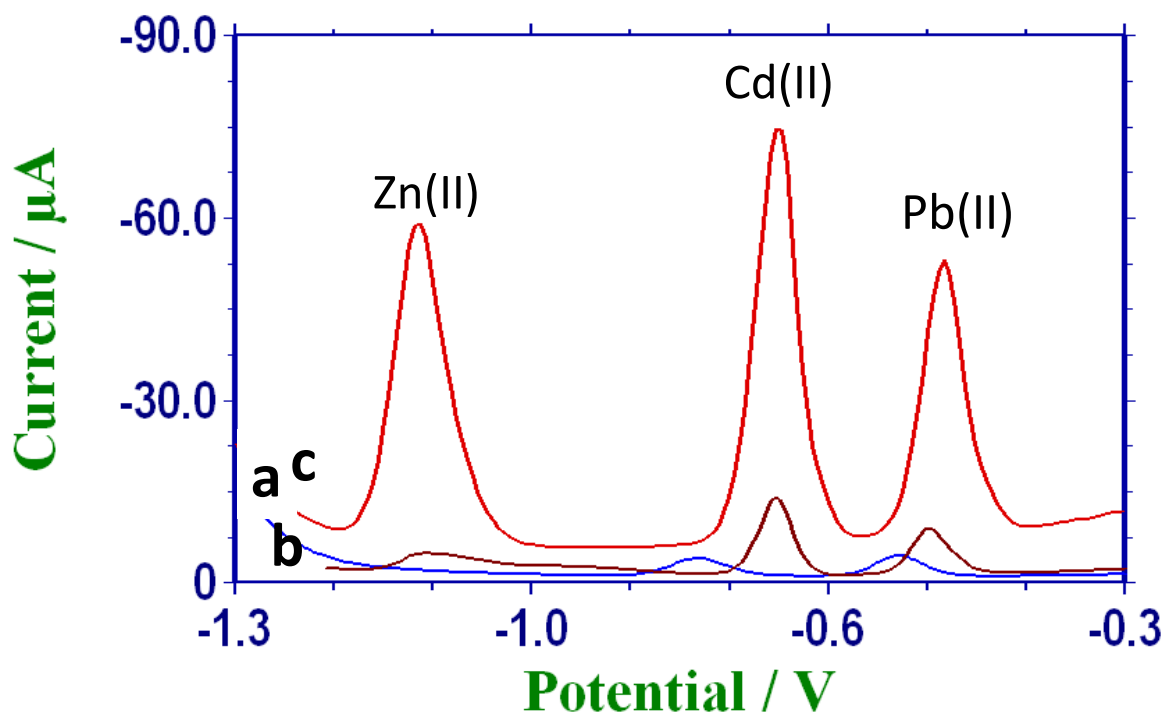


Figure 3.2: Square-wave stripping voltammograms of 20 ppb Zn(II), Cd(II) and Pb(II) at Glassy Carbon Electrode in presence of: (a) 600 ppb Bi(III), (b) 10 ppm Hg(II) and (c) 10 ppm Hg(II) and 600 ppb Bi(III) alloy, in acetate buffer solution (0.1 M, pH 4.5). Other conditions as in Figure 3.1.

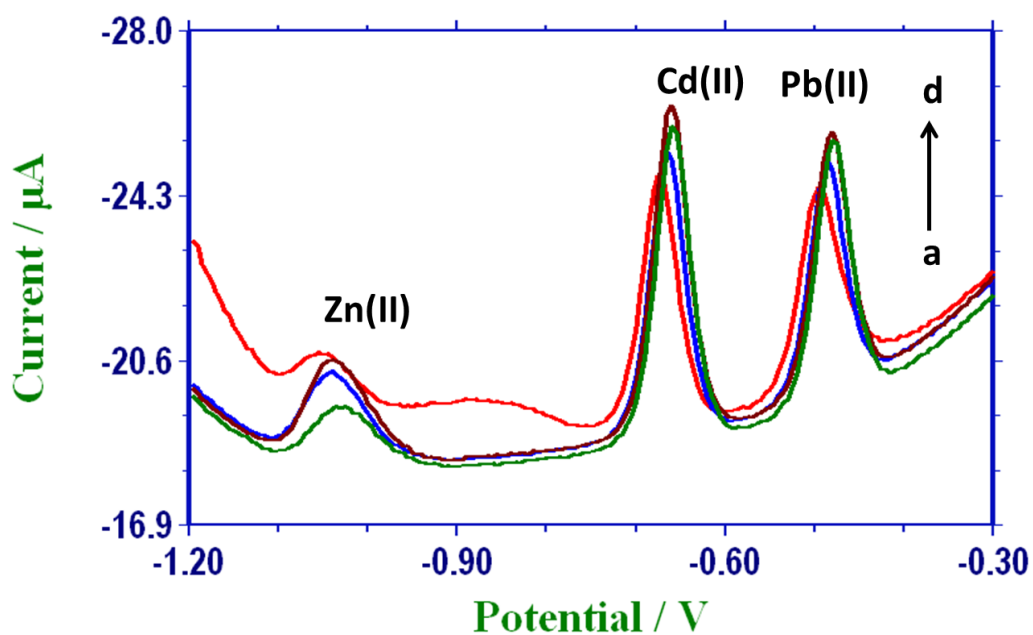


Figure 3.3: Square-wave stripping voltammograms of 20 ppb Zn(II), Cd(II) and Pb(II) using Glassy Carbon Electrode in acetate buffer solution (0.1 M, pH 4.5) containing 10 ppm Hg(II) and Bi(III) concentrations: (a) 100 ppb, (b) 400 ppb, (c) 600 ppb, (d) 800 ppb. Other working conditions as Figure 3.1.

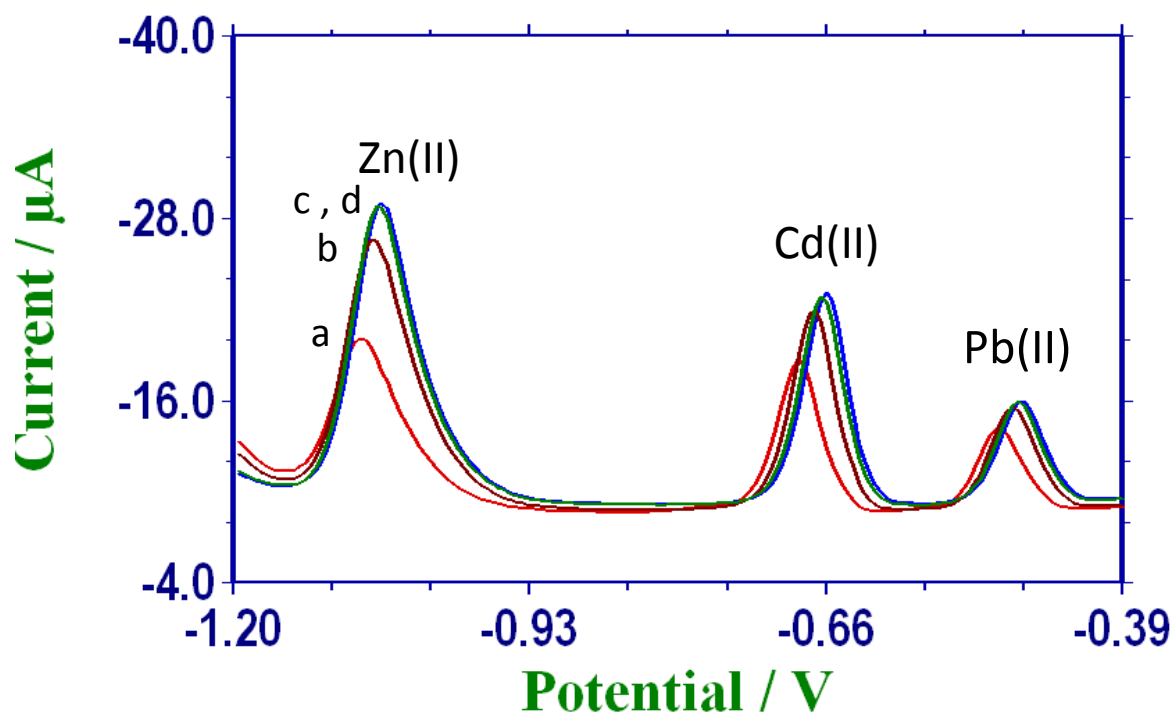


Figure 3.4: Square-wave stripping voltammograms of 20 ppb Zn(II), Cd(II) and Pb(II) using Glassy Carbon Electrode in acetate buffer solution (0.1 M, pH 4.5) containing 600 ppb Bi(III) and Hg(II) concentrations: (a) 1 ppm, (b) 5 ppm, (c) 10 ppm, (d) 15 ppm. Other working conditions as Figure 3.1.

Transducer Selection:

We have screened different transducers in the presence of Bi(III)/Hg(II). The transducers were used here are the Glassy carbon Electrode (GCE, Figure 3.5), the Glassy Carbon Paste Electrode (GCPE, Figure 3.6), the Graphite Pencil Electrode (GPE, Figure 3.7), the Graphite Paste Electrode (CPE, Figure 3.8) and the Carbon Nanotubes Past Electrode (CNPE, Figure 3.9). The response are shown for GCE-Bi/Hg at four different concentrations, 0.0, 20, 40 and 60 ppb, of Zn(II), Cd(II) and Pb(II). As shown clearly, GC is the best transducer among the tested transducers, and thus was used for the subsequent experiments.

Another method is to use CNT dissolved in several solvents (e.g. Nafion and DMF) and 20 μL was dropped at the GCE surface and allowed to dry. Then these surface modified CNT-GCEs were tested as shown in Figure 3.10.

Considering all the tested transducers, the Glassy Carbon Electrode (GCE) gave the best results for the current detection. So it was chosen to carry subsequent experiments.

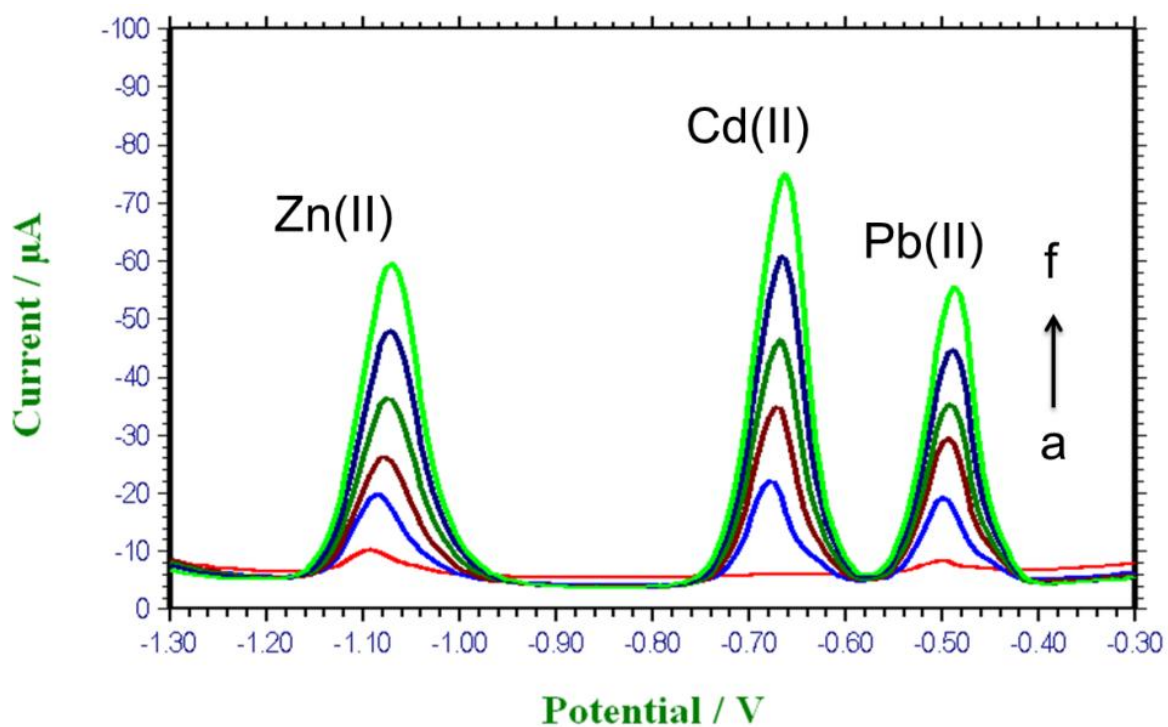


Figure 3.5: Square wave stripping voltammograms of Zn(II), Cd(II) and Pb(II) at Glassy Carbon Electrode (GCE) in presence of 600 ppb Bi(III) and 10 ppm Hg(II) in acetate buffer solution (0.1 M, pH 4.5); Amplitude, 40 mV; Frequency, 80 Hz; Potential increment, 6 mV; Accumulation time, 2.0 min at -1.4 V. For Zn(II), Cd(II) and Pb(II) concentrations: (a) 0.0, (b) 10 ppb, (c) 20 ppb, (d) 30 ppb, (e) 40 ppb, (f) 50 ppb.

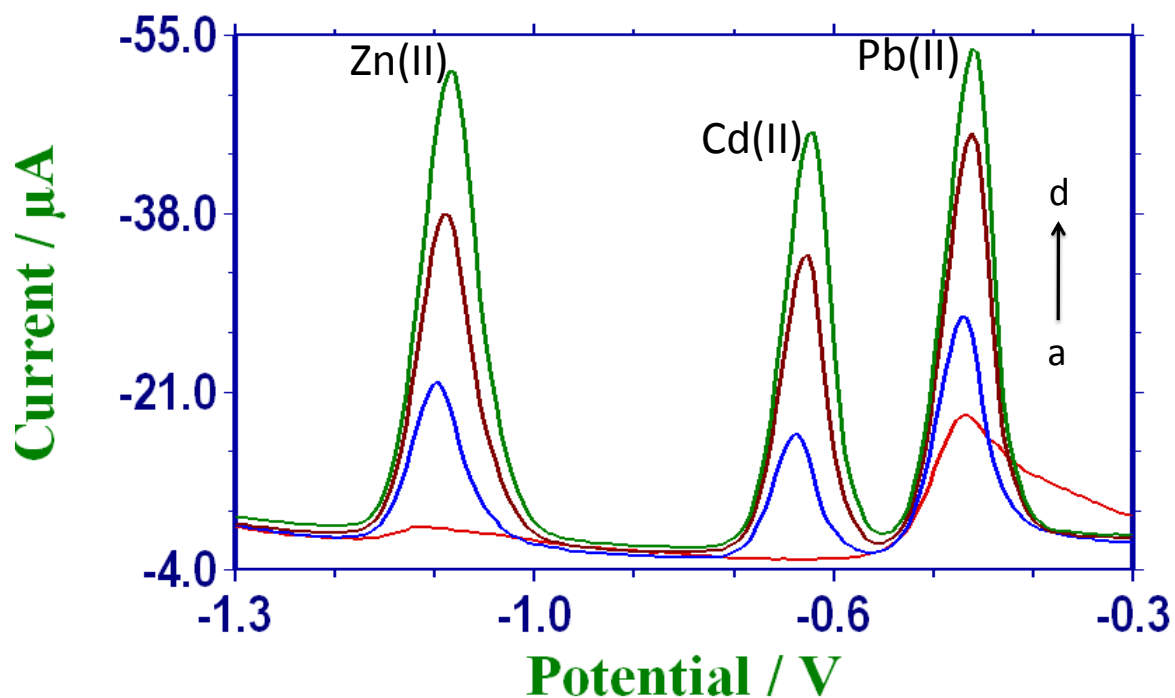


Figure 3.6: Square wave stripping voltammograms of Zn(II), Cd(II) and Pb(II) at Carbon Paste Electrode (CPE) in presence of 600 ppb Bi(III) and 10 ppm Hg(II) in acetate buffer solution (0.1 M, pH 4.5); Amplitude, 40 mV; Frequency, 80 Hz; Potential increment, 6 mV; accumulation time, 2.0 min at -1.4 V. For Zn(II), Cd(II) and Pb(II) concentrations: (a) 0.0, (b) 20 ppb, (c) 40 ppb, (d) 60 ppb.

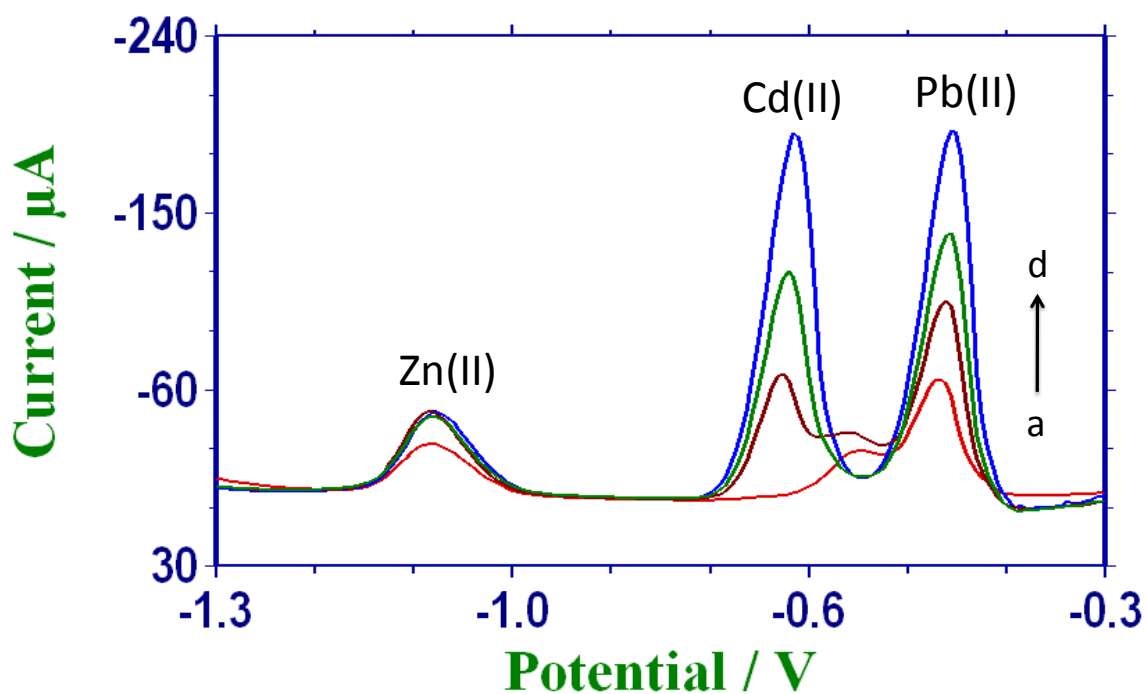


Figure 3.7: Square-wave stripping voltammograms of Zn(II), Cd(II) and Pb(II) at Graphite Pencil Electrode (GPE) in presence of 600 ppb Bi(III) and 10 ppm Hg (II) in acetate buffer solution (0.1 M, pH 4.5); Amplitude, 40 mV; Frequency, 80 Hz; Potential increment, 6 mV; Accumulation time, 2.0 min at -1.4 V. For Zn(II), Cd(II) and Pb(II) concentrations: (a) 0.0, (b) 20 ppb, (c) 40 ppb, (d) 60 ppb.

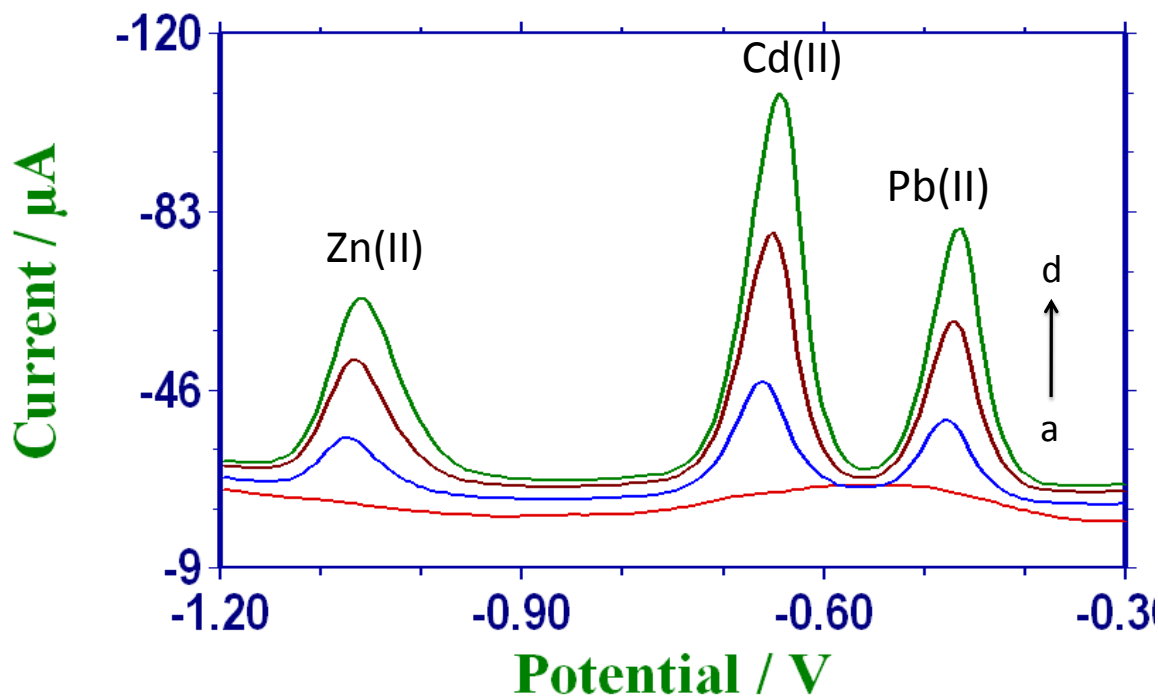


Figure 3.8: Square-wave stripping voltammograms of Zn(II), Cd(II) and Pb(II) at Glassy Carbon Paste Electrode (GCPE) in presence of 600 ppb Bi(III) and 10 ppm Hg (II) in acetate buffer solution (0.1 M, pH 4.5); Amplitude, 40 mV; Frequency, 80 Hz; Potential increment, 6 mV; Accumulation time, 2.0 min at -1.4 V. For Zn(II), Cd(II) and Pb(II) concentrations: (a) 0.0, (b) 20 ppb, (c) 40 ppb, (d) 60 ppb.

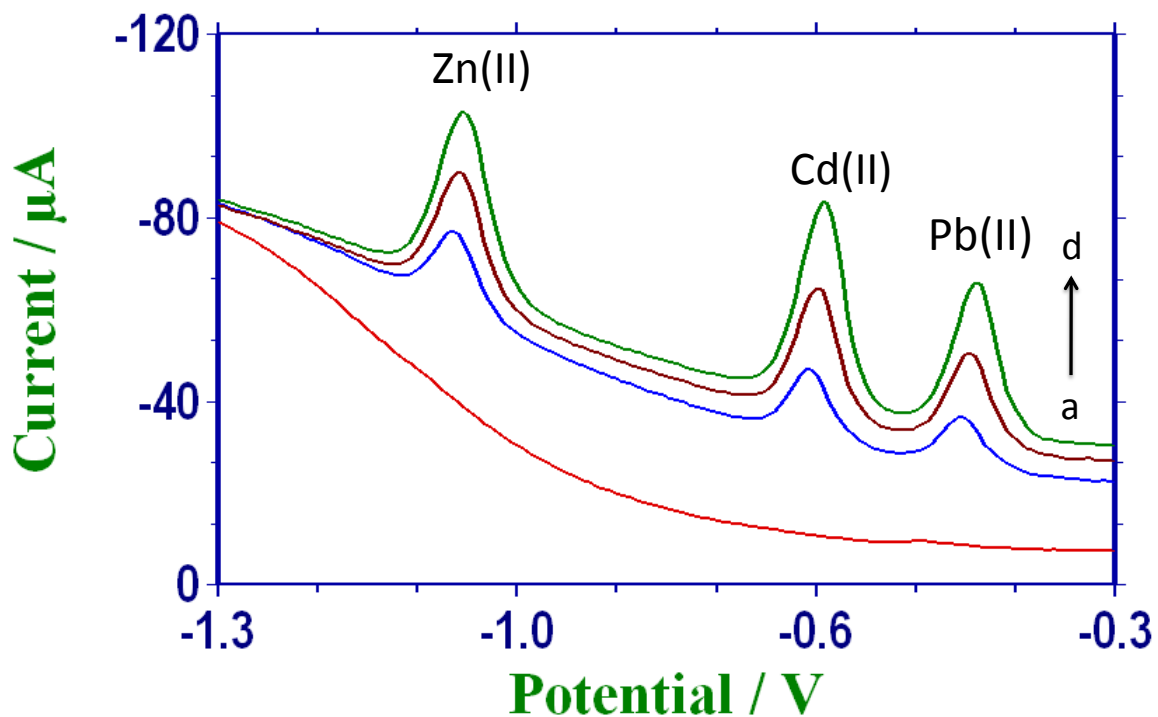


Figure 3.9: Square-wave stripping voltammograms of Zn(II), Cd(II) and Pb(II) at Carbon Nanotubes Paste Electrode (CNTPE) in presence of 600 ppb Bi(III) and 10 ppm Hg (II) in acetate buffer solution (0.1 M, pH 4.5); Amplitude, 40 mV; Frequency, 80 Hz; Potential increment, 6 mV; Accumulation time, 2.0 min at -1.4 V. For Zn(II), Cd(II) and Pb(II) concentrations: (a) 0.0, (b) 20 ppb, (c) 40 ppb, (d) 60 ppb.

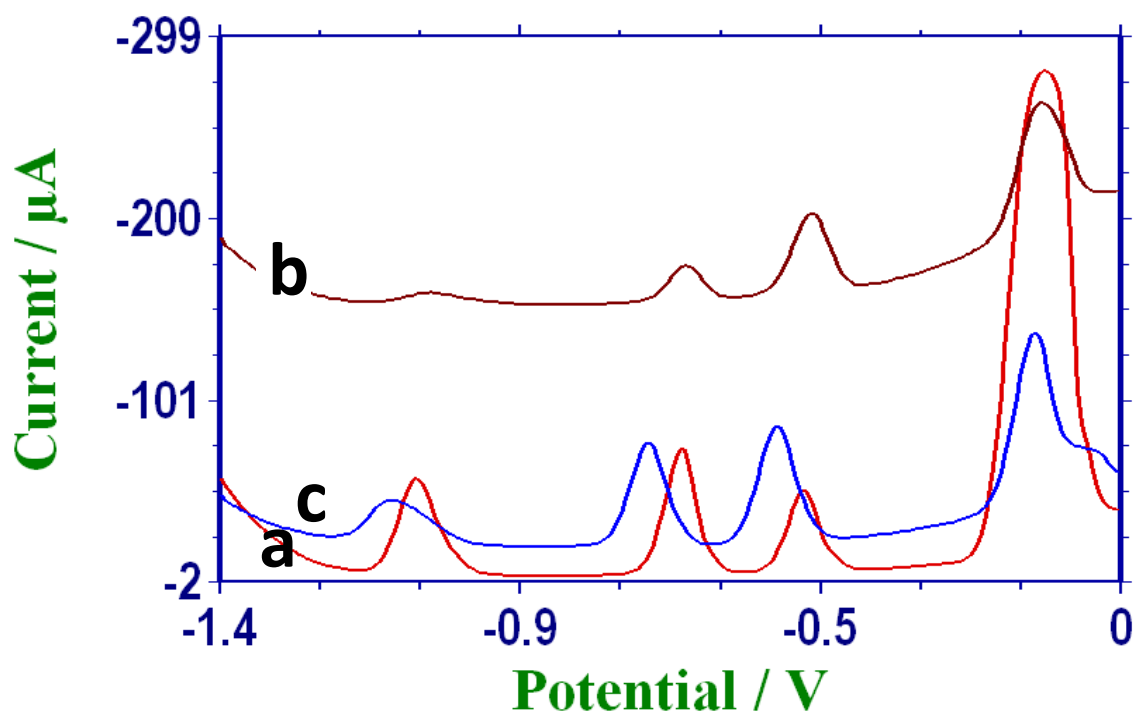


Figure 3.10: Square-wave stripping voltammograms of 20 ppb Zn(II), Cd(II) and Pb(II) at: (a) Bare GCE, (b) CNT/DMF-GCE and (c) CNT/Nafion-GCE. in acetate buffer solution (0.1 M, pH 4.5); Frequency, 80 Hz; Amplitude, 40 mV; Potential increment, 6 mV; Accumulation time 2.0 min at -1.4 V.

3.2.5.2 Optimization

Since the electrical response of the targeted heavy metals relies on the stripping voltammetric detection, it is essential to examine and optimize relevant experimental parameters.

The effect of buffer medium has been carried out by changing the pH value of the acetate buffer in two different analyte concentrations 20 ppb and 40 ppb of Zn(II), Cd(II) and Pb(II). Figure 3.11 and Figure 3.12 show the squarewave stripping voltammetric responses of 20 ppb and 40 ppb of Zn(II), Cd(II) and Pb(II) at the glassy carbon electrode (GCE) in acetate buffer solutions with different pHs. There was a cathodic potential shift for the Zn(II), Cd(II) and Pb(II) oxidation peak position with the increase of the pH. In the acetate medium, pH 4.5 was the optimum pH among all examined pHs with respect to the height and shape of the obtained oxidation peaks of the tested analytes.

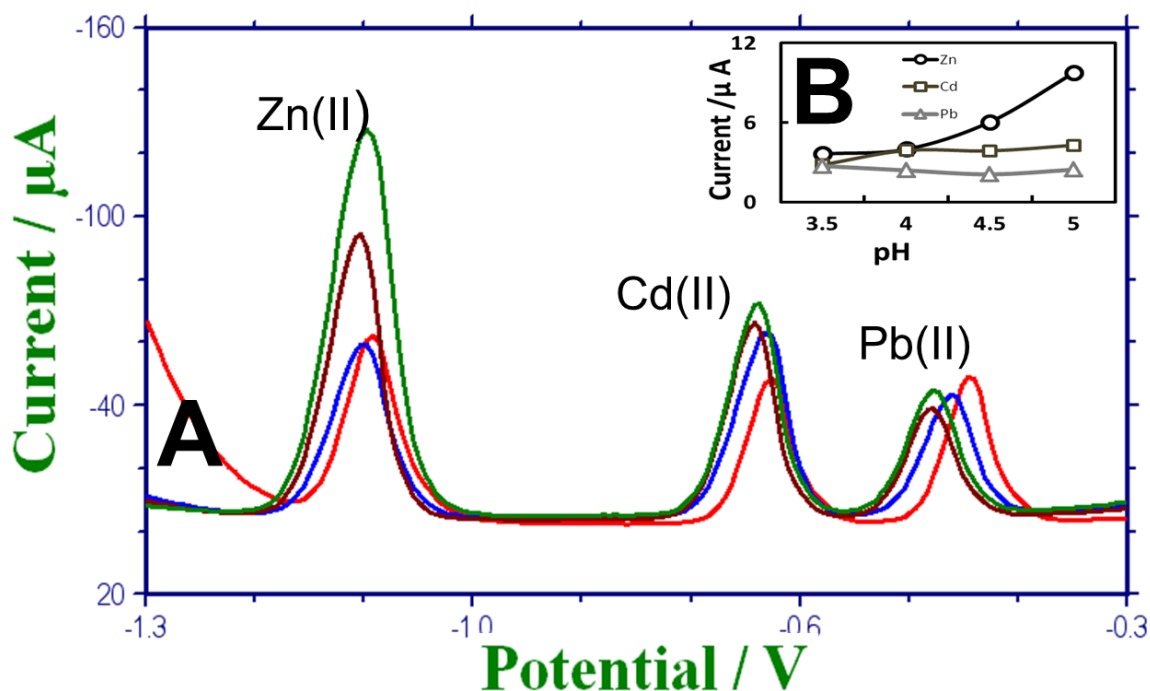


Figure 3.11: (A) Square-wave stripping voltammograms of 20 ppb of Zn(II), Cd(II) and Pb(II) heavy metals at GCE in the presence of 600 ppb Bi(III) and 10 ppm Hg(II), in acetate buffer solution (0.1M) at different pH values: (a) pH 3.5, (b) pH 4.0, (c) pH 4.5, (d) pH 5.0; Amplitude, 40 mV; Frequency, 80 Hz; Potential increment, 6 mV; Accumulation time, 2.0 min at -1.4V. (B) The corresponding plot.

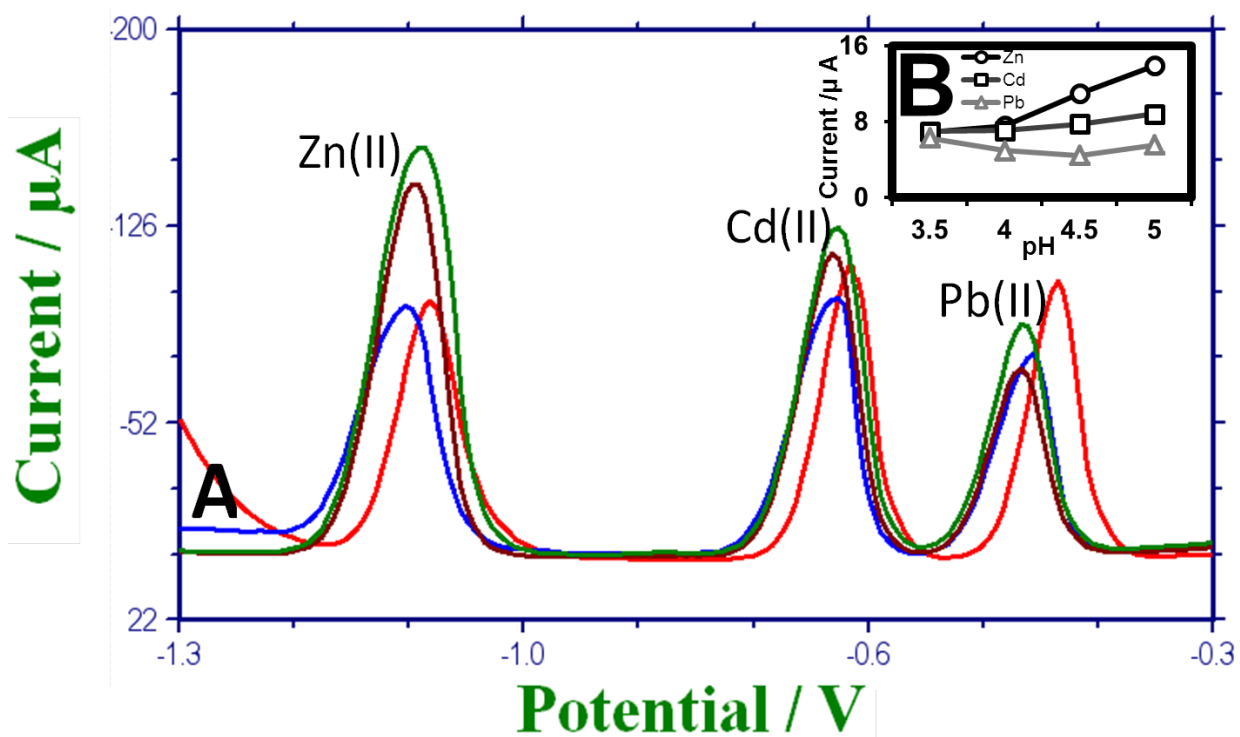


Figure 3.12: (A) Square-wave stripping voltammograms of 40 ppb of Zn(II), Cd(II) and Pb(II) heavy metals at GCE in the presence of 600 ppb Bi(III) and 10 ppm Hg(II), in acetate buffer solution (0.1M) at different pH values: (a) pH 3.5, (b) pH 4.0, (c) pH 4.5, (d) pH 5.0; Amplitude, 40 mV; Frequency, 80 Hz; Potential increment, 6 mV; Accumulation time, 2.0 min at -1.4V. (B) The corresponding plot.

Effect of frequency has been studied on the response of 20 ppb of Zn(II), Cd(II) and Pb(II) as shown in Figure 3.13A, the electrochemical responses of 20 ppb of Zn(II), Cd(II) and Pb(II) at frequencies from 10 to 100 in 10 Hz steps were obtained. Peak current versus frequency were plotted in Figure 3.13B. It has been noticed that the signal increases linearly up to 80 Hz and then levels off. For that 80 Hz was chosen for the optimum conditions.

It was found also that the larger the pulse amplitude, the higher the Zn(II), Cd(II) and Pb(II) as shown in Figure 3.14A. The responses were increasing is enhancing till 40 mV then it start to decrease (Figure 3.14B). For that 40 mV was chosen as the optimum pulse amplitude.

In Figure 3.15, we have studied the influence of varying the potential increment where the signals increased linearly and started to decrease after 6 mV. So we choose 6 mV as the optimum potential increment.

Since we are trying to detect Zn(II) at -1.1 V it will be convenient to go lower in potential. We have studied -1.2, -1.3, -1.4 and -1.5 V (vs. Ag/AgCl) accumulation potential as shown in Figure 3.16. We have found that there is an increase in the signal with decreasing the accumulation potential. That increase stops at -1.4 V for the Zn(II) and Cd(II) while it continues for the Pb(II). We choose the optimum potential at -1.4 V.

As expected increasing the accumulation time increases the signals for Zn(II), Cd(II) and Pb(II) yet after 600 Sec, the Zn(II) signal starts to decrease. We have decided to set the accumulation time at 240 Sec to have a good detection, yet with fast experiment (Figure 3.17).

3.2.5.3 Reproducibility

The reproducibility study has been carried out under the optimum parameters for a solutions contain 20 ppb of Zn(II), Cd(II) and Pb(II) (Figure 3.18), and another solution containing 40 ppb of Zn(II), Cd(II) and Pb(II) (Figure 3.19) at GCE in presence of 600 ppb Bi(III) and 10 ppm Hg(II) in acetate buffer solution (0.1 M, pH 4.5) and repeated for seven times. The RSD values were calculated and tabulated in Table 3.1.

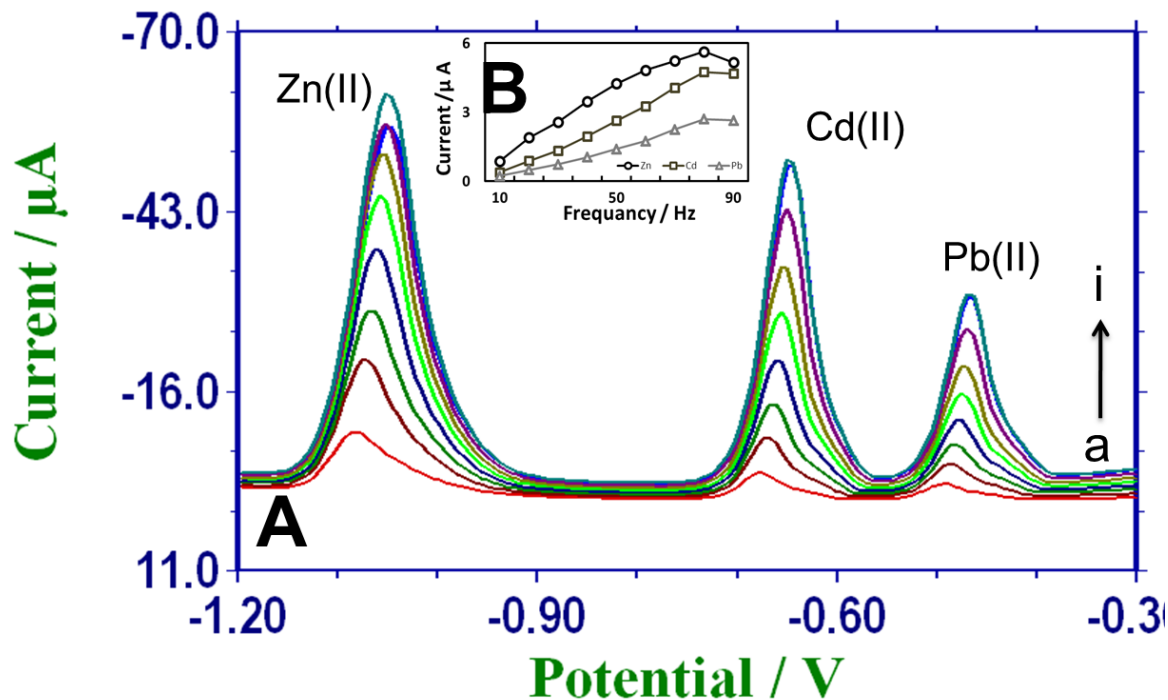


Figure 3.13: (A) Square-wave stripping voltammograms of 20 ppb Zn(II), Cd(II) and Pb(II) at GCE in presence of 600 ppb Bi(III) and 10 ppm Hg(II), in acetate buffer solution (0.1 M, pH 4.5); Accumulation time, 2.0 min at -1.4V; Amplitude, 40 mV; Potential increment, 6 mV; Frequency: (a) 10 Hz, (b) 20 Hz, (c) 30 Hz, (d) 40 Hz, (e) 50 Hz, (f) 60 Hz, (g) 70 Hz, (h) 80 Hz, (i) 90 Hz. (B) The corresponding plot.

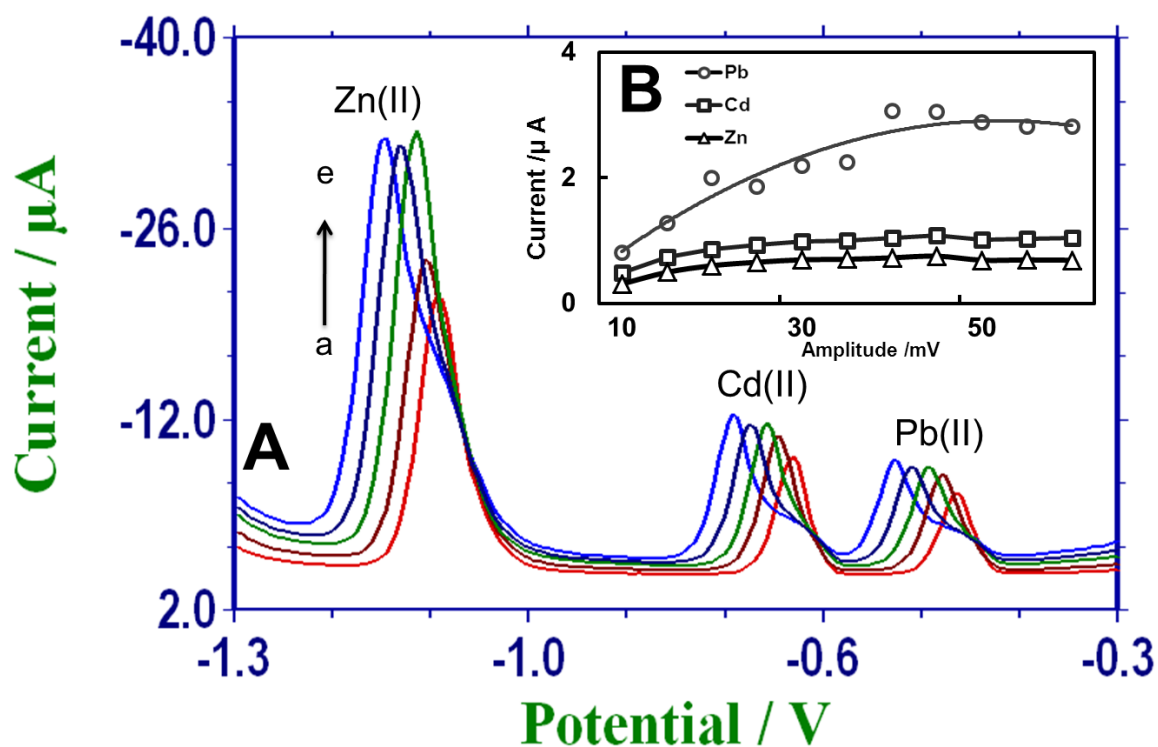


Figure 3.14: (A) Square-wave stripping voltammograms of 20 ppb Zn(II), Cd(II) and Pb(II) at GCE in presence of 600 ppb Bi(III) and 10 ppm Hg(II), in acetate buffer solution (0.1 M, pH 4.5); Accumulation time, 2.0 min at -1.4 V; Accumulation time, 2.0 min at -1.4V; Potential increment, 5 mV; Frequency, 25 Hz; Amplitude: (a) 20 mV, (b) 30 mV, (c) 40 mV, (d) 50 mV, (e) 60 mV. (B) The corresponding plot.

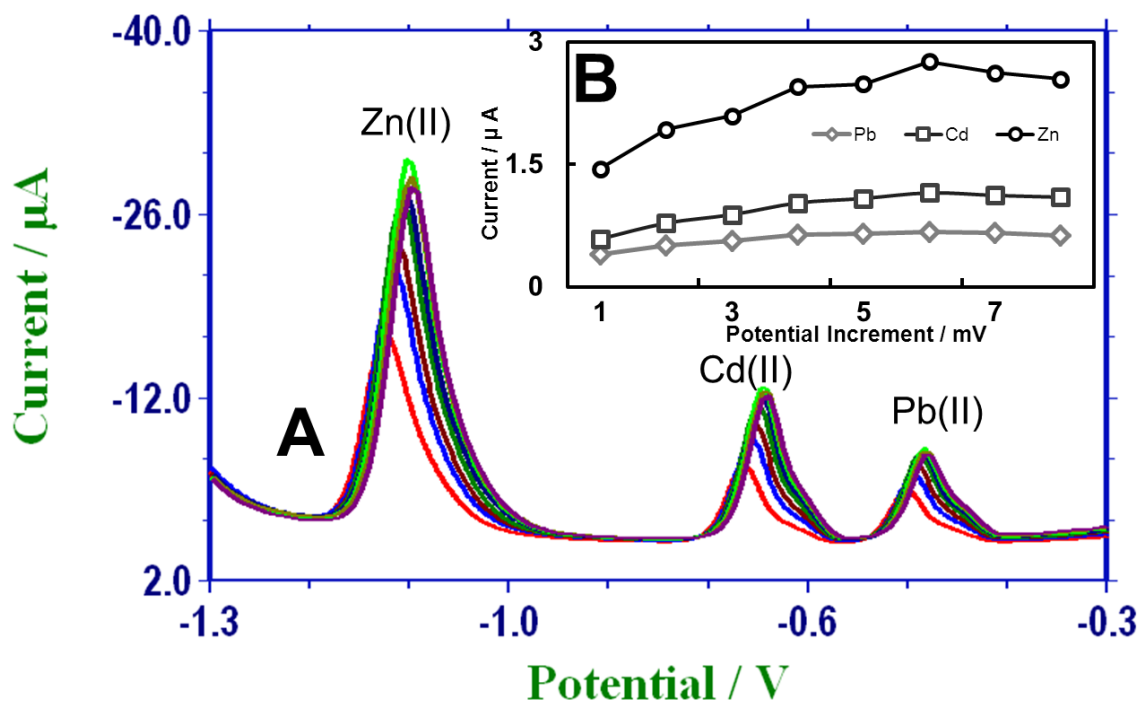


Figure 3.15: (A) Square-wave stripping voltammograms of 20 ppb Zn(II), Cd(II) and Pb(II) at GCE in presence of 600 ppb Bi(III) and 10 ppm Hg(II) in acetate buffer solution (0.1 M, pH 4.5); Accumulation time, 2.0 min at -1.4V; Frequency, 25 Hz; Amplitude, 40 mV; Potential increment: (a) 1 mV, (b) 2 mV, (c) 3 mV, (d) 4 mV, (e) 5 mV, (f) 6 mV, (g) 7 mV, (h) 8 mV. (B) The corresponding plot.

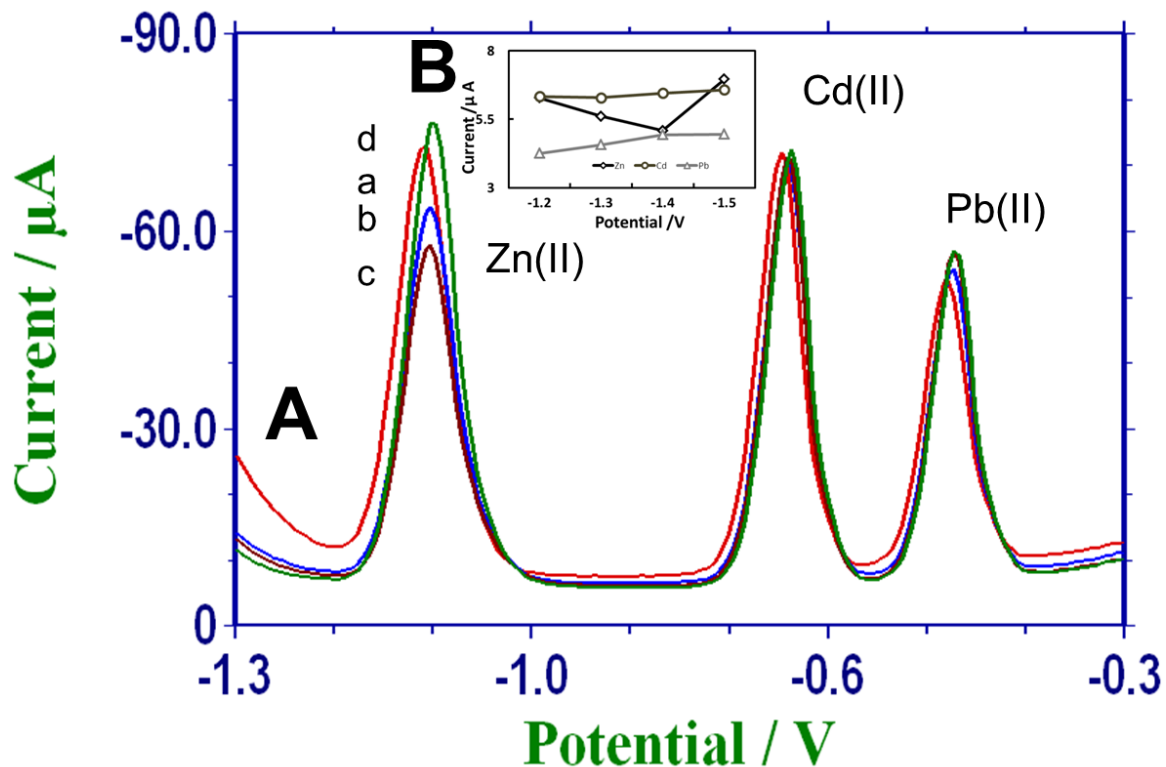


Figure 3.16: (A) Square-wave stripping voltammograms of 20 ppb Zn(II), Cd(II) and Pb(II) at GCE in presence of 600 ppb Bi(III) and 10 ppm Hg(II), in acetate buffer solution (0.1 M, pH 4.5). Amplitude 40 mV; Frequency, 80 Hz; Potential increment, 6 mV; Accumulation time, 2.0 min at: (a) -1.2 V, (b) -1.3 V, (c) -1.4 V, (d) -1.5 V. (B) The corresponding plot.

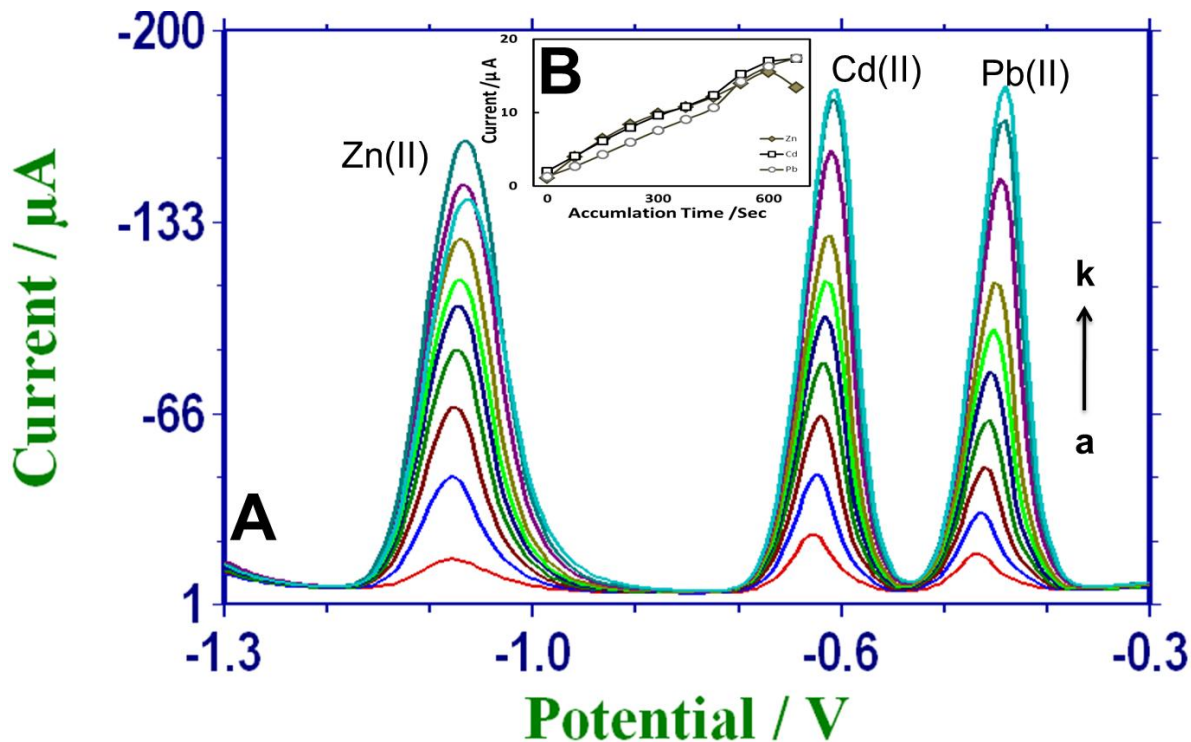


Figure 3.17: (A) Square-wave stripping voltammograms of 20 ppb Zn(II), Cd(II) and Pb(II) at GCE in presence of 600 ppb Bi(III) and 10 ppm Hg (II), in acetate buffer solution (0.1 M, pH 4.5); Amplitude, 40 mV; Frequency, 80 Hz; Potential increment, 6 mV; Accumulation Time at potential - 1.4 V for: (a) 60 Sec, (b) 120 Sec, (c) 180 Sec, (d) 240 Sec, (e) 300 Sec, (f) 360 Sec, (g) 420 Sec, (h) 480 Sec, (i) 540 Sec, (j) 600 Sec and (k) 660 Sec. (B) The corresponding plot.

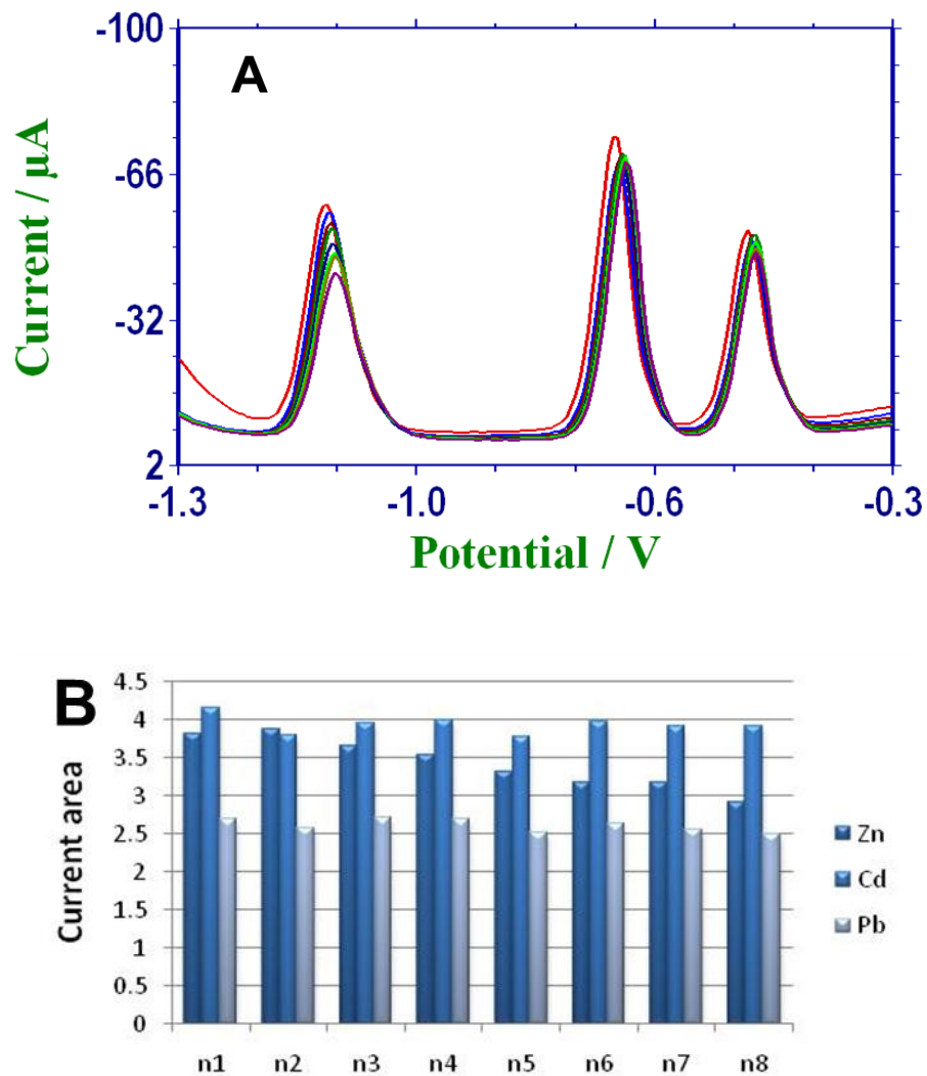


Figure 3.18: (A) Square-wave stripping voltammograms for 20 ppb Zn(II), Cd(II) and Pb(II) at GCE in presence of 600 ppb Bi(III) and 10 ppm Hg(II) in acetate buffer solution (0.1 M, pH 4.5); Amplitude 40 mV; Frequency, 80 Hz; Potential increment, 6 mV; Accumulation time, 2.0 min at -1.4 V. (B) The corresponding histogram showing the degree of reproducibility.

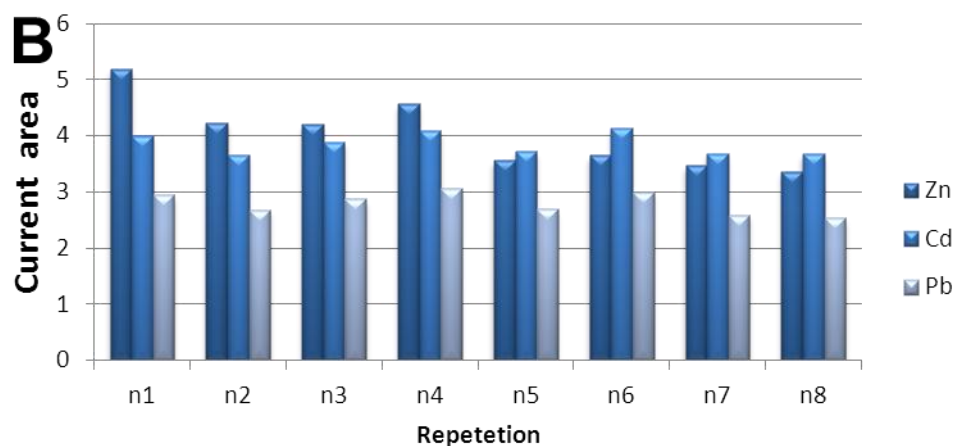
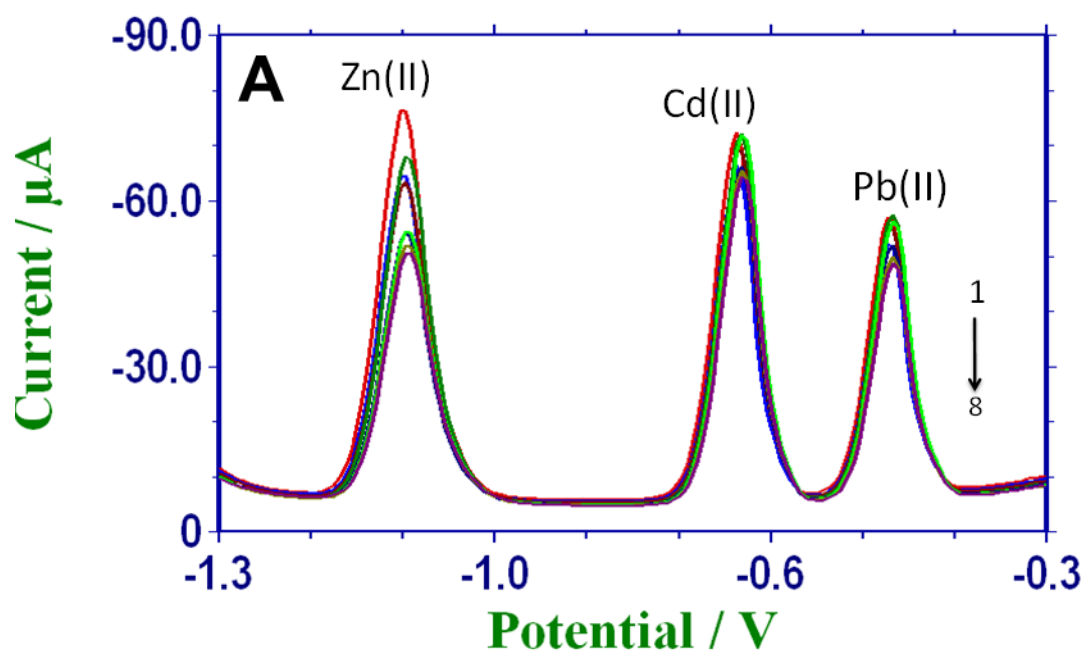


Figure 3.19: (A) Square-wave stripping voltammograms of 40 ppb Zn(II), Cd(II) and Pb(II) at GCE in presence of 600 ppb Bi(III) and 10 ppm Hg(II) in acetate buffer solution (0.1 M, pH 4.5); Amplitude 40 mV; Frequency, 80 Hz; Potential increment, 6 mV; Accumulation time, 2.0 min at -1.4 V. (B) The corresponding histogram showing the degree of reproducibility.

3.2.5.4 Analytical Determination

To study the calibration curve we have used the optimum parameters at a concentration range from 5 ppb to 250 ppb as shown in Figure 3.20A followed by constructing calibration plots as shown in Figure 3.20B. Limits of detection and quantitation are calculated as in Table 3.1.

3.2.5.5 Interferences

In this section we report on the effect of inorganic interferences such as Cu(II) as well as some organic compounds on the obtained Zn(II), Cd(II) and Pb(II) peaks. Copper ions (II) effect is shown in Figure 3.21. Where the Zn(II) signal was completely disappeared by adding 1 ppm of Cu(II).

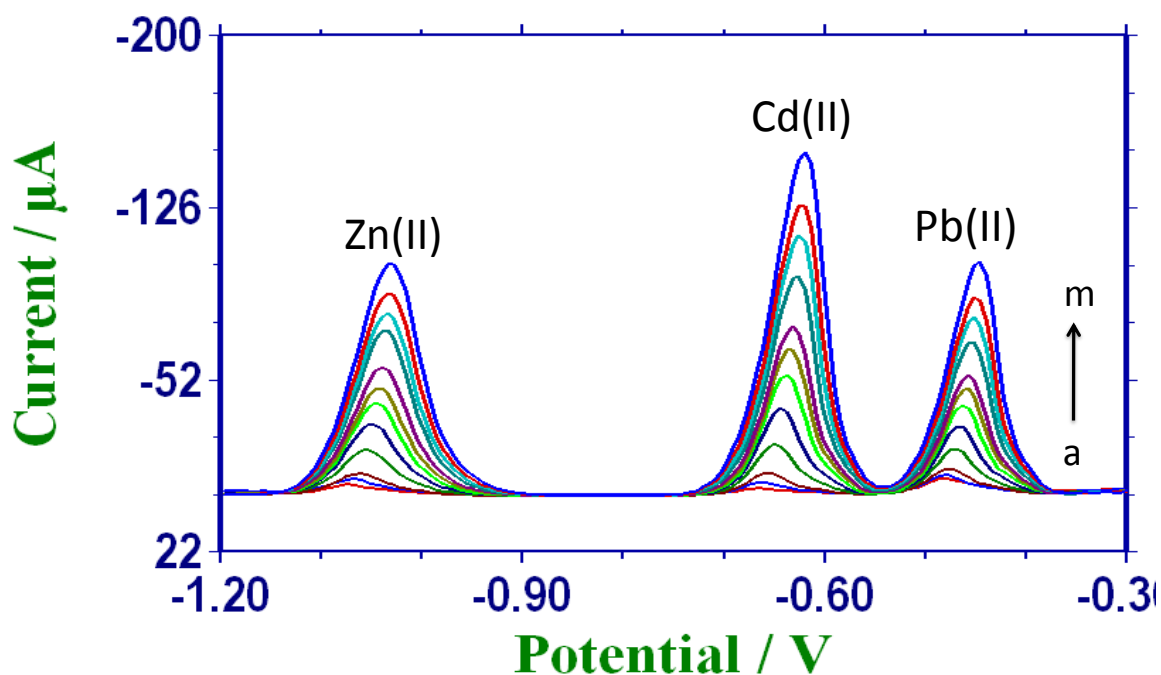


Figure 3.20A: Square-wave stripping voltammograms of Zn(II), Cd(II) and Pb(II) at GCE in presence of 600 ppb Bi(III) and 10 ppm Hg(II) in acetate buffer solution (0.1 M, pH 4.5); Amplitude, 40 mV; Frequency, 80 Hz; Potential increment, 6 mV; Accumulation time, 2.0 min at -1.4 V. A mixture of Zn(II), Cd(II) and Pb(II) concentrations: (a) 0.0, (b) 1, (c) 3, (d) 5, (e) 10, (f) 15, (g) 20, (h) 25, (i) 30, (j) 35, (k) 40, (l) 45, and (m) 50 ppb.

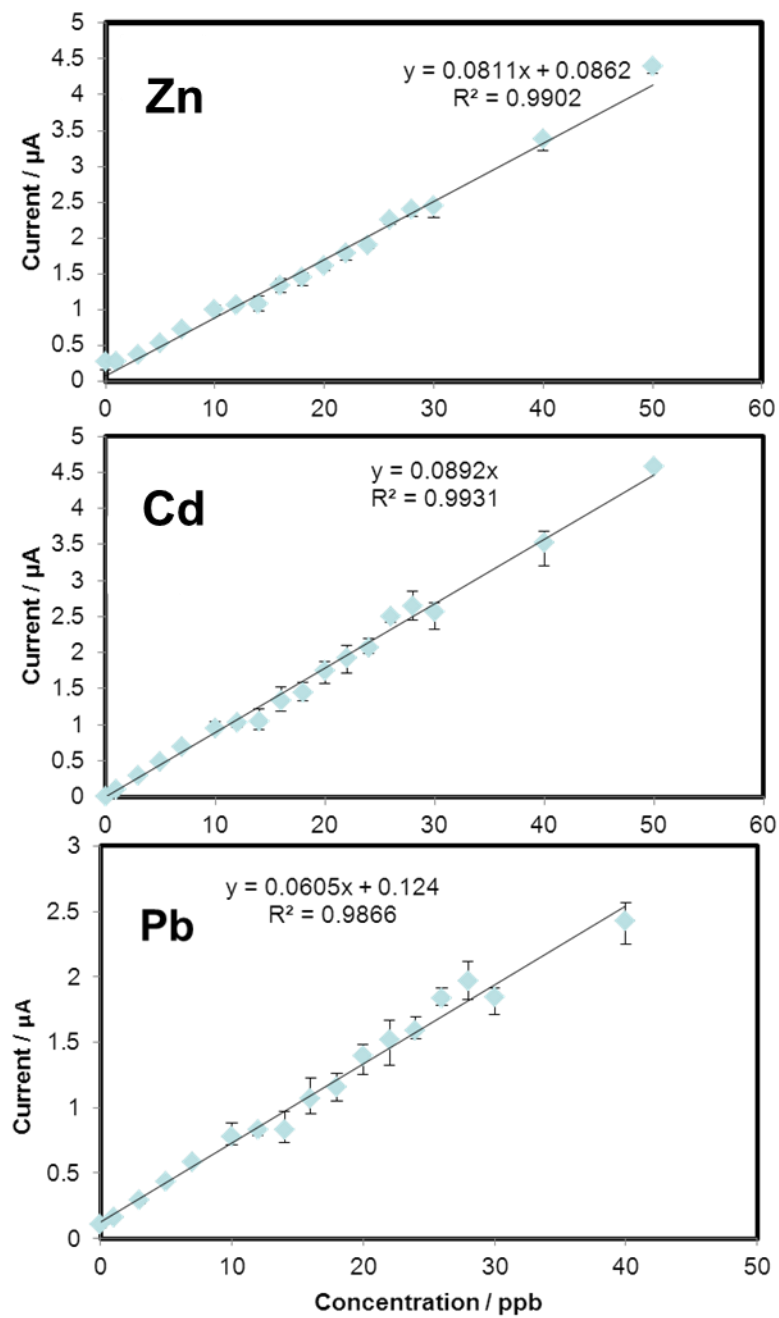


Figure 3.20B: The corresponding calibration plots of Figure 3.20A

Table 3.1: Limits of Detection and Quantification Obtained at GC-Hg(II)/Bi(III) alloy electrode.

Heavy Metal	LOD (ppb)	LOQ (ppb)	RSD (%)
Zn(II)	0.36	1.0	10.41
Cd(II)	0.01	1.0	2.72
Pb(II)	0.61	1.0	2.70

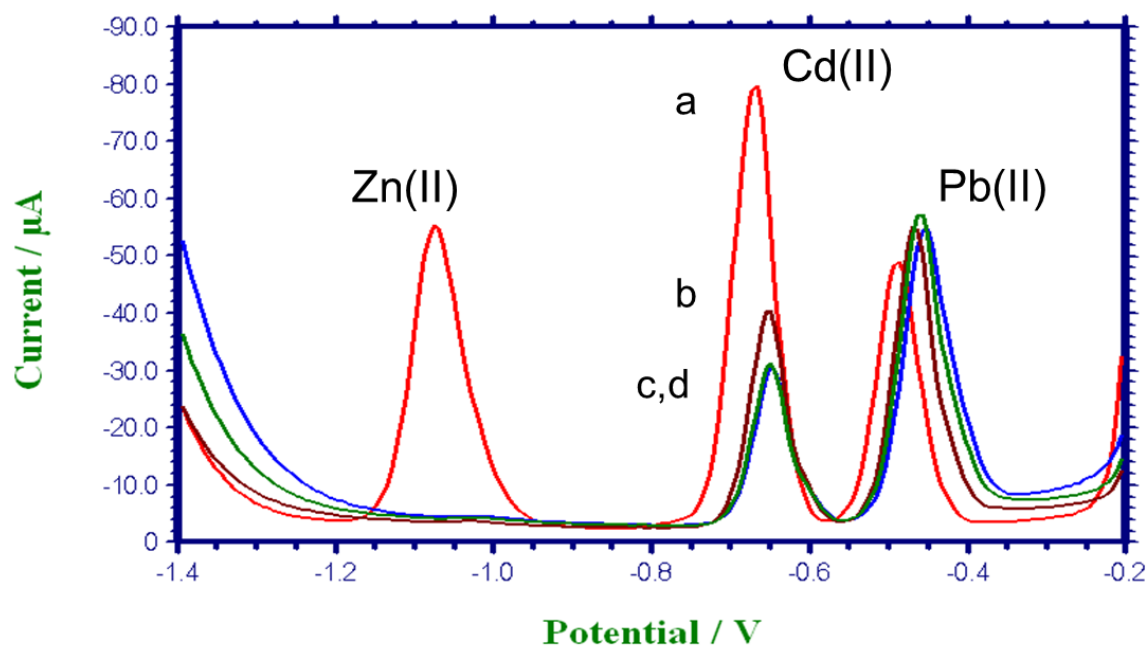


Figure 3.21: Effect of Cu(II) concentrations on the simultaneous determination of the 40 ppb Zn(II), Cd(II) and Pb(II) mixture at GCE in presence of 600 ppb Bi(III) and 10 ppm Hg(II) in acetate buffer solution (0.1 M, pH 4.5); Amplitude, 40 mV; Frequency, 80 Hz; Potential increment, 6 mV; Accumulation time, 2.0 min at -1.4 V. The Cu(II) concentrations: (a) 0.0 ppm, (b) 1.0 ppm, (c) 2.0 ppm, (d) 3.0 ppm.

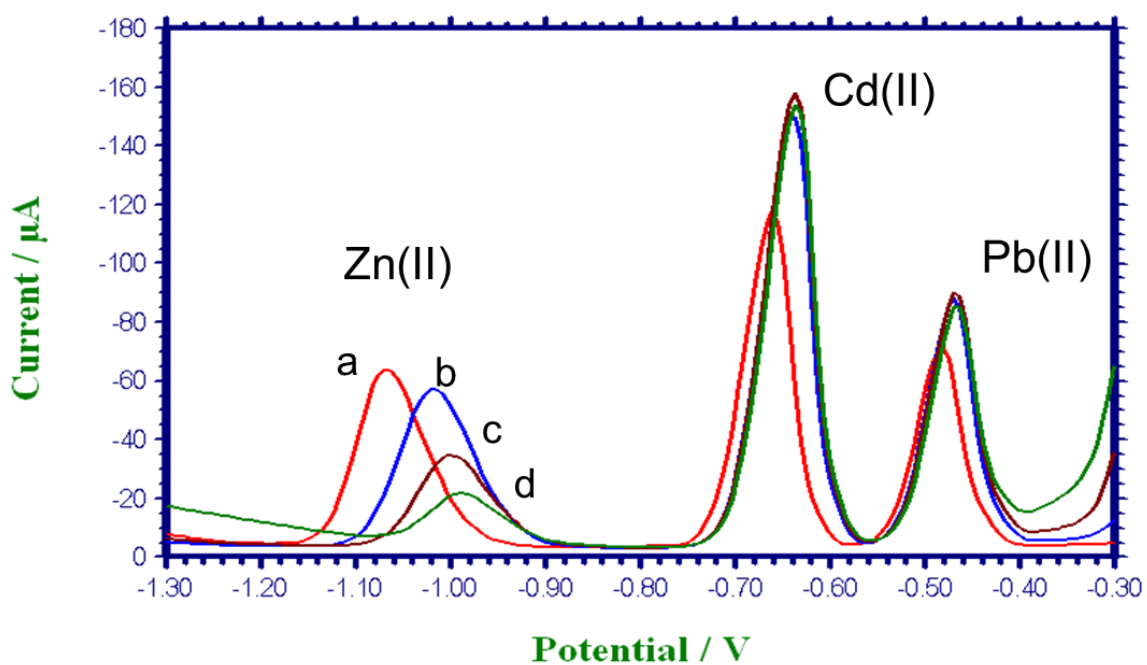


Figure 3.22: Effect of Fe(III) concentrations on the simultaneous determination of the 40 ppb Zn(II), Cd(II) and Pb(II) mixture at GCE in presence of 600 ppb Bi(III) and 10 ppm Hg(II) in acetate buffer solution (0.1 M, pH 4.5). Amplitude 40 mV; Frequency, 80 Hz; Potential increment, 6 mV; Accumulation time, 2.0 min at -1.4 V. The Fe(III) concentrations: (a) 0.0 ppm, (b) 1.0 ppm, (c) 2.0 ppm, (d) 3.0 ppm.

There is an obvious effect of Cu(II) on the detection especially for Zn(II). The Fe(III) effect has been studied as shown in Figure 3.22. We have noticed that the fast response of Zn(II) decreased with a shift in potential to more anodic direction. While the Pb(II) and Cd(II) have increased and then levels. The Ni(II) ions have a similar effect as shown in Figure 3.23.

We have also studied in this section the interference effect of some organic compounds such as adenosine on the Zn(II), Cd(II) and Pb(II) responses where the concentrations of the targeted metals were 40 ppb. The selectivity for the measurement was confirmed by measuring the responses after the addition of 1.0 ppm of the potential interferences, as shown in Tables 3.2A and B, Further study was obtained with adding different concentrations, there were small influences for the organic compounds tested which increase with adding more than 10 ppm of these organic compounds (Tables 3.2A and B).

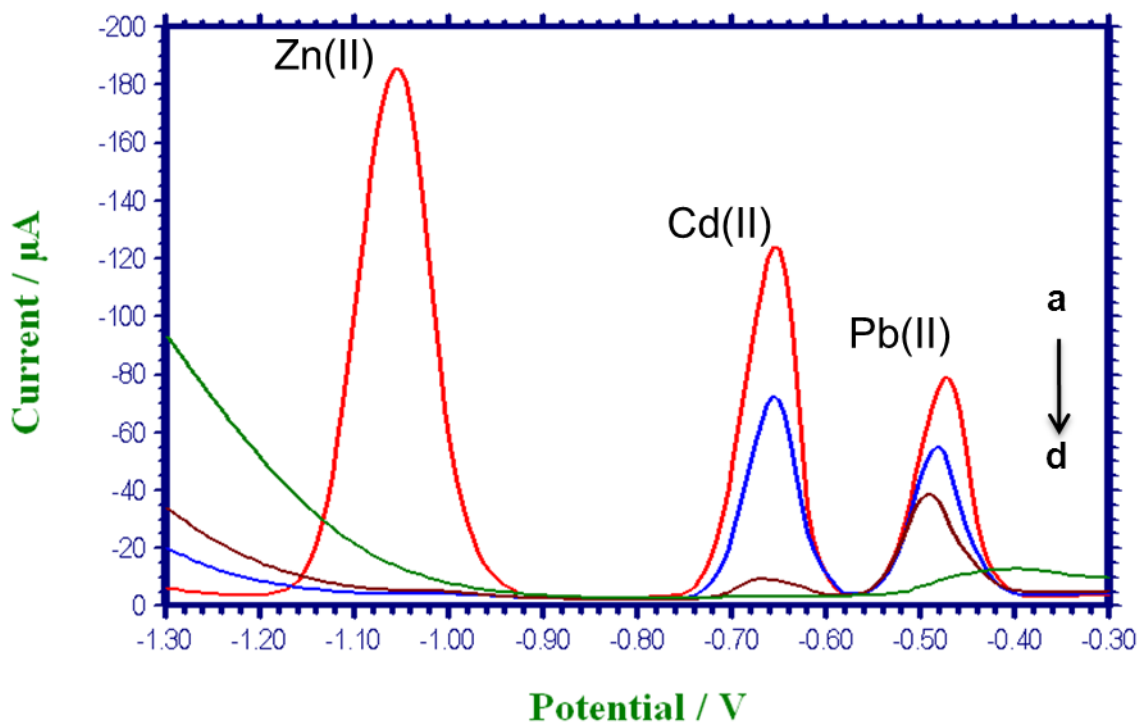


Figure 3.23: Effect of Ni(II) concentration on the simultaneous determination of the 40 ppb Zn(II), Cd(II) and Pb(II) mixture at GCE in presence of 600 ppb Bi(III) and 10 ppm Hg(II) in acetate buffer solution (0.1 M, pH 4.5); Amplitude, 40 mV; Frequency, 80 Hz; Potential increment, 6 mV; Accumulation time, 2.0 min at -1.4 V. The Ni(II) concentrations: (a) 0.0 ppm, (b) 1.0 ppm, (c) 2.0 ppm, (d) 3.0 ppm.

Table 3.2A: Influence of Several Organic Compounds.

Potential Interferent	concentration (ppm)	Change of Signal (%)		
		Zn(II)	Cd(II)	Pb(II)
Alanine	0	0.00	0.00	0.00
	1	-9.24	-1.05	1.88
	5	-4.46	-2.44	-0.15
	10	-9.37	-9.12	-7.25
	20	-19.11	-15.35	-13.03
Triton- X 100	0	0.00	0.00	0.00
	10	-34.39	-0.73	-2.74
	20	-60.36	-74.36	-25.96
	30	-42.81	-76.88	-40.64
	40	-38.36	-78.21	-47.81
Uric Acid	0	0.00	0.00	0.00
	1	24.74	0.87	1.69
	5	16.97	-4.88	-1.91
	10	-2.65	-10.15	-3.48
	20	-26.58	-26.97	-19.63
Cystine	0	0.00	0.00	0.00
	1	-8.06	-12.22	-0.02
	5	-14.34	-22.14	-9.58
	10	-11.22	-8.93	-10.40
	20	-34.33	-23.77	-30.61
Methionine	0	0.00	0.00	0.00
	1	-5.59	-1.73	-1.68
	5	-3.84	-5.12	-6.19
	10	-8.25	-6.38	-7.34
	20	-25.07	-16.67	-17.10

Table 3.2B: Influence of Several Organic Compounds.

Potential Interferent	concentration (ppm)	Change of Signal (%)		
		Zn(II)	Cd(II)	Pb(II)
Phenylalanine	0	0.00	0.00	0.00
	1	14.85	0.88	3.29
	5	18.19	-3.83	-0.51
	10	13.22	-6.69	-1.65
	20	-4.56	-16.48	-11.60
L. Tryptophane	0	0.00	0.00	0.00
	1	-2.51	8.41	4.32
	5	3.49	24.20	12.77
	10	22.08	71.85	48.59
	20	11.72	62.85	36.79
L. Tyrosine	0	0.00	0.00	0.00
	1	9.26	2.90	8.63
	5	1.78	-14.26	-8.70
	10	-10.40	-17.11	-7.71
	20	-20.77	-22.90	-11.75
Adenine	0	0.00	0.00	0.00
	1	4.14	-5.48	-5.39
	5	13.09	-2.09	0.42
	10	3.96	-12.23	-6.93
	20	-6.67	-19.72	-12.67
Guanine	0	0.00	0.00	0.00
	1	-0.16	-6.22	-9.05
	5	3.39	-2.17	-6.74
	10	5.19	1.14	-4.82
	20	-17.92	-3.43	-8.42

CHAPTER 4

4.0 FIELD-DEPLOYABLE ELECTROCHEMICAL SENSOR: SETUP AND REAL WATER SAMPLES APPLICATION.

4.1 INTRODUCTION

Due to possible sample contamination during the transportation from samples locations on the way to the laboratories, here we have tried to pack all needed components in a small package that could be taken into the field to do the on-field determination of heavy metals.

4.2 FIELD-DEPLOYABLE ELECTROCHEMICAL SENSORS

4.2.1 System Setup

The system consists of three main parts fixed in a hard suitcase (Figure 4.1)

- The potentiostat, a pocket-size electrochemical workstation (CHI1140A, CH Instruments Inc., Austin, TX, USA).
- The cell, Ag/AgCl reference electrode (in 3M KCl, CHI111, CH Instruments Inc.), Glassy carbon working electrode (CHI 112, CH Instruments Inc.) and platinum wire counter electrode (CHI115, CH Instruments Inc.) were inserted into a 5 ml small plastic cell through holes in its Teflon cover.
- The computer, a mini notebook computer is connected to the potentiostat by USB Port.

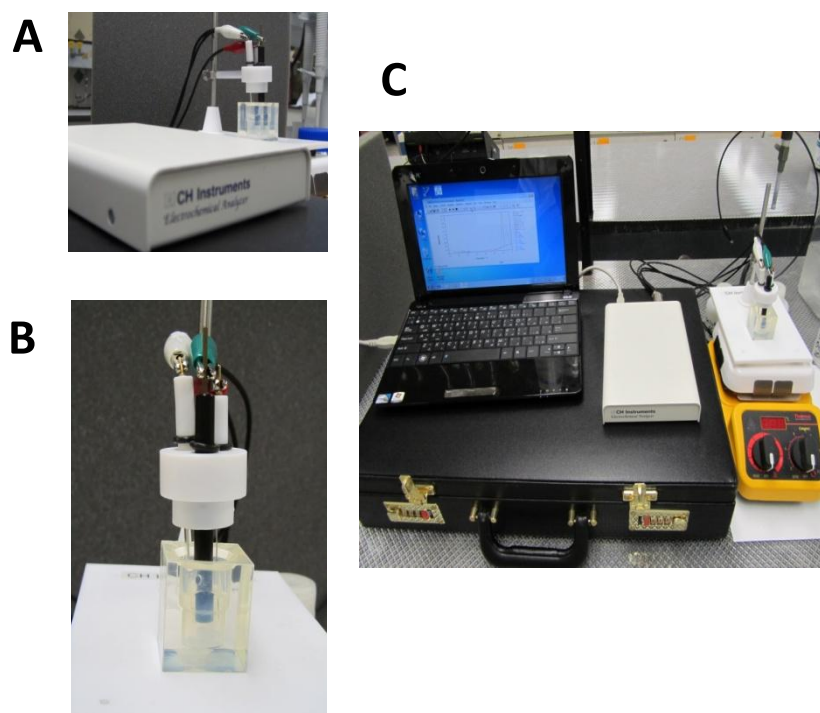


Figure 4.1: (A) The potentiostat, (B) The electrochemical, (C) The complete setup.

4.2.2 Procedure

Details of apparatus were described earlier on the subsection 3.2.4.

4.2.3 Results and Discussion

By applying the developed methods using the bench-top in laboratory potentiostat unit we have concluded that the same good response could be achieved by the on-field developed unit with the advantage of avoiding the transporting sample which could lead to contaminations. Glassy carbon electrode along with the screen printed electrodes has been used to determine the concentration of the targeted heavy metals in drinking water samples. More over the detected metal concentrations have been compared with the allowed values according to EPA, WHO and EU (Table 1.1).

We have tested the developed sensor to analyze heavy metals in drinking water samples. The samples were collected from Dhahran Vicinity, the high density polypropylene bottles were washed and acidified prior to collect these samples (Table 4.2).

Table 4.1: Locations of the Collected Water Samples.

	Place	Date	Time	Location
1	Mosque	14-10-2009	7:40 AM	Althogba Alryadhst. 20 St.
2	Mosque	14-10-2009	8:14 AM	Althogba King Fahad St.
3	Mosque	14-10-2009	8:41 AM	Alkhobar prince megrim St.
4	Privet school	14-10-2009	9:44 AM	Aldoha (northern) high pressure St.
5	Mosque	14-10-2009	10:02 AM	Aldoha (northern) Ahmed bin hanbel St.
6	KFUPM	15-10-2009	12:15 PM	House 6428 Alake

4.2.3.1 Real Drinking Water Samples Analysis Using Modified Glassy Carbon Electrodes

Square wave stripping voltammetry has been used as a technique to analyze real drinking water samples using glassy carbon electrode in the presence of

- a- Hg
- b- Bi
- c- Alloy

The data have been processed using the standard addition method.

4.2.3.1.1 Drinking Water Samples Analysis Using Glassy Carbon-Bi Modified Electrodes

The Samples have been analyzed by standard addition method, where a successive introduction of increments of the Zn(II), Cd(II) and Pb(II) heavy metals standard solutions were added to a single measured volume of the unknown water sample. Square wave stripping voltammetric measurements are made on the original water sample (Figure 4.2) and the water sample plus the standard heavy metal solution by spiking method.

4.2.3.1.2 Drinking Water Samples Analysis Using Glassy Carbon-Hg Modified Electrodes

The Samples have been analyzed by standard addition method, where a successive introduction of increments of the Zn(II), Cd(II) and Pb(II) heavy metals standard solutions were added to a single measured volume of the unknown water sample. Square wave stripping voltammetric measurements are made on the original water sample (Figure 4.3) and the water sample plus the standard heavy metal solution by spiking method.

4.2.3.1.3 Drinking Water Samples Analysis Using Glassy Carbon-Bi/Hg Alloy Modified Electrodes

The Samples have been analyzed by standard addition method, where a successive introduction of increments of the Zn(II), Cd(II) and Pb(II) heavy metals standard solutions were added to a single measured volume of the unknown water sample. Square wave stripping voltammetric measurements are made on the original water sample (Figure 4.4) and the water sample plus the standard heavy metal solution by spiking method.

4.2.3.2 Validation

The obtained data have been compared with the ICP-MS results as shown in Table 4.2. The obtained electrochemical results were quite comparable with the ICP-MS.

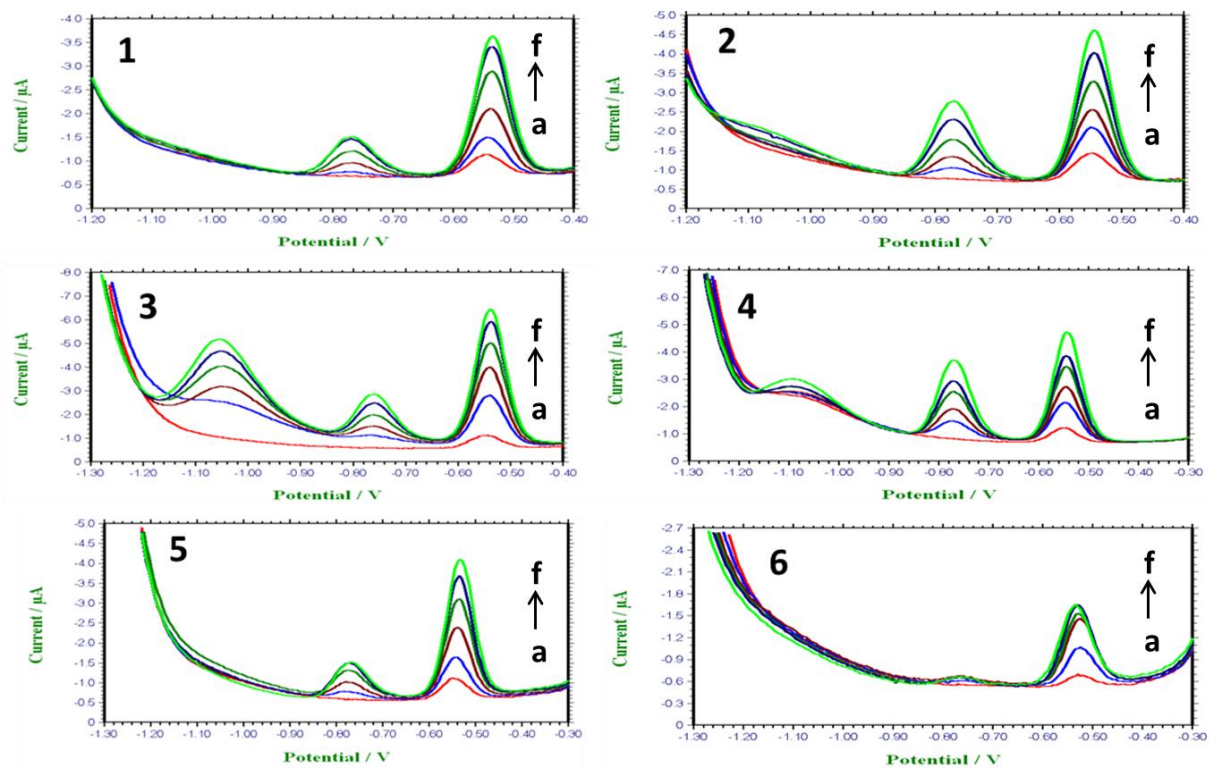


Figure 4.2: Square wave stripping voltammograms at GCE-Bi modified electrode of six (1- 6) different drinking water samples in acetate buffer solution (0.1 M, pH 3.5) with standard addition of different Zn(II), Cd(II) and Pb(II) heavy metals concentration: (a) water sample, (b) 2.0, (c) 4.0, (d) 6.0, (e) 8.0, (f) 10.0 ppb. Other working conditions as in Figure 2.12A.

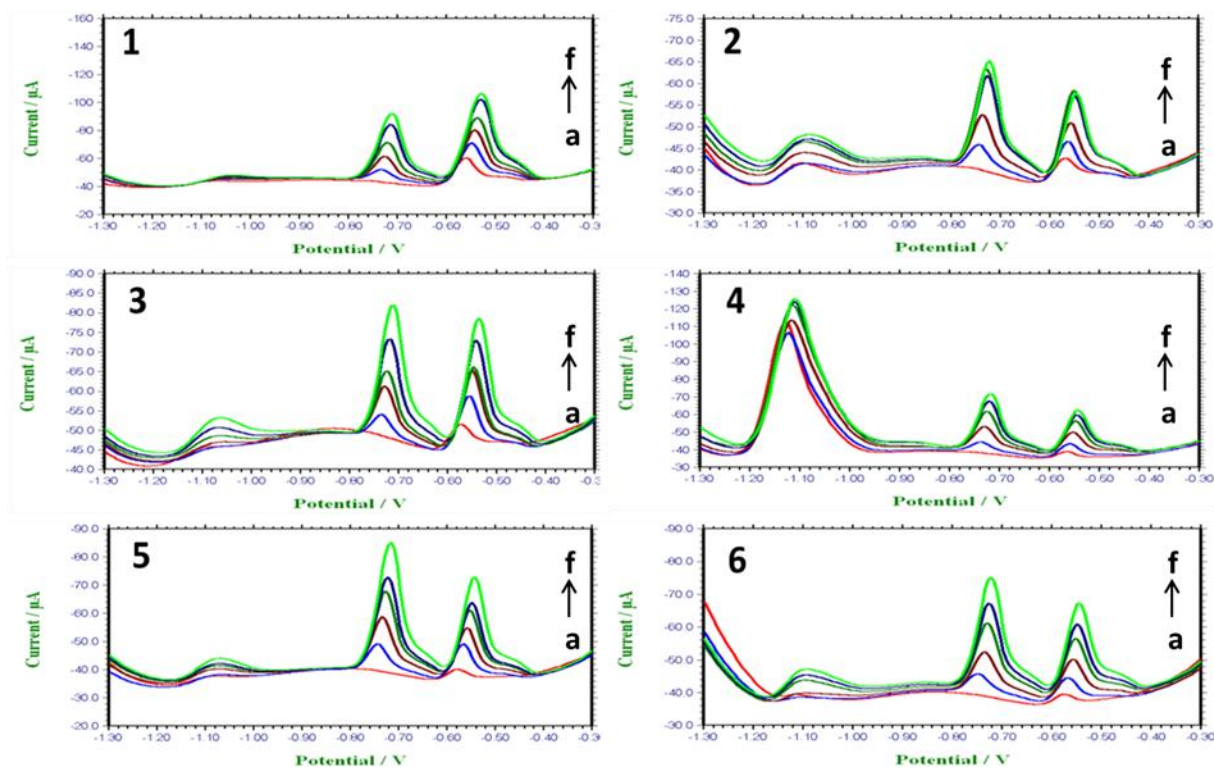


Figure 4.3: Square wave stripping voltammograms at GCE-Hg modified electrode of six (1- 6) different drinking water samples in acetate buffer solution (0.1 M, pH 3.5) with standard addition of different Zn(II), Cd(II) and Pb(II) heavy metals concentration: (a) water sample, (b) 2.0, (c) 4.0, (d) 6.0, (e) 8.0, (f) 10.0 ppb. Other working conditions as in Figure 2.23A.

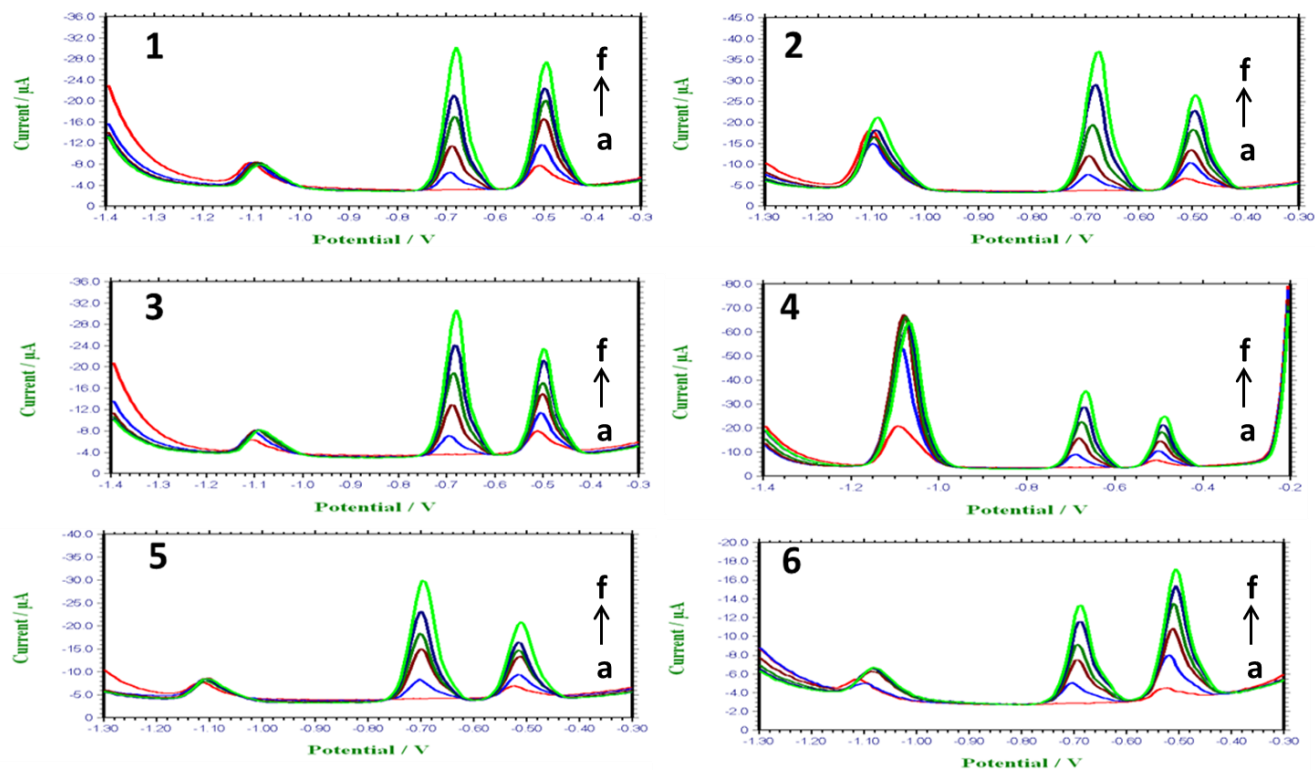


Figure 4.4: Square wave stripping voltammograms at GCE-Bi/Hg alloy modified electrode of six (1- 6) different drinking water samples in acetate buffer solution (0.1 M, pH 4.5) with standard addition of different Zn(II), Cd(II) and Pb(II) heavy metals concentration: (a) water sample, (b) 2.0, (c) 4.0, (d) 6.0, (e) 8.0, (f) 10.0 ppb. Other working conditions as in Figure 3.20A.

Table 4.2: Concentration Values of the Analyzed Water Samples.

Sample	Method	Zn (ppb)	Cd (ppb)	Pb (ppb)
1	GC-Hg	5.9	BDL*	3.6
	GC-Bi	BDL*	BDL*	1.4
	GC-Alloy	17.4	BDL*	2.2
	ICP	15.8	0.065	2.68
2	GC-Hg	9.8	BDL*	2.9
	GC-Bi	BDL*	BDL*	2.3
	GC-Alloy	18.1	BDL*	1.3
	ICP	19.26	0.02	0.07
3	GC-Hg	5.4	BDL*	2.2
	GC-Bi	BDL*	BDL*	0.9
	GC-Alloy	8.3	BDL*	2.3
	ICP	10.35	0.021	2.83
4	GC-Hg	4.8	BDL*	1.1
	GC-Bi	3.6	BDL*	1.5
	Alloy	31.2	BDL*	1.4
	ICP	37.89	0.02	0.11
5	GC-Hg	4.1	BDL*	0.8
	GC-Bi	BDL*	BDL*	ND*
	GC-Alloy	9.9	BDL*	1.5
	ICP	11.97	0.02	0.13
6	GC-Hg	0.4	BDL*	0.7
	GC-Bi	BDL*	BDL*	1.6
	GC-Alloy	13.7	BDL*	0.7
	ICP	18.59	0.01	0.10
BDL*	Below Detection Limit			

CHAPTER 5

5.0 CONCLUSION AND REFERENCES

5.1 CONCLUSION

- We have achieved all research objectives.
- We have studied the simultaneous detection of Zn(II), Cd(II) and Pb(II) in drinking water samples with the enhancement of the detection using bismuth, mercury and combination of the tow elements Bi/Hg alloy.
- We have developed a new portable electrochemical device to detect toxic heavy metals on field.
- We have reached comparable and even lower detection limits than that reported in the literature.
- We have studied several drinking water samples collected from Dhahran vicinity.

5.2 REFERENCES

1. F. Pontius, *Drinking Water Regulation and Health*, John Wiley & Sons, 2003.
2. J. Wang, K. Rogers, *Electrochemical Sensors For Environmental Monitoring: A Review Of Recent Technology*, 1995.
3. M. Rico, M. Marín, E. Gil, Modification of carbon screen-printed electrodes by Adsorption of Chemically Synthesized Bi Nanoparticles for the Voltammetric Stripping Detection of Zn(II), Cd(II) and Pb(II), *Talanta*, 80, 631. 2009.
4. M. Rico, M. Marín, E. Gil, A Novel Cell Design for the Improved Stripping Voltammetric Detection of Zn(II), Cd(II), and Pb(II) on Commercial Screen-Printed Strips by Bismuth Co-Deposition in Stirred Solutions, *Electroanalysis*, 24, 2608, 2008.
5. J. Janata, *Principles of Chemical Sensors*. Plenum Press, New York, 1989.
6. P. Richter, Review of Technologies Developed or Utilized in Europe and the Commonwealth of Independent States (CIS) for Use in Long Term Monitoring of Radionuclides and Heavy Metals in Water and Soils, Technical University of Budapest and Florida State University, 2004.
7. <http://www.palmsens.com/>
8. <http://www.physics.dcu.ie>
9. http://www.idronaut.it/metals_monit/main4.html
10. P. Kissinger, W. Heineman, *Laboratory Techniques in Electroanalytical Chemistry*, Dekker, 5, 1984.
11. J. Wang, *Analytical Electrochemistry*, John Wiley & Sons, 2006.

12. C. Brett, A. Brett, *Electrochemistry Principles Methods and Applications*, Oxford University Press. 1993.
13. A. Covington, *Ion-Selective Electrode Methodology*, CRC Press, 2, 1979.
14. A. Turner, I. Karube, G. Wilson, *Biosensors Fundamentals and Applications*, Oxford University Press, 1987.
15. J. Frew, H. Hil, Electrochemical Biosensor, *Analytical Chemistry*, 59, 933, 1987.
16. R. hobos, Enzyme-Based Electrochemical Biosensors, *TrAC Trends in Analytical Chemistry*, 6, 6, 1987.
17. J. Wang, L. Fang, D. Lopez, Amperometric Biosensor for Phenols Based on a Tyrosinase-Graphite-Epoxy Biocomposite, *Analyst*, 119, 455, 1994.
18. J. Wang, L. Fang, D. Lopez, Tyrosinase-based ruthenium dispersed carbon paste biosensor for phenols, *Biosensors and Bioelectronics*, 9, 9, 1994.
19. F. Pavinatto, E. Fernandes, P. Alessio, C. Constantino, J. de Saja, V. Zucolotto, C. Apetrei, O. Oliveira, M. Mendez, Optimized Architecture for Tyrosinase-Containing Langmuir–Blodgett films to Detect Pyrogallol, *Journal of Materials Chemistry*, 21, 4995. 2011.
20. L. Campanella, T. Beone, M.Sammartino, M. Tomassetti, Determination of Phenol in Wastes and Water Using an Enzyme Sensor, *Analyst*, 118, 979, 1993.
21. J. Wang, Q. Chen, Remote electrochemical biosensor for field monitoring of phenolic compounds, *Analytica Chimica Acta*, 312, 39,1995.
22. H. Kotte, B. Owndig, K. Vorlop, B. Strehlits, U. Stottmeister, Methylphenazonium- Modified Enzyme Sensor Based on Polymer Thick Films

- for Subnanomolar Detection of Phenols, *Anal. Chem.*, 67, 65, 1995.
23. J. Wang, Q. Chen, Microfabricated Phenol Biosensors based on Screen-Printing of Tyrosinase-Containing Carbon Ink, *Anal. Letters*, 7, 28, 1995.
 24. J. Marty, K. Sode, I. Karube, Biosensor for Detection of Organophosphate and Carbamate Insecticides, *Electroanalysis*, 4, 249, 1992.
 25. M. Smitt, G. Rechnitz, Toxin Detection Using a Tyrosinase-Coupled Oxygen Electrode, *Anal. Chem.*, 65, 380, 1993.
 26. I. Dolmanova, T. Shekhovtsova, V. Kutcheryaeva, Assay of Enzyme Effectors, *Talanta*, 34, 201, 1987.
 27. R. Baldwin, J. Christensen, L. Kryger, Voltammetric Determination of Traces of Nickel(II) at a Chemically Modified Electrode Based on Dimethylglyoxime-Containing Carbon Paste, *Anal. Chem.*, 58, 1790, 1986.
 28. J. Wang, M. Bonakdar, Preconcentration and Voltammetric Measurement of Mercury with a Crown-Ether Modified Carbon-Paste Electrode, *Talanta*, 35, 277, 1988.
 29. A. Downard, H. Kipton, J. Powell, S. Xu, Voltammetric Determination of Aluminium(III) Using a Chemically Modified Electrode, *Analytica Chimica Acta*, 251, 157, 1991.
 30. S. Sasso, R. Pierce, I. Walla, A. Yacynych, Electropolymerized 1,2-Diaminobenzene as a Means To Prevent Interferences and Fouling and To Stabilize Immobilized Enzyme in Electrochemical Biosensors, *Anal. Chem.*, 62, 1111, 1990.
 31. J. Wang, S. Chen, M. Lin, Use of Different Electropolymerization Conditions

- for Controlling the Size-Exclusion Selectivity at Polyaniline, Polypyrrole and Polyphenol Films, *Journal of Electroanalytical Chemistry and Interfacial Electrochemistry*, 273, 231, 1989.
32. T. Florence, Electrochemical Approaches to Trace Element Speciation in Waters A Review, *Analyst*, 111, 489, 1986.
 33. A. Zirino, S. Lieberman, C. Clavell, Measurement of Cu and Zn in San Diego Bay by Automated Anodic Stripping Voltammetry, *Environmental Science & Technology*, 12, 73, 1978.
 34. J. Wang, R. Setiadji, L. Chen, J. Lu, S. G. Morton, Automated System for On-Line Adsorptive Stripping Voltammetric Monitoring of Trace Levels of Uranium, *Electroanalysis*, 4, 161, 1992.
 35. B. Clark, D. DePaoli, D. McTaggart, B. Patton, An On-Line Voltammetric Analyzer for Trace Metals in Wastewater, *Analytica Chimica Acta*, 215, 13, 1988.
 36. J. Wang, B. Tian, Screen-Printed Stripping Voltammetric/Potentiometric Electrodes for Decentralized Testing of Trace Lead, *Anal. Chem.*, 64, 1706, 1992.
 37. M. Tercier, J. Buffle, A. Zirino, R. DeVitre, In Situ Voltammetric Measurement of Trace Elements in Lakes and Oceans, *Analytica Chimica Acta*, 237, 429, 1990.
 38. J. Wang, D. Larson, N. Foster, S. Armalis, J. Lu, X. Rongrong, Remote Electrochemical Sensor for Trace Metal Contaminants, *Anal. Chem.*, 67, 1481, 1995.

39. E. Jacobs, E. Vadasdi, L. Sarkozi, N. Colman, Analytical Evaluation of i-STAT Portable Clinical Analyzer and Use by Non laboratory Health-Care Professionals, *Clinical Chemistry*, 39, 1069, 1993.
40. M. de Grac, A. Korn, J. de Andrade, D. de Jesus, V. Lemos, M. Bandeira, W. dos Santos, M. Bezerra, F. Amorim, A. Souza, S. Ferreira, Separation and Preconcentration Procedures for the Determination of Lead Using Spectrometric Techniques: A review, *Talanta*, 69, 16, 2006.
41. A. Davisa, P. Wub, X. Zhangb, X. Houb, B. Jonesa, Determination of Cadmium in Biological Samples, *Applied Spectroscopy Reviews*, 41, 35, 2006.
42. J. Reyes, P. Barrales, A. Molina, Sensing of Trace Amounts of Cadmium in Drinking Water Using a Single Fluorescence-Based Optosensor, *Microchemical Journal*, 82, 94, 2006.
43. N. Stozhko, N. Malakhova, M. Fyodorov, K. Brainina, Modified Carbon-Containing Electrodes in Stripping Voltammetry of Metals Part I, *Jornal of Solid State Electrochem.*, 12, 1885, 2008.
44. J. Hart, A. Crew, E. Crouch, K. Honeychurch, R. Pemberton, *Anal. Letters.*, 37, 789, 2004.
45. O. Renedo, M. Lomillo, M. Martinez, Recent Developments in the Field of Screen-Printed Electrodes and their Related Applications, *Talanta*, 73, 202, 2007.
46. J. Wang, J. Lu, S. Hocevar, P. Farias, Bismuth-Coated Carbon Electrodes for

- Anodic Stripping Voltammetry, *Anal. Chem.*, 72, 3218, 2000.
47. E. Hutton, S. Hočevár, B. Ogorevc, Ex Situ Preparation of Bismuth Film Microelectrode for Use in Electrochemical Stripping Microanalysis, *Analytica Chimica Acta*, 17, 1354, 2005.
 48. R. Pauliukaite, C. Brett, Characterization and Application of Bismuth-Film Modified Carbon Film Electrodes, *Electroanalysis*, 17, 1354, 2005.
 49. R. Kachoosangi, C. Banks, X. Ji, R. Compton, Electroanalytical Determination of Cadmium(II) and Lead(II) Using an in-situ Bismuth Film Modified Edge Plane Pyrolytic Graphite Electrode, *Analytical Sciences*, 23, 283, 2007.
 50. L. Baldrianova, I. Svancara, S. Sotiropoulos, Anodic stripping voltammetry at a new type of disposable bismuth-plated carbon paste mini-electrodes, *Analytica Chimica Acta*, 599, 249, 2007.
 51. N. Naseri, S. Baldock, A. Economou, N. Goddard, P. Fielden, *Anal. Bioanal. Chem.*, 391, 1283, 2008.
 52. J. Wang, P. Hopke, Equation-Oriented System: an Efficient Programming Approach to Solve Multilinear and Polynomial Equations By the Conjugate Gradient Algorithm, *Chemometrics and Intelligent Laboratory Systems*, 55, 13, 2001.
 53. J. Marty, K. Sode, I. Karube, Biosensor for Detection of Organophosphate and Carbamate Insecticides, *Electroanalysis*, 4, 249, 1992.
 54. M. Smit, G. Rechnitz, Toxin Detection Using a Tyrosinase-Coupled Oxygen Electrode, *Anal. Chem.*, 65, 380, 1993.
 55. R. Baldwin, J. Christensen, L. Kryger, Voltammetric Determination of Ni(II)

- at a Chemically Modified Electrode Based on DMG Containing Carbon Paste, *Anal. Chem.*, 58, 1790, 1986.
56. J. Wang, M. Bonakdar, Preconcentration and Voltammetric Measurement of Mercury with Crown-Ether Modified Carbon Paste Electrode. *Talanta*, 35, 277, 1988.
 57. A. Downard, H. Kipton, J. Powell, S. Xu, Voltammetric Determination of Aluminum using a Chemically Modified Electrode, *Anal. Chim. Acta*, 251, 157, 1991.
 58. M. Rico, M. Marín, E. Gil, A Novel Cell Design for the Improved Stripping Voltammetric Detection of Zn(II), Cd(II), and Pb(II) on Commercial Screen-Printed Strips by Bismuth Co-Deposition in Stirred Solutions, *Electroanalysis*, 20, 2608, 2008.
 59. C. Brett, Electrochemical Sensors for Environmental Monitoring. Strategy and Examples, *Pure Appl. Chem.*, 73, 1969, 2001.
 60. K. Rajeshwar, What is Electrochemical and Solid-State Science, *The Electrochemical Society*, 15, 15, 2006.
 61. G. Budnikov, Biomedical Aspects of Electrochemical Methods of Analysis I, *Journal of Analytical Chemistry*, 55, 1014, 2000.
 62. J. Wang, Analytical Electrochemistry, VCH Publishers, New York, 1994
 63. A. Bard, L. Faulkner, Electrochemical Methods: Fundamentals and Applications, Wiley, 2001.
 64. P. Barlett, J. Cooper, A Review of the Immobilization of Enzymes in Electropolymerized Films, *Journal of Electroanalytical Chemistry*, 362, 1,

- 1993.
65. S. Kounaves, Voltammetric Techniques, Handbook of Instrumental Techniques for Analytical Chemistry, Upper Saddle River, 709, 1997.
 66. http://www.basinc.com/mans/EC_epsilon/Techniques/Pulse/pulse.html
 67. M. Frizzo, D. Lara, A. Prokopiuk, C. Vargas, C. Salbego, M. Wajner, O. Souza, Guanosine Enhances Glutamate Uptake in Brain Cortical Slices at Normal and Excitotoxic Conditions, *Cellular and Molecular Neurobiology*, 22, 353, 2002.
 68. J. wang, Analytical Chemistry, 3rd Edition wiley-VCH, 2006
 69. R. Wolf, What is ICP-MS , 2005.
 70. <http://www.britannica.com/EBchecked/topic/286745/Inductively-Coupled-Plasma-Mass-Spectrometer>
 71. D. Skoog, F. Holler, T. Nieman, Principles of Instrumental Analysis, 5th Edition, Brooks Cole, 1997.
 72. M. Dunlap, J. Adaskaveg, Introduction to the Scanning Electron Microscope Theory, Practice & Procedures, Facility For Advanced Instrumentation Davis, 1997.
 73. J. Hardcastle, G. Murcott, R. Compton, Sono-electroanalysis: Ultrasonically Facilitated Liberation and Determination of Copper in Whole Blood, *Electroanalysis*, 12, 559, 2000.
 74. M. de Oliveira, A. Saczk, A. de Moraes, N. Stradiott, Simultaneous Determination of Zinc, Copper, Lead, and Cadmium in Fuel Ethanol by Anodic Stripping Voltammetry Using a Glassy Carbon–Mercury-Film Electrode, *Anal.*

- Bioanal. Chem.*, 380, 135, 2004.
75. X. Dai, O. Nekrassova, M. Hyde, R. Compton, Anodic Stripping Voltammetry of Arsenic(III) Using Gold Nanoparticle-Modified Electrodes, *Anal. Chem.*, 76, 6924, 2004.
76. Z. Fijałek, A. Łozak, K. Sarna, Voltammetric and EQCM Studies on Selenium(IV) at Mercury, Gold and Glassy Carbon Electrodes in the Presence of Cu(II), Au(III), Pb(II) and Cd(II), *Electroanalysis*, 10, 846, 1998.
77. M. Korolczuk, K. Tyszczyk, M. Grabarczyk, Adsorptive stripping voltammetry of Nickel and Cobalt at In-Situ Plated Lead Film Electrode, *Electrochemistry Communications*, 7, 1185, 2005.
78. X. Dai, R. Compton, Detection of As(III) via Oxidation to As(V) using Platinum Nanoparticle Modified Glassy Carbon Electrodes: Arsenic Detection without Interference from Copper, *Analyst*, 131, 516, 2006.
79. C. Prior, C. Lenehan, G. Walker, Enhanced Resolution of Copper and Bismuth by Addition of Gallium in Anodic Stripping Voltammetry with the Bismuth Film Electrode, *Electroanalysis*, 18, 2468, 2006.
80. D. Li, J. Jia, J. Wang, A Study on the Electroanalytical Performance of a Bismuth Film-Coated and Nafion-Coated Glassy Carbon Electrode in Alkaline Solutions, *MicrochimActa*, 169, 221, 2010.
81. K. Armstrong, C. Tatum, R. Dansby-Sparks, J. Chambers, Z. Xue, Individual and Simultaneous Determination of Lead, Cadmium, and Zinc by Anodic Stripping Voltammetry at a Bismuth Bulk Electrode, *Talanta*, 82, 675, 2010.
82. M. Rico, M. Marín, E. Gil, Modification of Carbon Screen-Printed Electrodes

- by Adsorption of Chemically Synthesized Bi Nanoparticles for the Voltammetric Stripping Detection of Zn(II), Cd(II) and Pb(II), *Talanta*, 80 , 631, 2009.
83. D. Pan, L. Zhang, J. Zhuang, W. Lu, R. Zhu, W. Qin, New Application of Tin-Bismuth Alloy for Electrochemical Determination of Cadmium, *Materials Letters*, accepted 12 november 2011.
84. R. Ouyang, Z. Zhu, C. Tatum, J. Chambers, Z.Xue, Simultaneous Stripping Detection of Zn(II), Cd(II) and Pb(II) Using a Bimetallic Hg–Bi/Single-Walled Carbon Nanotubes Composite Electrode, *Journal of Electroanalytical Chemistry*, 656, 78, 2011.
85. H. Zheng, Z. Yan, H. Dong, B. Ye, Simultaneous Determination of Lead and Cadmium at a Glassy Carbon Electrode Modified with Langmuir–Blodgett Film of p-tert-butylthiacalixarene, *Sensors and Actuators B*, 120, 603, 2007.
86. E.Hasdemir, K. Karaboduk, Simultaneous Determination of Bismuth and Copper by Square Wave Voltammetry in The Presence of Ethylene Di Amine TetraAcetic Acid, *G.U. Journal of Science*, 23, 33, 2010.
87. A. Rahman, D. S. Park, M. Won, S. Park, Y. Shim, Selective Electrochemical Analysis of Various Metal Ions at an EDTA Bonded Conducting Polymer Modified Electrode, *Electroanalysis*, 16, 1366, 2004.
88. B. Lacka, J. Duncan, T. Nyokong, Adsorptive Cathodic Stripping Voltammetric Determination of Gold(III) in the Presence of Yeast Mannan, *Analytica Chimica Acta*, 385, 393, 1999.
89. C. Mousty, Sensors and Biosensors Based on Clay-Modified Electrodes- New

- Trends, *Applied Clay Science*, 27, 159, 2004.
90. D. Sun, X. Xie, Y. Cai, H. Zhang, K. Wu, Voltammetric Determination of Cd²⁺ Based on the Bi Functionality of Single-Walled Carbon Nanotubes–Nafion Film, *AnalyticaChimicaActa*, 581, 27, 2007.
 91. S. C. Petrovic, H. D. Dewald, Square-Wave Anodic Stripping Voltammetry of Zn(II) as a Method for Probing Instabilities at a Glassy Carbon Mercury Film Microelectrode, *AnalyticaChimicaActa*, 357, 33, 1997.
 92. N. Abo El-Maali, D. Abd El-Hady, Square-Wave Stripping Voltammetry of Uranium(VI) at the Glassy Carbon Electrode. Application to Some Industrial Samples, *Electroanalysis*, 11, 201, 1999.
 93. H. Diederich, S. Meyer, F. Scholz, Automatic Adsorptive Stripping Voltammetry at Thin- Mercury Film Electrodes (TMFE), *Anal. Chem.*, 349, 670, 1994.
 94. J. Hardcastle, G. Murcott, R. Compton, Sonoelectroanalysis: Ultrasonically Facilitated Liberation and Determination of Copper in Whole Blood, *Electroanalysis*, 12, 559, 2000.
 95. J. Di, F. Zhang, Voltammetry Determination of Trace Manganese with Pretreatment Glassy Carbon Electrode by Linear Sweep Voltammetry, *Talanta*, 60, 31, 2003.
 96. Nucleosides, Nucleotides & Nucleic Acids, Marcel Dekker, 25, 2006.
 97. E. Paleček, *Nature*, 188, 656, 1960.
 98. J. Wang, J. Mo, J. Lu, A. Kawde, A. Muck, Glassy Carbon Paste Electrodes, *Electrochemistry Communications*, 3, 203, 2001.

99. <http://www.inchem.org/documents/ehc/ehc/ehc214.htm>
100. http://en.wikipedia.org/wiki/Lead_poisoning
101. A. Economou, Bismuth-Film Electrodes: Recent Developments and Potentialities for Electroanalysis, *TrAC Trends in Analytical Chemistry*, 24, 334, 2005.
102. E. Hasdemir, K. Karaboduk, Simultaneous Determination of Bismuth and Copper by Square Wave Voltammetry in The Presence of Ethylenediaminetetraacetic Acid, *G.U. Journal of Science*, 23, 33, 2010.
103. J. Wang, Stripping analysis: principles, instrumentation and applications, VCH, Deerfield Beach 1985.
104. D. Li, J. Jia, J. Wang, A Study on the Electroanalytical Performance of a Bismuth Film-Coated and Nafion-Coated Glassy Carbon Electrode in Alkaline solutions, *MicrochimActa*, 169, 221, 2010.
105. F. Arduini, J. Calvo, A. Amine, G. Palleschi, D. Moscone, Bismuth-Modified Electrodes for Lead Detection, *Trends in Analytical Chemistry*, 29, 1295, 2010.
106. H. Duwensee, M. Adamovski, G. Flechsig, Adsorptive Stripping Voltammetric Detection Of Daunomycin At Mercury And Bismuth Alloy Electrodes, *Int. J. Electrochem. Sci.*, 2, 498, 2007.
107. J. Wang, J. Lu, S. Hocevar, P. Farias, Bismuth-Coated Carbon Electrodes for Anodic Stripping Voltammetry, *Anal. Chem.*, 72, 3218, 2000.
108. V. S. Ijeri, A. K. Srivastava, Voltammetric Determination of Lead at Chemically Modified Electrodes Based on Crown Ethers, *Analytical sciences*, 17, 605, 2001.

109. M. Rahman, D. Park, M. Won, S. Park, Y. Shim, Selective Electrochemical Analysis of Various Metal Ions at an EDTA Bonded Conducting Polymer Modified Electrode, *Electroanalysis*, 16, 1366, 2004.
110. J. Wang, Stripping Analysis at Bismuth Electrodes: A Review, *Electroanalysis*, 17, 1341, 2005.
111. M. Korn, J. Andrade, D. Jesus, V. Lemos, M. Bandeira, W. Santos, M. Bezerra, F. Amorim, A. Souza, S. Ferreira, Separation and Preconcentration Procedures for the Determination of Lead Using Spectrometric Techniques: A review, *Talanta*, 69, 16, 2006.
112. J. Wang, J. Lu, S. Hocevar, B. Ogorevc, Bismuth-Coated Screen-Printed Electrodes for Stripping Voltammetric Measurements of Trace Lead *Electroanalysis* (NY), 13, 13, 2001.
113. S. Hocevar, S. Daniele, C. Bragato, B. Ogorevc, Reactivity at the Film/Solution Interface of Ex-Situ Prepared Bismuth Film Electrodes: a Scanning Electrochemical Microscopy (SECM) And Atomic Force Microscopy (AFM) Investigation, *Electrochimica Acta*, 53, 555, 2007.
114. I. Svancara, L. Baldrianova, E. Tesarova, S. Hocevar, S. Elsuccary, A. Economou, S. Sotiropoulos, B. Ogorevc, K. Vytras, Recent Advances in Anodic Stripping Voltammetry with Bismuth-Modified Carbon Paste Electrodes, *Electroanalysis* (NY), 18, 177, 2006.
115. G. Kefala, A. Economou, A. Voulgaropoulos, M. Sofoniou, A study of bismuth-film electrodes for the detection of trace metals by anodic stripping voltammetry and their application to the determination of Pb and Zn in

- tapwater and human hair, *Talanta*, 61, 603, 2003.
116. R. Kachoosangi, C. Banks, X. Ji, R. Compton, Electroanalytical Determination of Cadmium(II) and Lead(II) Using an in-situ Bismuth Film Modified Edge Plane Pyrolytic Graphite Electrode, *Analytical Sciences*, 23,3,283, 2007.
117. M. Rico, M. Marín, E. Gil, Modification of Carbon Screen-Printed Electrodes by Adsorption of Chemically Synthesized Bi Nanoparticles for the Voltammetric Stripping Detection of Zn(II), Cd(II) and Pb(II), *Talanta*, 80 , 631, 2009.
118. W. Zhu, N. B. Li, H. Q. Luo, Anodic Stripping Voltammetry Determination of Pb(II) and Cd(II) at a Bismuth/Poly(aniline) Film Electrode, *Analytical Letters*, 39, 2273, 2006.
119. G. Yang, X. Qu, M. Shen, C. Wang, Q. Qu, X. Hu, Electrochemical behavior of lead(II) at poly(phenol red) modified glassy carbon electrode, and its trace determination by differential pulse anodic stripping voltammetry, *MicrochimActa*, 160, 275, 2008.
120. B. Privett, J. Shin, M. Schoenfisch, Electrochemical Sensors, *Anal. Chem.*, 82, 4723, 2010.
121. B. Janegitza, L. Marcolino-Junior, S. Campana-Filho, R. Fariaa, O. Fatibello-Filho, Anodic Stripping Voltammetric Determination Of Copper(Ii) Using A Functionalized Carbon Nanotubes Paste Electrode Modified with Cross Linked Chitosan, *Sensors and Actuators B*, 142, 260, 2009.
122. J. Morton, N. Havens, A. Mugweru, A. Wanekaya, Detection of Trace Heavy Metal Ions Using Carbon Nanotube-Modified Electrodes,

Electroanalysis, 21, 1597, 2009.

123. H. Xu, L. Zeng, S. Xing, Y. Xian, G. Shi, L. Jin. Ultrasensitive Voltammetric Detection of Trace Lead(II) and Cadmium(II) Using MWCNTs-Nafion/Bismuth Composite Electrodes,
Electroanalysis, 20, 2655, 2008.

VITA

- ABDULLAH ALI MOHAMMED AL-ALIWI
- Born in AlAhsa, Kingdom of Saudia Arabia 1980.
- Recived B.Sc. in Chemistry from King Faisal University, Saudia Arabia in June 2002.
- Worked as a teacher for high school students since late 2002.
- Joined KFUPM in October 2004 as a part time student in the M.S program in Chemistry.
- Awarded M.S degree in Chemistry from KFUPM in June 2012.
- Present address: Dammam, Saudia Arabia, Phone +966 50 3926122
- E-Mail: Ah_abdullh@hotmail.com